Study on Treatment of Oil Sands Process-Affected Water Using A Bioreactor Process Train

by

Lei Zhu

A thesis submitted in partial fulfillment of the requirements for the degree of

Doctor of Philosophy

in

Environmental Engineering

Department of Civil and Environmental Engineering
University of Alberta

ABSTRACT

With rapid development of Canadian Oil Sands industry, concerns about adverse impacts of oil sands process-affected water (OSPW) on aquatic resources are magnified. It has been found that biological process for removing organic chemicals in the oil industrial wastewater is environmentally friendly and economical. However, the application of conventional biological treatment to complex industrial wastewater has been hindered by the sensitivity of microorganisms to salinity and toxic recalcitrant organics, which are present in OSPW. In this work, a novel bioreactor process train was proposed, designed, fabricated and investigated for OSPW treatment.

Firstly, a comprehensive literature review about bioreactors with an emphasis on their performance in treating recalcitrant industrial wastewaters was conducted to screen the potential ones for OSPW treatment. Two sets of bench scale experiments were performed on biodegradation of raw OSPW and HiPOx-treated OSPW to cultivate proper seed for inoculating selected bioreactors. The promising results from those batch studies suggested that bioreactors with proper seed had the capacity of removing the biodegradable organics in OSPW and chemical oxidation process was useful and necessary for OSPW treatment. Based on the literature review and bench scale studies, a novel bioreactor process train was proposed for treating OSPW, which was composed of moving bed biofilm reactor (MBBR) for removing easily biodegradable organics at first, ozonation followed for decomposing the remaining recalcitrant organics, membrane aerated biofilm reactor (MABR) for degradation of decomposed organics and adsorption column for the removal of residual organics in OSPW.

Then, the selected bioreactors were designed, fabricated and continuously operated over 2 years. The entire operation was divided into different phases according to different influent

composition and hydraulic retention time (HRT). To evaluate the performance of the bioreactor process train, chemical oxygen demand (COD) and acid extractable fraction (AEF) measured by Fourier transform infrared spectrum (FT-IR) were applied in this study. When the state of the bioreactor process train was stable, MBBR removed 23% of COD and 16% of AEF from OSPW at HRT of 3 days. With the utilized dose of 35 mg/L of ozone, the biodegradability of MBBR effluent increased. At the same HRT, reductions of 44% COD and 24% AEF in MABR were achieved. After adsorption column, the average COD and AEF in the effluent of the process train was 17 mg/L and 2.9 mg/L, respectively.

Lastly, the demonstrated effective removal of chemical organics in OSPW present by this bioreactor process train inspired us to investigate the internal structure and microbial community of the biofilm inside each bioreactor by utilizing microsensor and molecular biological techniques together. It was found that nitrification and denitrification process existed in MBBR and MABR. Sulfate reduction process only existed in MABR biofilm, which was consistent with the H_2S profile measured by H_2S microsensor. The diversity of microbial community in the biofilm from MABR was higher than that in the biofilm from MBBR, which might explain the better performance on AEF removal in MABR. The influent composition and HRT were two main factors affecting the abundance and diversity of microbial communities inside bioreactors. Both bioreactors captured and enriched some specific microorganisms such as *Pseudomonas*, *Falvobacterium* and *Rhodobacter*, which showed great resistance to the harsh environment and the capability of degrading naphthenic acids in OSPW. Bioaugmentation happening inside MBBR and MABR made the biodegradation of recalcitrant organic chemicals in OSPW faster and reclamation of tailings pond promising.

ACKNOWLEDGEMENTS

Firstly, I would like to show my acknowledgement and thanks to my supervisor, Dr. Tong Yu, for his enlightening guidance, immense knowledge, invaluable encouragement and extraordinary patience throughout my research. It was my great honor and pleasure to work under his supervision.

Besides my supervisor, I would like to thank the professors in the Department of Civil and Environmental Engineering, including Dr. Ania Ulrich, Dr. Leonidas Perez- Estrada and Dr. Selma Guigard for their informative and enlightening courses. I feel grateful to the technicians in the department, including Chen Liang, Elena Dlusskaya, Jela Burkus and David Zhao. My gratitude also goes to members in Dr. Tong Yu's research group, including Kusumakar Sharma, Shuying Tan, Shujie Ren, Miao Yu, Hong Liu, Yijun Chen, Zi'ang Zhu, Hannah Kratky and Zhan Li. Thanks for the stimulating discussions, the sleepless nights we were working together, and all the fun we had together. In addition, Dr. Chunqiao Xiao, Dr. Yan Zhang, Xiaoyan Wu and Justin Dong Min are thanked for their valuable assistance during the continuous operation of bioreactors and data analysis that help me proceed this research smoothly.

Moreover, I would like to acknowledge the financial supports for my research from Natural Sciences and Engineering Research Council of Canada (NSERC) and China Scholarship Council (CSC).

Finally, I am very grateful to all family members. A special contributor to this research is my fiancée, Hui Huang. She and my parents were always there to support and encourage me especially when I was frustrated during the research. Without their selfless support and love, I would not have come this far.

TABLE OF CONTENTS

LIST OF TABLES ..... **viii**

LIST OF FIGURES ..... **ix**

NOMENCLATURE ..... **xii**

CHAPTER 1 Introduction **1**

1.1 Background 1

1.2 Challenges for Research 3

1.3 Research Objectives and Overall Approach 3

1.4 Thesis Outline 7

CHAPTER 2 STAGE I - Water Quality Analysis and Bioreactor Selection **9**

2.1 OSPW Water Quality Analysis 9

2.2 Potential Bioreactors for OSPW Treatment 11

2.3 Challenges for Bioreactors Application on OSPW Treatment 18

CHAPTER 3 STAGE II - Bench Test and Preliminary Results **20**

3.1 Sequencing Batch Reactor 20

3.2 Continuous Activated Sludge Reactor 24

3.2.1 Characteristics of the HiPOx-treated OSPW 24

3.2.2 Continuous Activated Sludge Reactor Setup and Results 25

3.3 Bioreactor process train 27

CHAPTER 4 STAGE III - Bioreactor Process Train Operation and Performance Evaluation **31**

4.1 Moving Bed Biofilm Reactor 31

4.1.1 MBBR Design and Fabrication 31

4.1.2 Materials and Methods 34
4.1.3 Operation and Performance Evaluation 37
4.2 Chemical Oxidation Process 45
4.2.1 Materials and Methods 45
4.2.2 Ozonation System Setup and Operational Procedure 46
4.2.3 Batch Test Experiment for Optimal Ozone Dose 47
4.2.4 Results and Discussion 48
4.3 Membrane Aerated Biofilm Reactor 50
4.3.1 MABR Design and Fabrication 50
4.3.2 Materials and Methods 53
4.3.3 Operation and Performance Evaluation 54
4.4 Adsorption Process 61
4.4.1 Materials and Methods 61
4.4.2 Results and Discussions 65
4.5 Performance Evaluation of the Process Train and Conclusions 69
CHAPTER 5 STAGE IV - Microbial Activity and Community Analysis of Biofilms in the Bioreactors 71
5.1 Background 71
5.2 Chemical Profiles inside Biofilms from MBBR and MABR Measured by Using Microsensor Techniques 76
5.2.1 Microsensors and Microsensor Measurements 76
5.2.2 Results and Discussion 79

5.3 Analysis of Microbial Community inside MBBR and MABR by Using Molecular Biological Techniques 85
5.3.1 Illumina MiSeq Sequencing 85
5.3.2 Sample Description 87
5.3.3 Results and Discussion 87
5.4 Conclusions 97
CHAPTER 6 Conclusions and Recommendations 99
6.1 Conclusions 99
6.2 Environmental Implications 102
REFERENCES 104
APPENDICES 122

LIST OF TABLES

Table 2-1 Water quality of OSPW from one Canadian oil sands company tailings pond..... 9

Table 2-2 Studty on xenobiotic contaminants biodegradation using a MABR 15

Table 3-1 Operational parameters and comments of the SBR..... 22

Table 3-2 Characterization of HiPOx-treated OSPW for the CASR..... 25

Table 4-1 Water quality of OSPW for the MBBR operation..... 35

Table 4-2 Composition of growth medium R2 36

Table 4-3 Results for the five scenarios ozonation in the batch test..... 49

Table 4-4 Main properties of two GAC columns 65

Table 4-5 Characteristic parameters of two adsorption isotherm models..... 66

Table 4-6 Performance of two GAC adsorption columns 67

Table 5-1 Description of six samples for Illumina MiSeq sequencing..... 87

Table 5-2 Alpha diversity parameters of microbial communities for all six samples 88

LIST OF FIGURES

Figure 1-1 Schematic diagram of the overall research approach 5

Figure 2-1 Schematic diagram of mass transfer pattern of oxygen and carbon substrate (C-substrate) in MABR (Casey et al., 1999) 13

Figure 3-1 Schematic diagram of the SBR 22

Figure 3-2 Ammonium, nitrite and nitrate concentration changes in the SBR on Day 1 23

Figure 3-3 Profile of COD concentrations and removal of SBR over the operation time 23

Figure 3-4 CASR system: ① air inlet; ② influent pump; ③ aerobic reactor; ④ stir plate; ⑤ settling flash; ⑥ recycle pump; ⑦ effluent storage tank 26

Figure 3-5 Profile of pH and DO of the CASR over the operation time 27

Figure 3-6 Profile of COD for the CASR over the operation time 27

Figure 3-7 Schematic graph of the bioreactor process train for OSPW treatment 28

Figure 4-1 Three-view diagram of the MBBR: (a) front view; (b) side view; (c) top view 32

Figure 4-2 Packing material in the MBBR: (a) PVC tubular packing material; (b) Mutag Biochip^{TM} 33

Figure 4-3 MBBR system: ① inlet; ② sampling port; ③ MBBR reactor; ④ mechanical mixer; ⑤ outlet; ⑥ settling flask; ⑦ mixer controller; ⑧ influent pump controller; ⑨ effluent storage tank; ⑩ influent pump; ⑪air inlet 34

Figure 4-4 Influent composition and HRT of MBBR at different phases 38

Figure 4-5 Biofilm grown on the PVC carrier in the MBBR system at different time: (a) Day 16; (b) Day 46; (c) Day 74 39

Figure 4-6 COD performance of MBBR during operation time at different phases 43

Figure 4-7 AEF performance of MBBR during operation time at different phases 44

Figure 4-8 Schematic diagram of chemical oxidation system 46
Figure 4-9 Picture of MABR with hollow fiber membrane module (white) 52
Figure 4-10 Schematic graph of the hollow fiber membrane module 52
Figure 4-11 MABR system: ① inlet; ② outlet; ③ effluent storage tank; ④ internal recycle outlet; ⑤ recycling pump; ⑥ internal recycle inlet; ⑦ nitrogen inlet; ⑧ compressed air inlet; ⑨ compressed air outlet; ⑩ sampling port; ⑪ MABR reactor 53
Figure 4-12 Influent composition and HRT of MABR at different phases 54
Figure 4-13 The state of biofilm formation inside MABR after 15 days' seeding period 55
Figure 4-14 COD performance of MABR during operation at different phases 59
Figure 4-15 AEF performance of MABR during operation at different phases 60
Figure 4-16 Schematic of GAC adsorption column 65
Figure 4-17 Adsorption isotherm of COD in MABR effluent onto GAC at 21°C 66
Figure 4-18 Breakthrough curve of the GAC column with 30 min EBCT 68
Figure 4-19 Performance of each operational component when the process train was at stable state 69
Figure 4-20 BOD value and BOD/COD ratio of each operational component when the process train was at stable state 70
Figure 5-1 An illustration diagram of microsensor measurement setup 78
Figure 5-2 Pictures of microsensor measurement setup for MBBR biofilm 79
Figure 5-3 Chemical profiles inside MBBR biofilm 80
Figure 5-4 Pictures of microsensor measurement setup for MABR biofilm 83
Figure 5-5 Chemical profiles inside MABR biofilm 83
Figure 5-6 The top 10 most relative abundance of the bacteria at the phylum level 92

Figure 5-7 The top 10 most relative abundance of the bacteria at the class level 92

Figure 5-8 Heat map for top 50 most abundant bacteria at genus level 95

Figure 5-9 PCoA analysis 96

NOMENCLATURE

Symbol	Explanation
AEF	Acid extracted fraction
AMO	Ammonia monooxygenase
AOB	Ammonia oxidizing bacteria
BOD	Biological oxygen demand
BTEX	Benzene, ethylbenzene, toluene and xylenes
CASR	Continuous activated sludge reactor
CFBR	Continuously flow biofilm reactor
COD	Chemical oxygen demand
CSTR	Continuous stirred-tank reactor
DCM	Dichloromethane
DO	Dissolved oxygen
DOC	Dissolved organic carbon
EBCT	Empty bed contact time
EGSB	Expanded granular sludge bed
FISH	Fluorescent *in situ* hybridization
FT-IR	Fourier transform infrared spectrum
GAC	Granular activated carbon
HRT	Hydraulic retention time
IC	Ion chromatography
IFAS	Integrated fixed-film activated sludge
LPM	Liter per minute
MABR	Membrane aerated biofilm reactor
MBBR	Moving bed biofilm reactor
MBR	Membrane biofilm reactor
MFTs	Mature fined tailings
MLSS	Mixed liquor suspended solids

MLVSS	Mixed liquor volatile suspended solids
MSBR	Moving-bed sequencing batch reactor
MTZ	Mass transfer zone
NAs	Naphthenic acids
ORP	Oxidation-reduction potential
OSPW	Oil sands process-affected water
OTU	Operational taxonomic units
PAHs	Polycyclic aromatic hydrocarbons
PCE	Perchloroethylene
PCoA	Principal coordinate analysis
PHC	Petroleum hydrocarbon
PVC	Polyvinylchloride
qPCR	Quantitative polymerase chain reaction
RPM	Revolutions per minute
rRNA	Ribosomal ribonucleic acid
SBR	Sequencing batch reactor
SRA	Sequence read archive
SRB	Sulfate reducing bacteria
SRT	Sludge retention time
SSBR	Sequencing batch biofilm reactor
TCE	Trichloroethylene
TDS	Total dissolved solids
TKN	Total Kjehldahl nitrogen
TN	Total nitrogen
TOC	Total organic carbon
TSS	Total suspended solid
UASB	Up-flow anaerobic sludge blanket reactor

CHAPTER 1 Introduction

1.1 Background

The Athabasca oil sands deposit, covering more than 75,000 km^2 in Alberta, Canada, is the third-largest proven oil reserves in the world with approximately 170.4 billion barrels of recoverable bitumen (Kannel and Gan, 2012). The Clark Hot Water Extraction Process, which uses a combination of hot water, steam, and caustic (NaOH), is used to separate the bitumen from the surface-mined oil sands. During this process, a large quantity of fresh water is consumed and results in large volumes of high-water content tailings. Tailings are a mixture of sand, silt, clay, water and a small amount of residual bitumen. The acute and chronic toxicity of fresh oil sands process-affected water (OSPW) to aquatic biota are commonly attributed to the fact that this OSPW contains a complex mixture of organic acids including naphthenic acids (NAs) (Afzal et al., 2012).

For every unit volume of bitumen recovered, there are 7 to 8 volume units of wet sand and mature fine tailings (MFTs) that need to be handled, and 10 volume units of water (recycled and fresh) that are pumped around the system (Flint, 2005). Although 80%-88% of the water used in the extraction process is recycled (Kannel and Gan, 2012), there are still numerous volumes of water trapped in the tailings pond and the pores of the sand in beaches and dykes (Flint, 2005). At current production rates, it is estimated that over 1 billion m^3 of OSPW will be accumulated in the Athabasca area by the year 2025 (Kannel and Gan, 2012).

With the rapid growth of oil production industry in the Athabasca area, concerns about possible adverse impacts of NAs in OSPW on aquatic resources are magnified. Environmental management of OSPW is becoming more stringent and its treatment is becoming a critical issue

for researchers, regulators and engineers, both in terms of sustaining bitumen recovery, reducing water consumption and protecting freshwater resources.

Based on the review of emerging technologies for OSPW treatment (Allen, 2008b), there are three kinds of technologies: 1) physical processes; 2) chemical oxidation processes; 3) biological processes. Physical processes have been proven to be capable of removing pollutants by transferring them from water phase to solid phase without degradation. Adoption of physical processes for full scale commercial use in OSPW will depend on operating costs, capital investment, footprint, and waste disposal requirements (Allen, 2008b). Chemical oxidation processes are useful on decomposition of recalcitrant organics in OSPW. For treatment of large volume of water containing organic contaminants, when biological processes are feasible, they are almost always more economical in comparison to chemical processes. For biological process, the OSPW related challenges are toxicity, low biodegradability due to recalcitrant organics, low temperature and high salt concentration (Allen, 2008b).

I believe that biological processes are promising for OSPW treatment. There are some reviews on the microbial degradation in remediation research of NAs in aquatic environments (Clemente et al., 2005; Headley et al., 2004) and on options for *in situ* bioremediation of OSPW NAs (Quagraine et al. 2005; Whitby, 2010). It has been shown that microbial communities exposed to NA-contaminated environments have certain specific metabolic capabilities to degrade organic acids with alkyl-substituted aliphatic chains (Marchal et al., 2003). These microbial communities could also degrade the NAs in OSPW faster than those from non-process-affected wetlands (Del Rio et al., 2006). Furthermore, some recent research has demonstrated that biological treatment can effectively degrade the organic components in OSPW (Allen, 2008b; Quinlan and Tam, 2015). Therefore, it is hypothesized that biological treatment

using bioreactors inoculated with indigenous microbial communities from OSPW tailings ponds may likely be a feasible, environmentally friendly and economical way for treating OSPW.

1.2 Challenges for Research

At the beginning of my research in 2010, there was no demonstrated biological process that had been used successfully to treat OSPW except one paper using synthesized NAs, nor consensus on how to select, design and start up bioreactors for treating OSPW based on literature review in the Chapter 2. Firstly, it is very critical and necessary to establish a set of criteria to select potential bioreactors by analyzing dozens of bioreactors in terms of their mechanism, configuration, and applications for recalcitrant organics biodegradation.

Secondly, the need to develop "seed" for reactor start-up and operation had just been realized in our research group when I began my research, but the method was far from mature. The seeding and start-up procedure for selected bioreactors needed to be explored from previous bioreactor applications on recalcitrant industrial wastewater which is similar to OSPW.

Lastly, I speculated and believed that biofilms would likely play a key role in the bioreactors treating OSPW based on literature review in Chapter 2 and experience; but the knowledge on this particular type of biofilm treating the challenging OSPW was quite limited. If the performance of bioreactors is promising, the biofilm internal structure, microbial community composition and related functions will be the key to interpret operational results, and to improve the performance and design of bioreactors. These application and knowledge gaps interested and challenged me to proceed with research in my PhD study.

1.3 Research Objectives and Overall Approach

In view of the above gaps, the aim of this research is to: (i) establish a proper and feasible bioreactor process train for OSPW treatment; (ii) expand our fundamental understanding of the

structure and function of the biofilm grown inside of the selected and designed bioreactors; and (iii) provide information for future improvements in the design and operation of wastewater bioreactors and in the reclamation of oil sands tailings. To achieve this aim, there were many unknowns and uncertainties at the beginning of my research. Some proposed studies could only become feasible when the previous one was accomplished with promising results. Therefore, an exploratory approach was used, with the aim as the guidance, and many revisions of proposed studies followed. At the end, the entire research was retrospectively organized into four stages, including seven steps.

Stage 1: Literature Review

Objective 1: Screen potential types of bioreactors based on literature review and select the promising ones for OSPW treatment;

Stage 2: Bioreactor Process Train Establishment

Objective 2: Use lab-scale prototype of bioreactors to cultivate proper seed;

Objective 3: Establish a feasible bioreactor process train using selected bioreactors, as well as necessary supporting chemical and physical processes;

Stage 3: Bioreactor Process Train Operation and Evaluation

Objective 4: Seed designed bioreactors and improve the performance of these bioreactors by changing operational conditions;

Objective 5: Evaluate the performance of bioreactors in the process train to find out the optimal operational conditions for this bioreactor process train;

Stage 4: Biofilm Exploration and Correlation inside Bioreactor Process Train

Objective 6: Investigate on the structure and microbial community inside biofilm of each bioreactor by using microsensor and molecular biological techniques;

Objective 7: Correlate and illustrate the relationship between bioreactors operation performance and biofilm internal structure and functions.

Figure 1-1 lists the following specific objectives of each stage and shows the relationship between stages and steps.

Figure 1-1 Schematic diagram of the overall research approach

The details and relationship between each stage are explained in the following paragraphs. In Stage 1, the focus was to develop a set of criteria to find out potential bioreactors that could treat OSPW. This stage included OSPW water quality analysis (Step 1) and critical review of

hundreds of research papers directly related to the technical applicability of biological treatment for industrial wastewater similar to OSPW (Step 2). From these two steps, biofilm-based bioreactors were our best choice to serve Objective 1 well.

In Stage 2, the goal was to establish a bioreactor process train with bioreactors, chemical oxidation and adsorption for treating OSPW. At the beginning, several bench scale experiments were carried out (Step 3) to provide preliminary data, which were necessary for achieving Objective 2. With the analysis of the experimental results, it became clear and confident to establish a feasible bioreactor process train with those selected bioreactors, which was Objective 3. After this point, the first two stages' preparation for the entire OSPW treatment system setup was finished.

In Stage 3, the start-up, operation and performance evaluation of designed bioreactors for OSPW treatment was critical and time-consuming, which determined the success of this research. During the start-up period, continuous and intense monitoring was involved to make inoculated biofilm attach, grow and become thicker on the inside packing material (Step 4), which was the key to make Objective 4 achievable. After the start-up period, bioreactors were evaluated to find out the optimal operational conditions for OSPW treatment by gradually changing influent composition and flow rate (Step 5). When the capability of the bioreactor process train to treat OSPW had been demonstrated, it indicated that Objective 5 was accomplished. Our research interest switched to understand the biofilm inside the bioreactors, which was the key component of bioreactors.

In Stage 4, the biofilm inside the bioreactors was the focus. Firstly, I explored the microbial communities and chemical profiles related to major microbial metabolic activities inside the biofilm by microsensor and molecular biological techniques (Step 6), which was helpful to

accomplish Objective 6. The following step was to correlate and elucidate the relationship between bioreactors operation performance and the biofilm internal structure by combining performance data and microbial communities' dynamic shift under each operational condition (Step 7). All these improved understandings about biofilm would be beneficial for further improvement of bioreactor design and performance for OSPW treatment. Therefore, the aim of this research was finally testified and realized.

1.4 Thesis Outline

There are six chapters present in this dissertation. Its structure is as follows:

Chapter 1 introduces the background information and present situation of OSPW treatment. It also includes the overall aim, specific objectives and the approach used in this research.

Chapter 2 provides a literature review to understand the characteristics, mechanism and real industrial applications of different types of bioreactors. OSPW water quality analysis was utilized to find out the challenges for biological treatment of OSPW. Based on this literature review and OSPW water quality analysis, the potential bioreactors for OSPW treatment were selected, in which Stage 1 was accomplished.

Chapter 3 presents the bench scale test and preliminary results, which gives us a solid foundation and promising direction to establish the proper bioreactor process train for OSPW treatment. Then, a feasible bioreactor process train was proposed in this chapter, which is the focus of Stage 2.

Chapter 4 describes each component of the established bioreactor process train in detail. The entire process train includes four operational components: moving bed biofilm reactor (MBBR), chemical oxidation, membrane-aerated biofilm reactor (MABR) and adsorption. The

materials and methods of each unit are fully described. The performance of each operational component was evaluated to find the optimal conditions. The promising final effluent quality shown in this chapter signals the achievement of Stage 3.

Chapter 5 examines the internal structure and function of biofilm inside bioreactors when the performance of the bioreactor process train was stable. That is the main objective of Stage 4. In the first section, several microsensors were fabricated and applied to picture the profile of related chemicals, such as nitrate and H_2S, inside the biofilm. A literature review of microsensor and molecular biological techniques used in biofilm research was covered in the first section of this chapter to support my research tools selection. High-throughput sequencing technology was used to investigate microbial community shift during operation and specific microorganisms were identified to be responsible for related biological processes in OSPW treatment.

Chapter 6 illustrates conclusions and environmental implications of this research.

CHAPTER 2 STAGE I - Water Quality Analysis and Bioreactor Selection

2.1 OSPW Water Quality Analysis

Tailings are composed of water, dissolved salts, organics, minerals, and a small amount of residual bitumen. The composition of oil sands tailings varies with ore quality, source, extraction processes, and age, but generally contain approximately 70 to 80 wt% water, 20 to 30 wt% solids (such as sand, silt, and clay) and 1-3 wt% bitumen (Kasperski, 1992). Table 2-1 presents OSPW water characteristics from a tailings pond of one Canadian oil sands company.

Table 2-1 Water quality of OSPW from one Canadian oil sands company tailings pond

Parameter	Units	Range
TDS	mg/L	1740-2110
pH	-	8.1-8.3
Total alkalinity	mg/L as $CaCO_3$	690-720
HCO_3^-	mg/L	844-878
CO_3^{2-}	mg/L	< 5
Cl^-	mg/L	350-419
NH_4^+-N	mg/L	13-19
NO_3^--N+NO_2^--N	mg/L	< 0.07 - < 0.1
SO_4^{2-}	mg/L	199-389
Total phosphorus	mg/L	0.1-0.223
DOC	mg/L	70-90
BOD	mg/L	49-69
COD	mg/L	299-318
Ca^{2+}	mg/L	13-44
Mg^{2+}	mg/L	6-16
Na^+	mg/L	551-683
AEF	mg/L	46-63
Benzene	µg/L	8.0-31.8
Ethylbenzene	µg/L	8.6-84
Toluene	µg/L	126-417
Xylene	µg/L	171-501

OSPW is hard (13-44 mg/L Ca^{2+}, 6-16 mg/L Mg^{2+}) with a pH of 8.1-8.3 and an alkalinity of 690-720 mg/L as $CaCO_3$. Total dissolved solids (TDS) concentrations (1740-2110 mg/L) are in the slightly brackish range. Dissolved solids are dominated by sodium (551-683 mg/L), chloride (350-419 mg/L), bicarbonate (844-878 mg/L), and sulfate (199-389 mg/L). The ammonium-nitrogen is in the range of 13-19 mg/L, while phosphate is <1 mg/L. For biological treatment, the OSPW is slightly brackish with high alkalinity but little nutrients, especially phosphate. Therefore, it is harsh and stressful for microorganisms to grow in OSPW.

Organic compounds detected in OSPW include bitumen, naphthenic acids, asphaltenes, benzene, creosols, humic and fulvic acids, phenols, phthalates, polycyclic aromatic hydrocarbons (PAHs), and toluene (Allen, 2008a). Dissolved organic carbon (DOC) ranges in concentration from 70 to 90 mg/L, and is mostly comprised of organic acids, 80% of which are NAs. NAs are a family of alicyclic and alkyl-substituted aliphatic carboxylic acids with a generalized formula of $C_nH_{2n+z}O_2$, where n stands for carbon number, z specifies a homologous series resulting double bond formation or cyclicity. Values of n range from 5 to 33, which results the molecular weight of NAs between 100 to 500 g/mol (Islam et al., 2014). The most important characteristics of tailings water is its toxicity mainly due to NAs on aquatic and terrestrial biota (Allen, 2008a). Among the aromatic compounds detected in tailings water are several toxicants of concern including benzene, ethylbenzene, toluene, xylenes (BETX), phenol, and PAHs, which are groups of recalcitrant substrates for microorganisms. The scarcity of easily biodegradable carbon in tailings water, as shown by BOD/COD ratio of 0.16-0.21, makes it recalcitrant for biological degradation.

Although tailings water is toxic, the microbial activity of degrading the petroleum hydrocarbons has been found in sediments of oil sands tailings ponds, which is also known as

mature fine tailings (MFTs) (Siddique et al., 2006). Diverse methanogenic communities have been discovered and identified in MFTs (Penner et al., 2010). Also, microbial activities have been reported in fine tailings that reduce sulfate and produce methane (Holowenko et al., 2000) and reduce amended sulfate in MFTs (Salloum et al., 2002). These findings encouragingly indicate the biological treatability of tailings water. Also, NAs of OSPW can be degraded by using indigenous microorganisms from the sediment (Del Rio et al., 2006). These indigenous mixed microbial species could potentially be selected for tolerance to the complex and toxic properties of tailings waters and used as seed capable of remediation of tailings water.

2.2 Potential Bioreactors for OSPW Treatment

Engineered bioreactors of various types have been successfully used in wastewater treatment for decades (Farhadian et al., 2008). The experience on the design and applications of bioreactors to industrial wastewater provides a rich source of knowledge that can be transferred to treatment of OSPW. For biological treatment of OSPW, the challenges are related to toxicity, low biodegradability, low temperature and high salt concentration. Therefore, the criteria for selecting potential bioreactors for OSPW treatment are as follows:

1) Bioreactors which can support different types of microorganisms to adapt the stressing and inhibitory environment;
2) Bioreactors which have been applied to degrade the recalcitrant organics in the industrial wastewater;
3) Bioreactors which are relatively easy to operate and tolerant to shock loading.

Compared to suspended growth bioreactors, such as activated sludge reactors, biofilm reactors exhibit significantly improved performance due to the unique structure of biofilm. Depending on the water characteristics and treatment objective, aerobic, anaerobic, or combined

processes could be employed for pollutant degradation. Aerobic bioreactors can reduce NAs toxicity and oxidize ammonia, while anoxic bioreactors can remove total nitrogen by denitrification. The anaerobic bioreactors are most suitable for degrading recalcitrant and toxic organics, sulfate reduction, producing acids to neutralize alkalinity and methanogenesis (Frankin, 2001).

The moving-bed biofilm reactor (MBBR) is a highly effective biological treatment process that was developed on the basis of conventional activated sludge process and fluidized-bed reactor. MBBR can be easily alternated between aerobic and anaerobic conditions, to achieve nitrification, COD and phosphorous removal (McQuarrie et al., 2011).

Because of the biofilm diffusion limit, MBBR exhibits greater resistance to the adverse chemical conditions presented by industrial wastewaters than conventional biological treatment. It is because MBBR can provide suitable microenvironment for specialized microorganisms to degrade toxic organic compounds including aromatic compounds, organic chlorides, and other contaminants. Bassin et al. (2011) found that in a bench scale MBBR nitrification percentage of the treated domestic sewage was higher than 90% for all tested chloride concentrations up to 8000 mg/L. MBBR can provide adequate conditions for adaptation of nitrifying microorganisms even under stressing and inhibitory conditions. In the study by Moussavi et al. (2009), the performance of a moving-bed sequencing batch reactor (MSBR) to remove phenol from wastewater was tested. The effects of phenol concentration (50-3325 mg/L), filling time (0-4 h) and aerating time (4-18 h) on the performance of the MSBR are given in terms of phenol as COD removal efficiencies. The optimum hydraulic retention time (HRT) for the MSBR was 40 h and the maximal phenol loading rate was 83.4 g phenol/(m^3·h), which gives a phenol removal efficiency of 99%.

For oil refinery wastewater, Schneider et al. (2011) tested a MBBR and produced the best performance of 89% COD removal and 86% NH_4^+-N removal at HRT of 6 h. After ozonation in series with a biological activated carbon column, the effluent obtained at the end of this process train presented a quality that meets the requirements for water reuse in the oil refinery. These results support that MBBR is a promising technology for being used in the OSPW treatment.

The membrane aerated biofilm reactor (MABR) is a novel kind of reactor, which uses gas-permeable hydrophobic hollow fiber membranes for bubbleless aeration and also as the carrier of the biofilm (Casey et al., 1999). Figure 2-1 shows the schematic mass transfer pattern in this reactor. Such a configuration can provide high oxygen transfer efficiency and have the potential advantage to lower the treatment operational cost (Brindle et al., 1996).

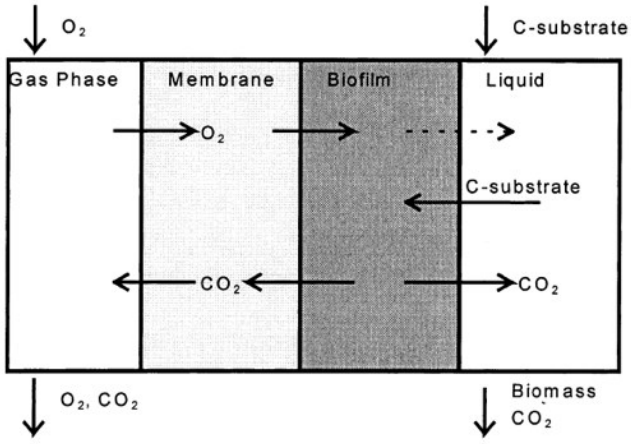

Figure 2-1 Schematic diagram of mass transfer pattern of oxygen and carbon substrate (C-substrate) in MABR (Casey et al., 1999)

The unique capability of a MABR to accommodate both aerobic and anaerobic zones has led to the application of this type of bioreactor to biodegradation of compounds requiring both aerobic and anaerobic environments. A MABR has been developed for the complete degradation of perchloroethylene (PCE) to ethane without the build-up of harmful intermediates. Due to the long sludge retention time (SRT), MABR has the capacity to retain slow growing rate

microorganisms, which will enrich diverse microbial communities that can degrade a wide range of contaminants (Syron and Casey, 2008). Table 2-2 shows some lab scale studies that investigated the potential of using a MABR for the biodegradation of synthetic wastewater with xenobiotics constituents causing toxicity. From these studies reported, it suggests that MABR has the potential for effective removal of toxic and recalcitrant organic compounds in OSPW.

For anaerobic process, up-flow anaerobic sludge blanket reactor (UASB) and expanded granular sludge bed (EGSB) reactor are used commonly. The latter one is a variant of the UASB concept (Kato et al., 1994). Granulation in UASB reactors is important in the treatment of various industrial wastewaters containing toxic substances due to their compact structure which protects the bacteria from inhibitory and toxic pollutants.

Petrochemical wastewater and effluents from similar industries include complex organic constituents that exert high organic loading on treatment reactors and besides, mostly contain toxic compounds that may shock the anaerobic biodegradation processes due to their toxicity for treatment systems. These characteristics are similar to those of the OSPW.

However, in an UASB, the structural characteristics of bacterial aggregates and high biomass retention increase the tolerance of anaerobic bacteria to toxic compounds. For example, phenol in wastewater could be effectively degraded in a UASB reactor. With a 1:1 effluent recycle ratio, over 97% of phenol was removed at 37°C and pH 6.9-7.5 with 12 h of HRT for phenol concentration up to 1260 mg/L, corresponding to 3000 mg/L of COD and a loading rate of 6 g COD/(L·d) (Fang et al., 1996).

Table 2-2 Studies on xenobiotic contaminants biodegradation using a MABR

Reactor configuration	Aeration mode	Target contaminant	Influent concentration	Removal	HRT (h)	Reference
Single silicone tubing membrane reactor, continuous flow with internal recirculation	CH_4/air mixture	Trichloroethylene (TCE)	4.6 mg TCE/L	80-90%	26	(Clapp et al., 1999)
Air-tight completely mixed reactor with immersed silicone tubing membrane by magnetic stirrer	Air/O_2	Xylene	275 mg COD/L	52%	6	(Debus and Wanner, 1992)
Sequencing batch biofilm reactor with immersed silicone tubing membrane, mixed by magnetic stirrer	O_2	Phenols	120 mg Phenol/L	99%	12	(Woolard et al., 1995)
Sequencing batch biofilm reactor with immersed spiral wound silicone tubing membrane, external recycle	O_2	Chlorophenol	8 mg chlorophenol/L	95%	6	(Wobus et al., 1995)
Sequencing batch biofilm reactor with immersed spiral wound silicone tubing membrane, external recycle	O_2	Monochlorophenol (MCP)	207 mg MCP/L	95%	6	(Wobus and Roske, 2000)
MABR with polypropylene flat sheet membrane, continuous flow with internal recirculation	O_2	PCE	70 mg PCE/L	99%	9	(Ohandja and Stuckey, 2007)

Anaerobic digestion of long-chain fatty acids by using UASB and EGSB reactors was investigated in early 1990's (Rinzema, 1993). The inoculums in this experiment were from potato processing wastewater and sugar-beet refinery wastewater, respectively. Concentrated stock solutions of sodium caprate and sodium laurate were used as the target pollutants. From the results obtained, the conventional UASB reactors cannot achieve efficient contact between the substrate and all the biomass when lipids contribute 50% or more to the COD of the wastewater. However, EGSB reactors did perform well in mixing and contacting between substrate and biomass. They can accommodate loading up to 30 kg COD m^3/day with COD removal efficiency of 83-91% and can be operated at HRT of 2 h without problem.

For oil produced water, Rincon et al. (2003) reported on the anaerobic treatment of three different waters from the extraction of light, medium and heavy crude oils using lab-scale UASB reactors. Granular sludge from a UASB reactor treating brewery wastewater was used as the inoculum. Vieira et al. (2005) investigated the anaerobic biodegradability of oil produced water from an offshore oilfield in a batch reactor. The salinity and COD in the influent water was 7.6% TDS and 4700 mg/L, respectively. After an incubation of 6-15 days, reductions of about 57% COD, 44-78% total phenols and 42-62% oil and grease were achieved.

There have been many research reports on psychrophilic anaerobic treatment by the EGSB reactor (Collins et al., 2005; Collins et al., 2006; Enright et al., 2005; Enright et al., 2007; Rebac et al., 1999). It is because the EGSB reactor has been shown to be a feasible system for anaerobic treatment at low temperature. Connaughton et al. (2006) showed that there has no difference between the mesophilic EGSB reactor and the psychrophilic one.

Furthermore, sulfide concentration will not have much impact on the performance of EGSB. It is reported that the incubated granules converted sulfide, nitrate, and acetate simultaneously in

the same EGSB reactor to S^0, N-containing gases and CO_2 at loading rates of 3.0 kg S/(m^3·d), 1.45 kg N/(m^3·d), and 2.77 kg C/(m^3·d), respectively, and was not inhibited by sulfide concentration up to 800 mg/L (Chen et al., 2008). Also, a set of bench scale anaerobic EGSB studies showed that COD conversion could be achieved at the influent concentration of approximately 150 mg COD/L. The maximum COD conversion efficiency was 78% at 10 hours HRT and 20°C (Collins et al., 1998).

Although UASB and EGSB have the potential for treating recalcitrant organics in industrial wastewater based on the above applications, there are three limitations about them for OSPW treatment: (1) hard formation of granular sludge due to low organic loading for OSPW treatment. The flocculent sludge cannot grow fast and much enough to form granular sludge due to the shortage of biodegradable organic compounds in OSPW. Therefore, the performance of UASB and EGSB will not be good. (2) long time needed for reactor start-up. Sludge granulation is complex and affected by many factors; and is not clearly understood yet. Most microorganisms existed in granules are denitrifying, nitrifying, acidogenic, and methanogenic bacteria. However, several factors determine characteristics of granules, including: characteristics of organisms, growth rate of organisms, and death rate and decay rate of the organisms (Lettinga, 1995). So gradually increasing inlet flow rate and organic load is needed. Seeding of granular sludge from another operating reactor is highly recommended, which is the disadvantage for my study. (3) no good removal of suspended solids and colloidal matter can be achieved. Soluble pollutants are efficiently treated in UASB and EGSB, but suspended solids are not substantially removed from the wastewater stream due to the high up-flow velocities applied. Therefore, post-treatment of EGSB effluent is required which will increase the investment of the wastewater treatment plant.

In summary, the selection of UASB and EGSB on OSPW treatment in this research is not recommended.

From the above literature study, it is found that biofilm reactor has the advantage of protecting bacteria under harsh environment due to biofilm unique structure; can be operated under both anaerobic and aerobic conditions, which gives more capacity for recalcitrant organics digestion by different kinds of bacteria; and can be easily started up comparing with UASB and EGSB. Therefore, MBBR and MABR were selected for OSPW treatment.

2.3 Challenges to Run Bioreactors Continuously for OSPW Treatment

Biological treatment has been tested extensively in the oil industry for removal of organic carbon and nitrogen compounds. There are also studies about using bioreactors for several kinds of commercial NAs removal (Huang et al., 2012; Toor et al., 2013). However, there was no publication about treating raw OSPW by bioreactors at the time of the literature review for bioreactor selection. Because there are several challenges encountered during the bioreactor application on OSPW treatment:

1) Fluctuation of the influent water quality. It is known that the water quality of OPSW varies largely from different tailings ponds. However, a stable influent quality is important for bioreactor operation, because the environment inside the bioreactor needs to be controlled for microbial growth during the process. Without a stable influent water quality, it is not possible to maintain and evaluate the performance of the bioreactor.
2) An affordable and efficient monitoring method for bioreactor performance evaluation is needed. During the operation, the performance of bioreactor should be monitored and evaluated timely to guide the further operation. Recently, the

3) Start-up of bioreactors. The procedure of starting up a bioreactor for OSPW treatment is unknown and need to be determined based on bench tests. Furthermore, seeding plan and pre-treatments are critical issues for bioreactor start-up. It is a big challenge to keep the indigenous microorganisms in OSPW alive and growing inside the selected bioreactor.

With the bioreactors selected (MBBR and MABR) and challenges related to bioreactor operation identified, the objective of Stage 1 was achieved. Next, it is needed to find suitable seed for inoculating the selected bioreactor and to establish a proper biological process train with selected bioreactors. They are objectives of Stage 2 and are described in Chapter 3. Those challenges for bioreactor application on OSPW treatment will be illustrated in Chapter 3 and 4.

CHAPTER 3 STAGE II - Bench Test and Preliminary Results

In this chapter, the main objective was to find the proper seed for inoculating the bioreactor selected in Chapter 2 and to establish a feasible bioreactor process train based on preliminary bench scale tests, which are also tasks of Stage 2. Two sets of bench scale experiments were conducted: (1) using a sequencing batch reactor (SBR) to cultivate and testify the sludge from a commercial biofilm reactor with biosolids from OSPW as a proper seed; (2) using a continuous activated sludge reactor (CASR) seeded with the cultivated sludge in the first experiment to treat chemically oxidized OSPW. The results from those two sets of experiments combined with literature review in Chapter 2 are used to support the development of the bioreactor process train.

3.1 Sequencing Batch Reactor

It is known that the key of successful bioremediation is to utilize microorganisms with survivability and proven remediation capability in the contaminated environment. For OSPW biological treatment, the selection and cultivation of proper microorganisms is the key to this research. The purposes of experiments in this section were 1) to cultivate the activated sludge from a commercial membrane biofilm reactor and biosolids from OSPW by using an SBR; 2) to testify whether microorganisms in the culture are capable of tolerating the toxic environment and utilizing the petroleum hydrocarbon.

There are two main reasons for choosing SBR for seed cultivation. Firstly, in the case of organic compounds with a low biodegradability in OSPW, when specialized microorganisms are required, SBR is preferable (Dollerer and Wilderer, 1996). SBR will be beneficial for the selection of proper microorganisms as seed. Secondly, the SBR is an activated sludge process but operates in a true batch mode. It means that one SBR tank performs functions such as equalization, aeration, and sedimentation in a time rather than in a space sequence. Therefore,

SBR can offer high degree of process flexibility in terms of cycle time and sequences (Kennedy and Lentz, 2000), which will be necessary and helpful for seed cultivation.

COD test is a common test for wastewater treatment, the change of which can be used for observing the substrate utilization by microorganisms in aqueous phase. Although it is not capable of reflecting concentration changes of organic chemicals with long chains and large molecular weight (such as NAs) due to limitations of this method, COD test is fast and applicable for identifying the microbial activity indirectly, which meets the requirement in this section of experiment. The closed reflux colorimetric method was used for COD analysis (APHA, 2005). Every sample was duplicated in the COD test and the average COD value was present in this study.

Mixed liquor volatile suspended solids (MLVSS) inside the SBR was measured to evaluate the biomass growth according to Standard Methods for Examination of Water and Wastewater (APHA, 2005).

In this experiment, a 5 L Pyrex® bottle (Catalog No. 06-414-1F, Fisher Scientific Company, ON, Canada) was used as a SBR and was placed on a magnetic stir plate. There was 2 L of solution inside the SBR in the beginning, which was composed of 600 mL activated sludge with biosolids extracted from OSPW and 1400 mL of raw OSPW. Biosolids was collected from OSPW by centrifuging at 6000 revolutions per minute (RPM) for 20 min, in which microorganism from OSPW could be extracted. Activated sludge from an operating biofilm reactor was also used as seed for the SBR. The initial MLVSS concentration inside the SBR was approximately 3000 mg/L. There was a magnetic stir bar inside for mixing. Compressed air was introduced for aeration through air diffuser and controlled by a flow meter to maintain the DO in the SBR around 2 mg/L. No pH adjustment was needed because the high alkalinity existed in the

raw OSPW. Figure 3-1 is the schematic diagram of the SBR. During the operation, pH did not change significantly (shown in Table 3-1). One liter of raw OSPW was introduced every two days with one liter supernatant out of the SBR at the same time. The influent OSPW was from a Canadian oil sands company, whose characteristics were listed in Table 2-1 in Chapter 2. The operational parameters of the SBR are shown in Table 3-1.

Table 3-1 Operational parameters and comments of the SBR

Parameter	Value	Comments
Reaction time	46 h	Aeration and mixing applied
Settling time	2 h	No aeration and mixing applied
HRT	48 h	Raw OSPW 1 L/day fed
DO	2 mg/L	By a constant air flow rate
pH	7-8	Using the alkalinity of OSPW to maintain pH
Mixing rate	300 RPM	To make a complete mixing

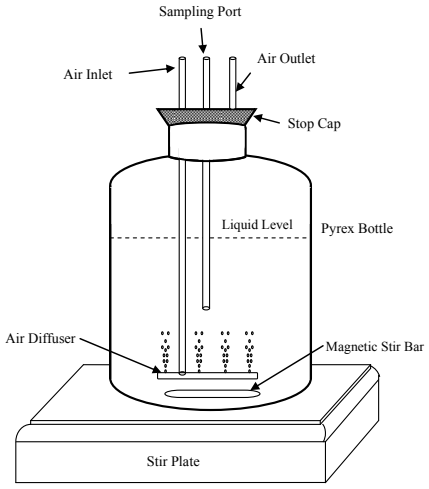

Figure 3-1 Schematic diagram of the SBR

The SBR was operated for one month with 46 h reaction time and 2 h settling time alternating to testify the feasibility of the seed added and to cultivate it. Figure 3-2 shows the ammonium, nitrite and nitrate concentration changes in SBR on Day 1. It indicated that ammonium in OSPW could be quickly utilized by microorganisms in the seed. Nitrite, as the metabolic intermediate, was oxidized to nitrate after 12 h, which demonstrated that the

nitrification process was occurring in the SBR under aerobic condition. Figure 3-3 presents the monitored COD concentration in the influent and effluent of the SBR and COD removal over the operation. It took 7 days for the SBR to reach a stable operational condition with almost 20% removal of COD. The MLVSS inside reactor was about 4100 mg/L when reactor performance was stable. These results demonstrated that bacteria inside the SBR survived in the harsh environment of OSPW and utilized organic compounds and nutrients in it for growth, which made Objective 2 achieved. It also proves that biological treatment is promising for OSPW treatment.

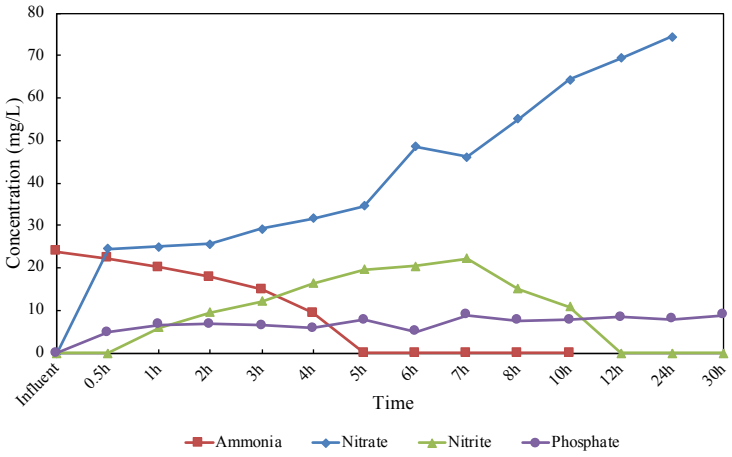

Figure 3-2 Ammonium, nitrite and nitrate concentration changes in the SBR on Day 1

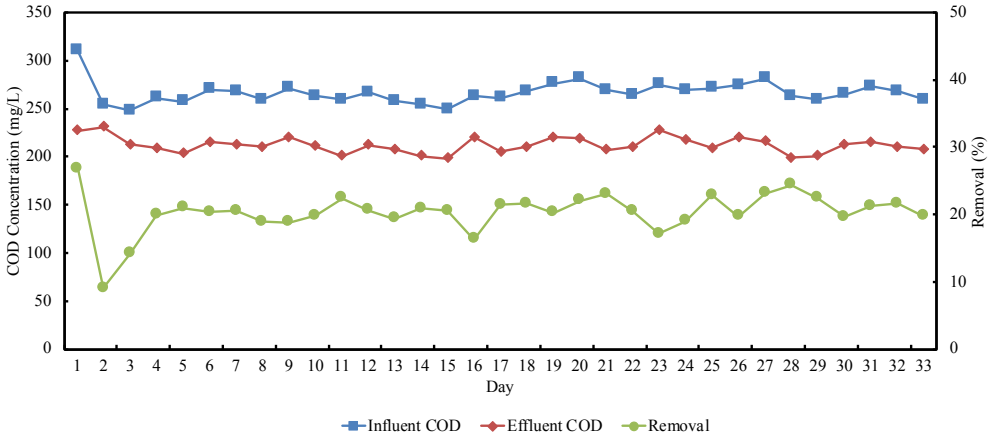

Figure 3-3 Profile of COD concentrations and removal of the SBR over the operation time

3.2 Continuous Activated Sludge Reactor

In Chapter 2, it is known that naphthenic acids are toxic organic components and the main concern for OSPW treatment. The complex molecular structure of NAs like long carbon chains and more rings is the reason of their recalcitrance for degradation in the environment. Biodegradation is usually able to remove NAs with low molecular weight and cyclicity based on recent studies (Kannel and Gan, 2012; Han et al., 2008). After biological treatment, there will be remaining nonbiodegradable NAs in OSPW. In order to improve the removal efficiency of NAs in OSPW, another treatment in addition to biological treatment will be necessary. Chemical oxidation such as ozonation is a proven effective method for decomposing the most bio-persistent NAs in OSPW (Martin et al., 2010). In the present study, it is necessary to determine the effect of chemical oxidation on the following biological process for OSPW further treatment, which will be beneficial for establishment of the bioreactor process train.

3.2.1 Characteristics of the HiPOx-treated OSPW

In this experiment section, HiPOx-treated OSPW was used as the influent of CASR. HiPOx treatment utilizes ozone and hydrogen peroxide to break down long chain organic compounds that are not biodegradable. Table 3-2 characterizes the HiPOx-treated OSPW and raw OSPW. Compared to the raw OSPW, NAs concentration was significantly reduced indicating the long chain organic compounds were broken down after HiPOx treatment. The short chain organic compounds were more easily biodegradable than those with long chain. Slight COD removal from raw OSPW suggested that HiPOx treatment could not achieve complete mineralization.

Fourier transform infrared spectrum method (FT-IR) described by Holowenko et al. (2001) was used to quantify NAs concentration in HiPOx-treated OSPW. It is now suggested as a standard method for routine monitor of NAs in OSPW. The result tested by FT-IR is named as

acid extractable fraction (AEF) of NAs and is expressed as mg/L of the Fluka commercial NAs standards purchased from Sigma-Aldrich (ON, Canada). Fluka commercial NAs were selected as standards due to comprehensive characterization of compositions, which have been used in several studies (Barrow et al., 2004; Headley et al., 2009; McMartin et al., 2004; Mishra et al., 2010; Rudzinski et al., 2002).

Table 3-2 Characterization of HiPOx-treated OSPW for the CASR

Parameter	HiPOx-treated OPSW	Raw OSPW
pH	7.1-7.2	8.1-8.3
COD	285-310 mg/L	299-318 mg/L
AEF	1.0-1.4 mg/L	46-63 mg/L
Alkalinity	523-526 mg/L as $CaCO_3$	690-720 mg/L as $CaCO_3$
Sulfate	371-411 mg/L	199-389 mg/L
Nitrate	under detection limit	<0.07-<0.1 mg/L

As listed in Table 3-2, pH dropped to 7.2 along with a loss of 181 mg/L as $CaCO_3$ in alkalinity. It indicated that alkalinity may be consumed during reaction with hydroxyl radicals resulting in a neutral pH value. Sulfate concentration increased to 390.9 mg/L in HiPOx-treated OSPW. This might be due to oxidation of organic and inorganic sulfides. Nitrate was under detection limit suggesting potential nutrients deficiency during aerobic sludge treatment. Therefore, nutrients additions would be needed for the following bioreactor operation after OSPW being treated by chemical oxidation process.

3.2.2 Continuous Activated Sludge Reactor Setup and Results

In this section, a 2 L volume flask was used as a CASR. Figure 3-4 shows the CASR system setup in the lab. The operation volume of this CASR was 2 L. The activated sludge was inoculated from the SBR in Section 3.1. The volume ratio of activated sludge and HiPOx-treated OSPW was 1:4, which made the sludge concentration inside reactor around 4000 mg/L. The HRT of the reactor was 24 h. The stir bar mixing rate was 300 RPM for complete mixing. The

effluent of the CASR flowed into another 2 L volumetric flask, in which the washed-out activated sludge was settled and recycled into the CASR by the recycling pump to maintain sludge concentration in the CASR during the entire operation.

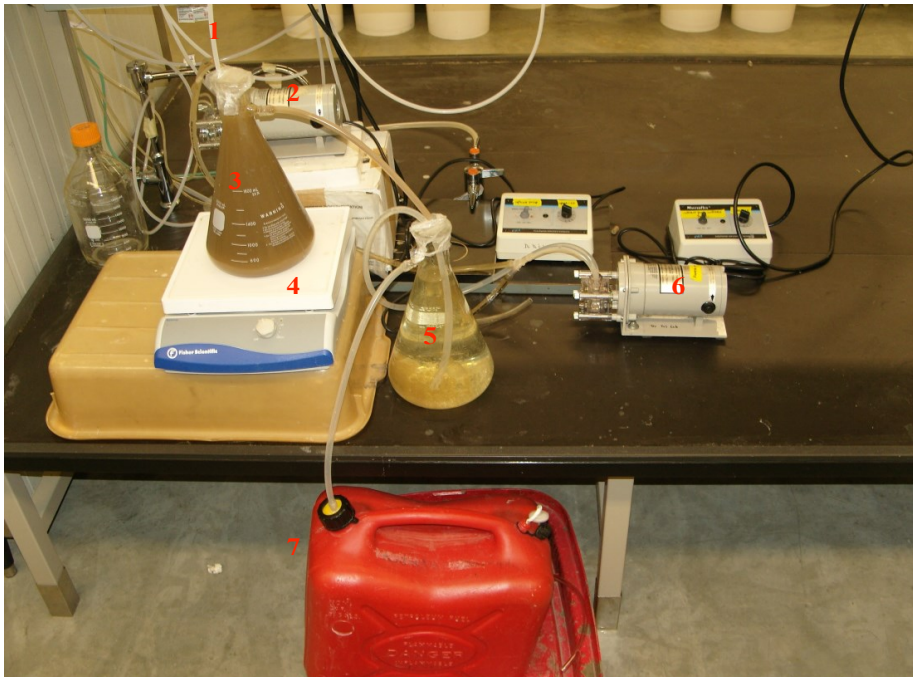

Figure 3-4 CASR system: ① air inlet; ② influent pump; ③ aerobic reactor; ④ stir plate; ⑤ settling flask; ⑥ recycle pump; ⑦ effluent storage tank

Figure 3-5 shows the pH and DO profile over the operation time. It was proven that the reactor operation was stable after 10 days. DO range was 2.5-3.5 mg/L, which was the indication of aerobic condition. Because of the high alkalinity in HiPOx-treated OSPW, pH kept around 7.8 when the reactor was stable.

Figure 3-6 presents the COD concentration in the influent and effluent of continuous aerobic reactor and COD removal during the operation time. The average COD removal in this CASR was 43% when reactor performance was stable. It was almost double the COD removal in the SBR. Furthermore, the HRT of CASR was shorter than that in the SBR. After 10 days' start-up phase, the effluent COD was around 170 mg/L, which was lower than that in the SBR. It

demonstrated that chemical oxidation process increased the biodegradability of OSPW and the following bioreactor utilized the decomposed organics for OSPW further treatment. Therefore, chemical oxidation process should be an essential part in the proposed bioreactor process train for OSPW treatment.

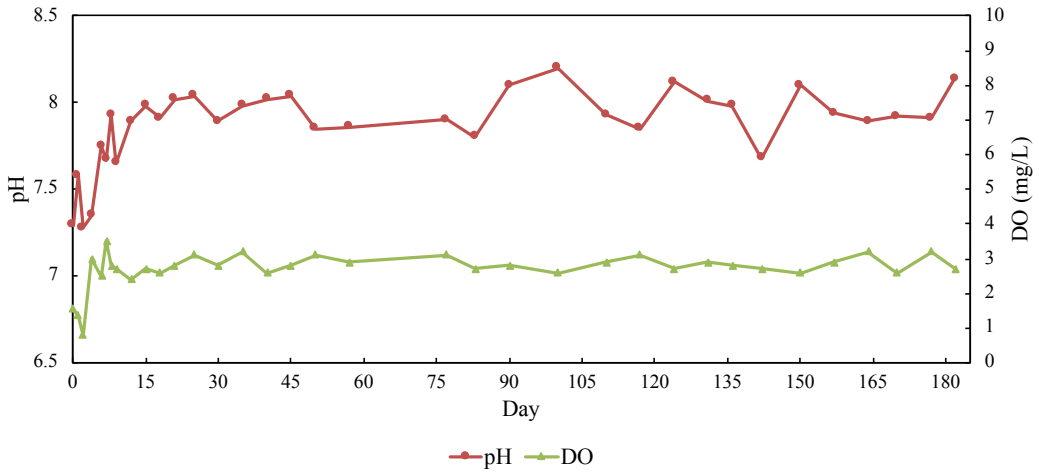

Figure 3-5 Profile of pH and DO of the CASR over the operation time

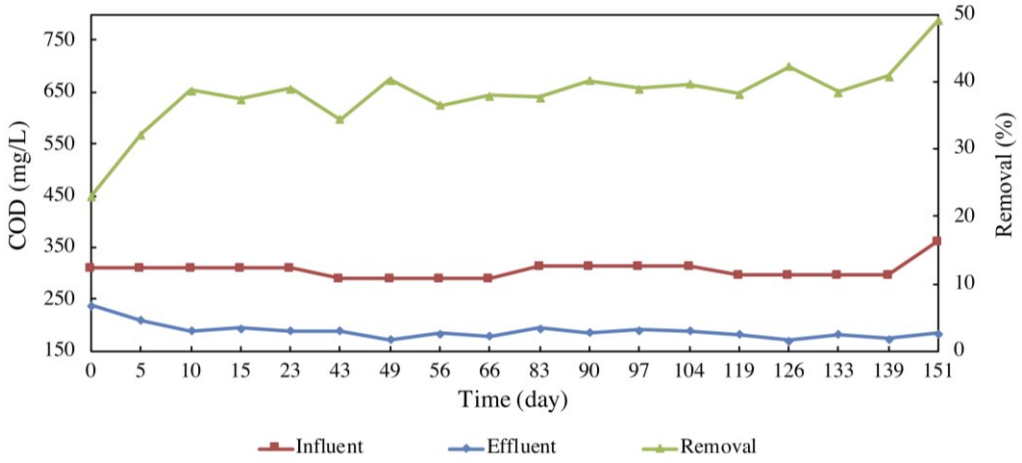

Figure 3-6 Profile of COD for the CASR over the operation time

3.3 Bioreactor process train

Based on the literature review in Chapter 2 and the preliminary results in Sections 3.1 and 3.2, it is proven that bioreactors with proper seed have the capacity of surviving and removing

the biodegradable organics in OSPW; chemical oxidation process is useful and necessary for decomposing the large, complex organics in OSPW, which can be utilized by the microorganism in the subsequent bioreactor for further treatment. Therefore, the bioreactor process train including four components was proposed, which is shown in Figure 3-7. The considerations and justifications of each component are described in the following paragraphs.

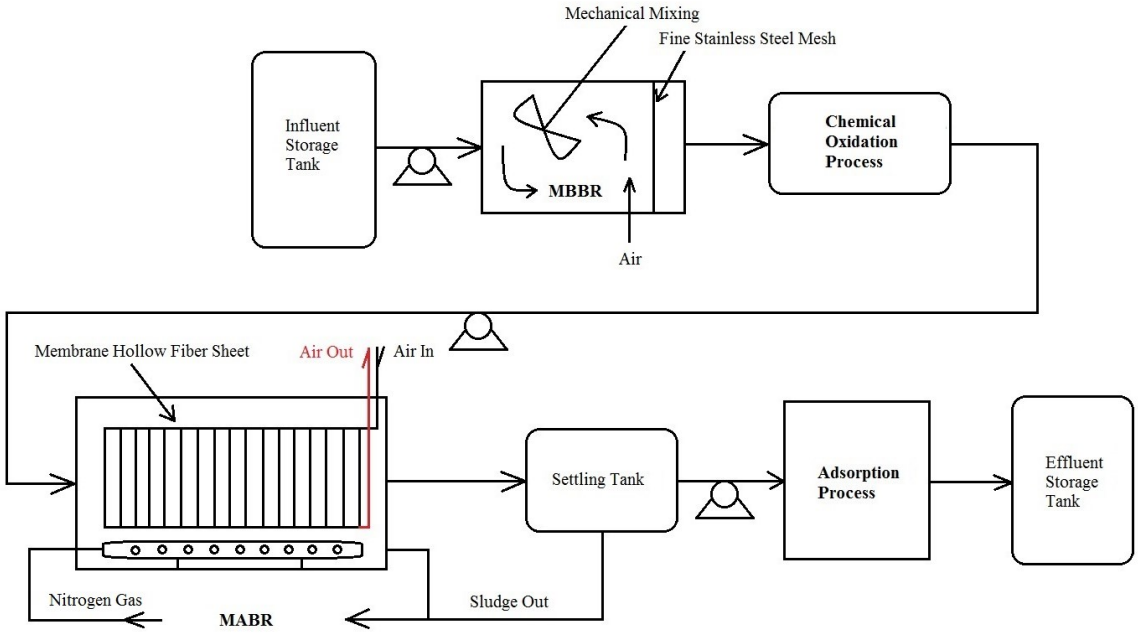

Figure 3-7 Schematic graph of the bioreactor process train for OSPW treatment

Component 1: MBBR – Biological process

In this bioreactor process train, MBBR is chosen to be the first bioreactor. Because that a MBBR has 1) a long sludge retention time: to keep the bacteria of low growth rate surviving inside the reactor; 2) high usage of the tank volume for biomass growth and improvement on mass transfer of pollutants: to enhance the performance of reactor; 3) operational stability: to make bioreactor start-up easier and faster. MBBR can lower the suspended solid concentration and remove some easily biodegradable organic compounds and inorganic compounds from

OSPW. It is beneficial for the following chemical oxidation process by saving the dosage of ozone.

Component 2: Ozone – Chemical oxidation process

For chemical oxidation process, ozone is applied for breaking down the remaining organic compounds in MBBR effluent, which have long carbon chain and large molecular weight, into relative-easily biodegradable smaller compounds, which will be introduced into MABR for further degradation. Several batch tests will be conducted for the optimal ozone dosage for the MBBR effluent.

Component 3: MABR – Biological process

As the second bioreactor, MABR can provide aerobic and anaerobic environment for different metabolic types of bacteria to grow, which will make the degradation of those complex organic compounds in OSPW as much as possible. MABR also has long sludge retention time to prevent the bacteria of slow growth rate from being washed out. Those two main advantages of MABR will give us more confidence on the performance of this process train for OSPW treatment. The settling tank followed can lower the suspended solid concentration of MABR effluent, which is the pre-treatment for adsorption process followed.

Component 4: Adsorption column – Physical process

As explained in Chapter 1, adsorption process was not proposed in the beginning of this stage (Stage 2) because the outcome of MABR was unknown and unpredictable at that time. Therefore, if there is a gap between the water quality of MABR effluent and the final discharge requirement for OSPW, adsorption process will be considered. Because adsorption process will be more efficient and cost-effective to remove low level of nonbiodegradable organic

compounds left in MABR effluent, comparing with chemical oxidation and biological process. Adsorption column filled with granular activated carbon is capable of further polishing the MABR effluent, which makes the final discharge or reclamation of OSPW achievable.

For the four operational components, the main focus of this study is on the biological process, including MBBR and MABR, for OSPW treatment. The role of chemical oxidation process is to enhance the biodegradability of MBBR effluent for further biodegradation by MABR. The application of physical process is to improve the performance of the proposed bioreactor process train for accomplishing the final discharge of OSPW. Therefore, chemical oxidation and physical process in the bioreactor process train are supportive for the biological process.

Based on the above analysis, it is believed that this bioreactor process train could be a feasible option for OSPW treatment, which makes the Objective 3 accomplished. In the next stage (Stage 3), MBBR and MABR will be designed, fabricated, seeded and operated to investigate the feasibility of the proposed bioreactor process train and find out the performance of each component for OSPW treatment, which will be described in Chapter 4.

CHAPTER 4 STAGE III - Bioreactor Process Train Operation and Performance Evaluation

In this chapter, the proposed bioreactor process train in Chapter 3 was designed, fabricated, started up, and operated to remove recalcitrant organics such as NAs in OSPW, which are the main task of Stage 3. There are four operational components in this entire process train, including MBBR, chemical oxidation, MABR and adsorption. The objectives of this chapter are 1) to investigate the feasibility of this process train, including bioreactor seeding, start-up and performance improvement, for OSPW treatment; and 2) to determine the optimal operational conditions for each component.

4.1 Moving Bed Biofilm Reactor

4.1.1 MBBR Design and Fabrication

The MBBR, the Component 1 in the bioreactor process train, serves as (1) exploration of proper seeding procedure for biofilm reactor for OSPW treatment, which would accelerate the start-up of MABR; (2) pretreatment for the chemical oxidation process, because MBBR can remove some easily biodegradable organics and reduce the alkalinity of OSPW, which will lower the required dosage of ozone; (3) seed source for MABR. This MBBR system was designed by me with help from my supervisor Dr. Tong Yu. It was fabricated by the machine shop in Department of Chemical and Materials Engineering in University of Alberta. The detailed design and related accessories like fittings, tubing and pump type was provided in Table A-1 in Appendix A. The design draft of MBBR is illustrated in Figure B-1 in Appendix B. The completed MBBR is shown in Figure 4-1.

The operational volume of MBBR reactor is 4.5 L. It is made of poly (methyl methacrylate), also known as acrylic glass. In Figure 4-1 (a), the two ports attached to the wall at the lower part

are the influent port and the sampling port. The opposite one at the lower part is used for introducing air into the reactor. Therefore, an air diffuser is connected to the inside port for aeration. There is a stainless-steel mesh inside the reactor for sludge separation, which can be slid out of the reactor for cleaning. The port at the upper part is the effluent port, which is larger than influent port to prevent water overflow. The slot on the removal cover of the reactor is used for adjusting the angle of mechanical mixer shaft (see Figure S-2 in Appendix B), which will supply the power for mixing to prevent packing material from floating inside the reactor.

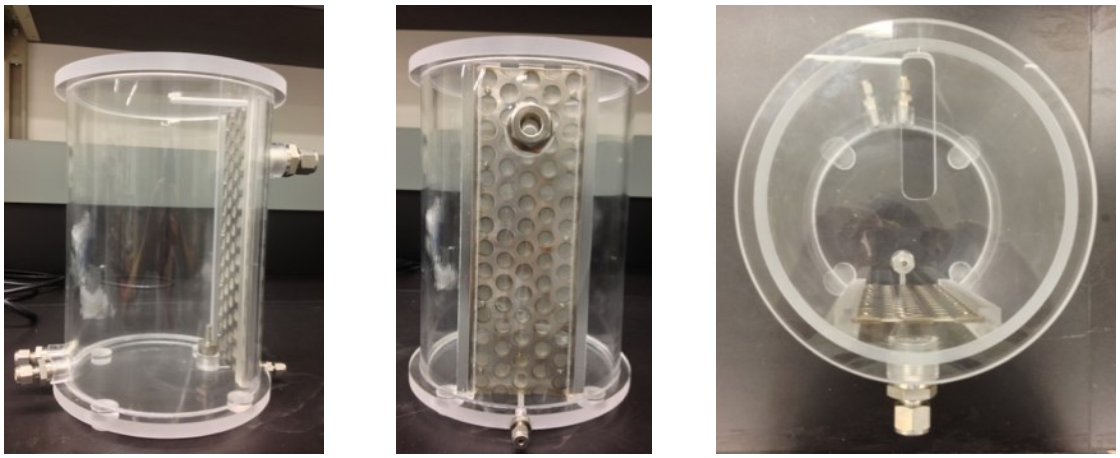

(a) (b) (c)

Figure 4-1 Three-view diagram of the MBBR: (a) front view; (b) side view; (c) top view

This MBBR contains the volume of packing material up to 50% of its empty bed liquid volume. There are two kinds of packing material inside the reactor: polyvinyl chloride (PVC) tubular black carrier and flat white Mutag Biochip^{TM} (Multi Umwelttechnologie AG, Germany) shown in Figure 4-2. The PVC carrier with an active surface area of 440 m^2/m^3 is used to supply surface for biofilm growth; the biochip carrier with an active surface area of more than 3000 m^2/m^3 is used to increase the biomass concentration inside the reactor.

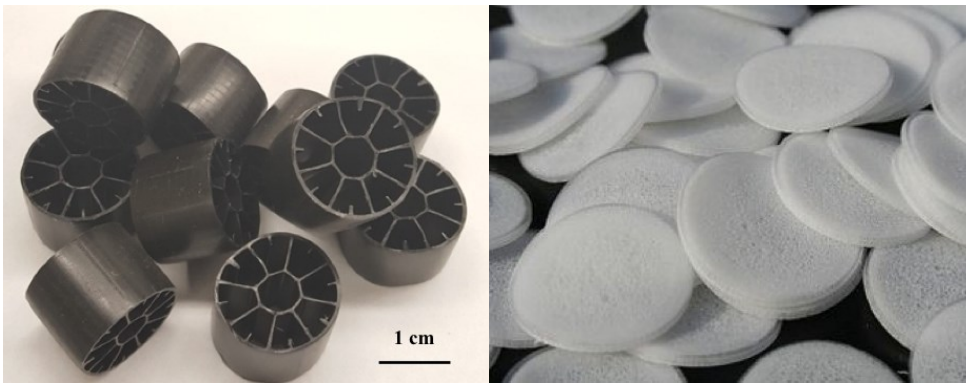

(a) (b)

Figure 4-2 Packing material in the MBBR: (a) PVC tubular packing material; (b) Mutag Biochip™

The MBBR system in the lab is shown in Figure 4-3. A 15 L plastic influent pail was stored in a walk-in cooler under 4℃. The influent was pumped by a peristaltic pump ⑩ into the MBBR reactor ③ from the inlet port ①. When the sample was collected from sampling port ②, the influent pump was shut down to avoid the interference from the coming influent. The influent rate was controlled by influent pump controller ⑧. The air was introduced from the air let ⑪, whose flow rate was controlled by a flow meter to make reactor bulk liquid phase under aerobic condition. The settling flask ⑥ was used to let sludge from effluent settle down, which lowered suspended solid concentration in the final effluent. The final effluent was stored in the effluent storage tank ⑨. The flow rate of the influent was manipulated by influent pump controller ⑧, which made the hydraulic retention time of the reactor change accordingly. Mechanical mixing rate was in the range of 90-120 RPM, depending on the sludge growth condition inside MBBR. It was controlled by the mixer controller ⑦.

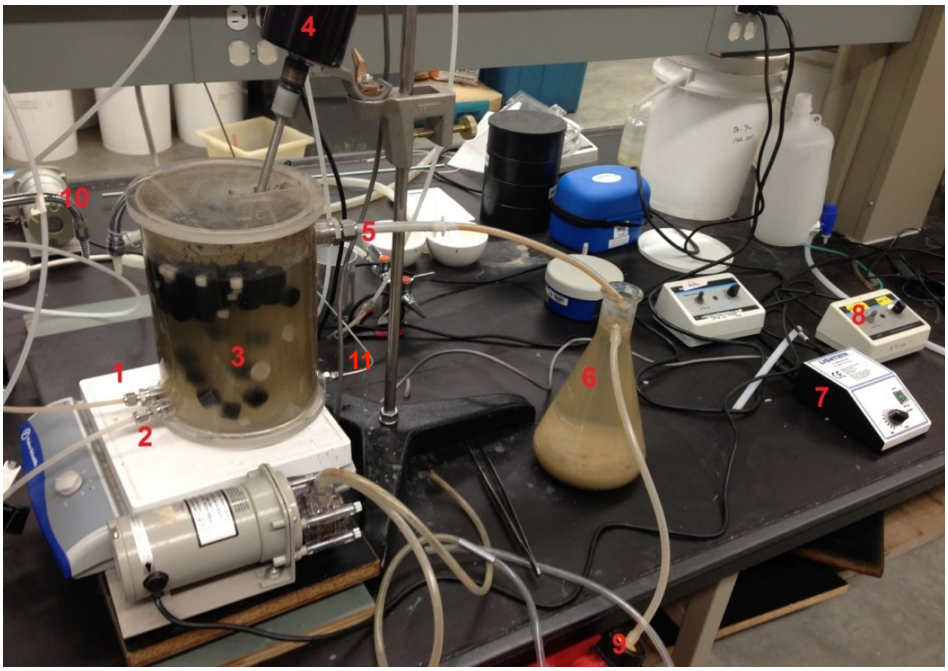

Figure 4-3 MBBR system: ① inlet; ② sampling port; ③ MBBR reactor; ④ mechanical mixer; ⑤ outlet; ⑥ settling flask; ⑦ mixer controller; ⑧ influent pump controller; ⑨ effluent storage tank; ⑩ influent pump; ⑪ air inlet

4.1.2 Materials and Methods

4.1.2.1 Influent Preparation for MBBR

In order to deal with the challenge of water quality fluctuation for bioreactor operation described in Chapter 1, a large quantity of raw OSPW is needed for influent preparation during the entire bioreactor operation. Due to limitations of reality, 1 m^3 of raw OSPW was obtained from a different tailings pond of the same Canadian oil sands company as mentioned in Chapter 2, which was able to support almost two and a half years' continuous operation for the bioreactors. After complete mixing, the OSPW was distributed into 20 L plastic pails and stored in the cold room at 4°C, which will further eliminate the interference of water quality fluctuation during the operation of bioreactors. The water quality of the OSPW is shown in Table 4-1. By comparing with the water quality in Table 2-1, it is found that pH, nitrogen, phosphorus, AEF

and COD concentration of these two OSPW are close to each other. It means that the sludge from CASR in Chapter 3 can be seeded for MBBR. However, the BOD concentration inside the OSPW for MBBR operation is much lower than that in Table 2-1, indicating that the biodegradability of OSPW for MBBR operation is even lower than that of OSPW used in Chapter 3. Considering the shortage of nutrients, raw OSPW cannot be used as influent of MBBR without any nutrient amendment.

Table 4-1 Water quality of OSPW for the MBBR operation

Item	Value
pH	7.9 ± 0.4
Alkalinity	501.3 ± 2.4 mg/L as $CaCO_3$
$NO_3^- + NO_2^-$	2.4 ± 0.2 mg N/L
NH_4^+	1.95 ± 0.14 mg/L
Total phosphorus	0.2 ± 0.1 mg/L
AEF	56.1 ± 2.3mg/L
BOD	2.1± 0.4 mg/L
COD	239 ± 7 mg/L

A growth medium R2 (Reasoner and Geldreich, 1985) was used to supply easily biodegradable carbon source for bacteria growth and to ensure nitrogen and phosphorus were not limiting nutrients. The composition of growth medium R2 is listed in Table 4-2. The influent of the MBBR was composed of raw OSPW and growth medium R2 with different volume ratio at different operational phases. Due to the addition of growth medium R2, the COD level of influent was much higher than that of raw OSPW. In this study, it was assumed that the portion of influent COD contributed by growth medium R2 was completely utilized by microorganisms inside bioreactor, which was not counted into the performance of bioreactor on OSPW treatment. Therefore, the COD removal mentioned in Section 4.1.3 referred to the percentage of COD removed from raw OSPW by calculation based on the removal performance shown in Figure 4-6.

Table 4-2 Composition of growth medium R2

Chemicals	Concentration (g/L)
Peptone	0.525
Yeast extract	0.35
Dextrose	0.35
Starch	0.35
KH_2PO_4	0.21
Sodium pyruvate	0.21
Tryptone	0.175
$MgSO_4$	0.0168

4.1.2.2 Water Quality Analyses

In this experiment, the influent and effluent of the reactor were collected every day at the seeding phase and when the operational conditions changed. When bioreactors performance was stable, samples of influent and effluent were collected every two days. After pH and DO measurement, samples were filtered through a 0.45μm nylon filter (Whatman) before performing COD and AEF analysis. Daily measurement of pH was performed with an Accumet® AR 20 pH/conductivity electrode (Cole-Parmer, IL, USA) connected to a digital pH meter (Orion 720A, Thermo Fisher Scientific Inc, MA, USA). DO was measured at 22℃ daily by an LDO 101 model dissolved oxygen electrode (HACH company, Loveland, CO, USA).

The closed reflux colorimetric method was used for COD analysis, which is a quick and reliable parameter for reactor performance monitoring (APHA, 2005). FT-IR spectroscopy was adopted for AEF analysis (BioRad, FTS-6000, Cambridge, MA, USA), which is the current industry standard employed by oil sands companies in the Athabasca oil region. Prior to FT-IR analysis, 30 mL sample was acidified to pH 2.0 and organics were extracted by liquid-liquid extraction with portions of dichloromethane (DCM) in a separatory funnel (Catalog No. 10-437-11E, Fisher Scientific Company, ON, Canada). After the separation, DCM was evaporated with

compressed air flow, leaving the extracted AEF in the glass tube. The extracted AEF was reconstituted with a known mass of DCM and subjected to FT-IR spectral analysis. Sample absorbance was measured at wave numbers of 1743 and 1706 cm^{-1}, which correspond to adsorption bands characteristic of monomeric and dimeric carboxylic groups, respectively (Clemente, et al., 2005). Fluka commercial NAs mixture was used as standards, whose information was illustrated in Section 3.2.1. Furthermore, recent studies (Ibrahim, 2018; Islam et al., 2014) suggest that AEF and COD can be used as surrogate parameters to monitor the performance of bioreactors on NAs removal due to the high correlation found between AEF and COD removals and NAs degradation. For sample analysis, duplicate tests of COD and AEF for each sample were conducted over the experiment duration.

All the other chemical analysis was done according to Standard Methods for Examination of Water and Wastewater (APHA, 2005).

4.1.3 Operation and Performance Evaluation

The MBBR system, which is shown in Figure 4-3, began to run on March 8, 2013. The operation of MBBR system lasted almost twenty-seven months. The experimental run was divided into three phases. Each phase served different purpose for MBBR operation and had different operational conditions due to the influent composition and HRT. Figure 4-4 shows the influent composition and HRT under each phase for MBBR.

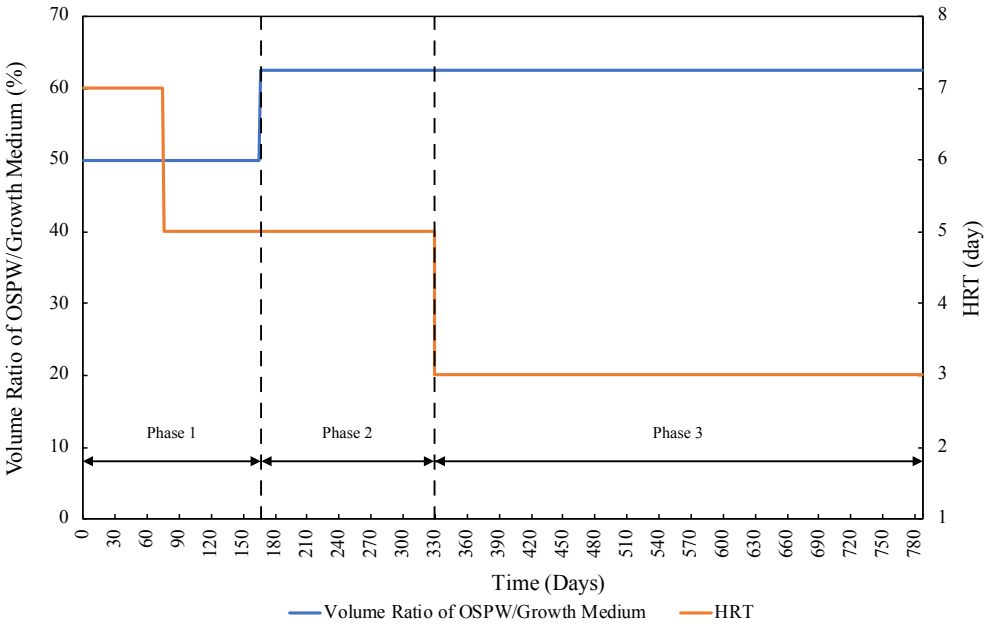

Figure 4-4 Influent composition and HRT of MBBR at different phases

In phase 1, the main objective was to successfully seed and grow bacteria attached on the carriers inside MBBR. The inoculums for seeding MBBR had three sources: indigenous bacteria extracted from MFT in the research work by Yu (2014), bacteria centrifuged from raw OSPW and activated sludge from the CASR in Chapter 3. The initial MLVSS concentration inside MBBR was around 3200 mg/L. The influent of the reactor was composed by raw OSPW and growth medium R2 with a volume ratio of 1:1. This synthetic influent could supply more easily biodegradable organics and make inoculum microorganism grow faster. pH and DO in the reactor were controlled at 7.5-8.0 and 2 mg/L, respectively. HRT of the reactor was set at 7 days based on preliminary results in Section 3.1 of Chapter 3. Mechanical mixing rate is in the range of 90-120 RPM to ensure packing material submerged in the bulk liquid.

The seeding period lasted about 45 days for biofilm growth on the PVC tubular carriers. To make biofilm attach and grow on the surface of the carriers, fill-and-draw procedure was repeated for the operation of the reactor at the start-up period. It simulated the operation pattern

of SBR described in Chapter 3. After 15 days, a thin layer of biofilm was observed on the inner wall of the carriers, which was shown in Figure 4-5 (a). Then the feed mode of influent was changed into continuous flow mode and the other operational conditions were maintained the same. One month later, the biofilm layer grew thicker (seen in Figure 4-5 (b)) and MLVSS concentration inside reactor increased to 4800 mg/L. When the MBBR had a stable COD removal efficiency, it was considered as the accomplishment of biofilm cultivation and proliferation. In order to increase the biomass concentration inside reactor, which is necessary and beneficial for increasing the organic loading in the next phase, MBBR continued to operate for another one month. The thickness of the biofilm increased to 1-2 mm (seen Figure 4-5 (c)), which was more condensed than that on Day 46. The MLVSS concentration inside reactor was almost 5500 mg/L. During the operation, there were also suspended sludge existed inside reactor. The average COD removal from OSPW was 17% when MBBR performance was stable, as shown in Figure 4-6.

(a) (b) (c)

Figure 4-5 Biofilm grown on the PVC carrier in the MBBR system at different time: (a) Day16; (b) Day 46; (c) Day 74

When the biomass condition inside MBBR was stable, the organic loading was increased to investigate the performance of MBBR. Then, the HRT was decreased from 7 days to 5 days during Day 77 to Day 166. The average COD removal of OSPW was 19%, which was a little higher than that in the seeding period. It meant that the MBBR developed the capacity to degrade

organic compounds inside OSPW even under a shorter time due to abundant biomass, which was one of the advantages for MBBR. In phase 1, it was found that the removal performance of AEF in MBBR shown in Figure 4-7 changed dramatically. The main reason was the fluctuation of influent water quality, which demonstrated the challenge and importance of constant influent water quality for biological treatment, especially for the start-up period. The more unstable AEF concentration in the influent gave more loading shock on the fragile engineered ecosystem built inside MBBR in the start-up period. More carefulness and attention would be involved in the influent preparation to avoid this issue.

In phase 2, in order to select bacteria which are capable to adapt harsher environment with high level of NAs and to testify the stability and performance of MBBR facing organic loading change, I lowered the portion of growth medium R2 and enlarged the portion of raw OSPW inside the synthetic influent. Considering the organic loading shock as the main factor leading to sudden failure of reactor in real applications, the volume ratio of OSPW and growth medium R2 inside the influent changed slightly from 1:1 to 5:3. The HRT was maintained at 5 days during phase 2.

It was found that COD removal dropped dramatically at the beginning of the changing. It took almost two months for the MBBR to reach the performance at phase 1 and maintain it afterwards, which illustrated that bioreactor operation conditions should change gradually to avoid the sudden performance deterioration. The average COD removal maintained around 21% when reactor performance was stable. It demonstrated that the MBBR exhibited great resistance to the adverse environment because MBBR can provide suitable microenvironment for specialized microorganisms to survive and utilize toxic organics, which will be investigated in Chapter 5.

In phase 3, the organic loading rate was increased further by shorting HRT to test the capacity of MBBR on OSPW treatment. From Day 331 to Day 788, the HRT of MBBR changed gradually from 5 days into 3 days to avoid organic loading shock for the MBBR. However, a noticeable decrease in the COD removal efficiency was still observed in the beginning. One month later, the COD removal was recovered to 23% on average and 35% alkalinity was reduced when the performance was stable. The COD and alkalinity of MBBR effluent was 115 ± 3 mg/L and 204 ± 9 mg/L as $CaCO_3$, respectively. The removal of COD would lower the dosage of oxidant added in the following chemical oxidation process. Because the radicals produced by oxidant added is nonselective (AWWARF, 1998) and can be exhausted by the organic or inorganic compounds present in OSPW other than NAs the concerned contaminants in this study. Both carbonate and bicarbonate as main portions of alkalinity will scavenge radicals to create carbonate radicals, which will lower the reaction rate with NAs. Therefore, MBBR, as the first operational component in the bioreactor process train, plays an important and necessary role as the pretreatment for the next chemical oxidation process for removing the easily biodegradable organics and some inorganics in OSPW.

Figure 4-7 shows AEF performance of MBBR during each phase. It was illustrated that MBBR could achieve 16% removal of AEF from OSPW at HRT 3 days. In comparison, Hwang et al. (2013) reported that a continuous flow biofilm reactor could remove 13.8% AEF in OSPW. In the research by Shi et al. (2015), 18.3% of AEF was removed from OSPW in MBBR. A batch study conducted by Han et al. (2008) suggested that the half-life for OSPW NAs was 44-240 days. The estimated half-life of residual recalcitrant organics in OSPW tailings pond that undergo slow biodegradation was 12.8-13.6 years (Han et al., 2009). With high NAs removal under such a short HRT, the MBBR in this study shows great capability for OSPW treatment.

Our long period MBBR operation proved that our seeding process was feasible to inoculate bacteria into bioreactor. Due to the biofilm diffusion limit, the concentration of chemicals inside and outside of the biofilm was different. This difference made some specialized microorganisms from the inoculum survive and utilize recalcitrant organic compounds from OSPW to grow up, which was verified by COD and AEF reduction during the entire operation. Comparing to months' or years' half-life of NAs degradation in tailings pond, the MBBR could achieve high and rapid NAs removal, which indicates the feasibility and effectiveness of biological process on OSPW treatment. At the end of operation, the COD and AEF concentration of MBBR effluent was 115 ± 3 mg/L and 32.8 ± 0.3 mg/L, respectively. MBBR could remove average 23% COD, 35% alkalinity, and 16% AEF from OSPW at HRT of 3 days. These promising results gave us more confidence to proceed to the next operational component, chemical oxidation process, to break down the remaining nonbiodegradable recalcitrant organics in the MBBR effluent.

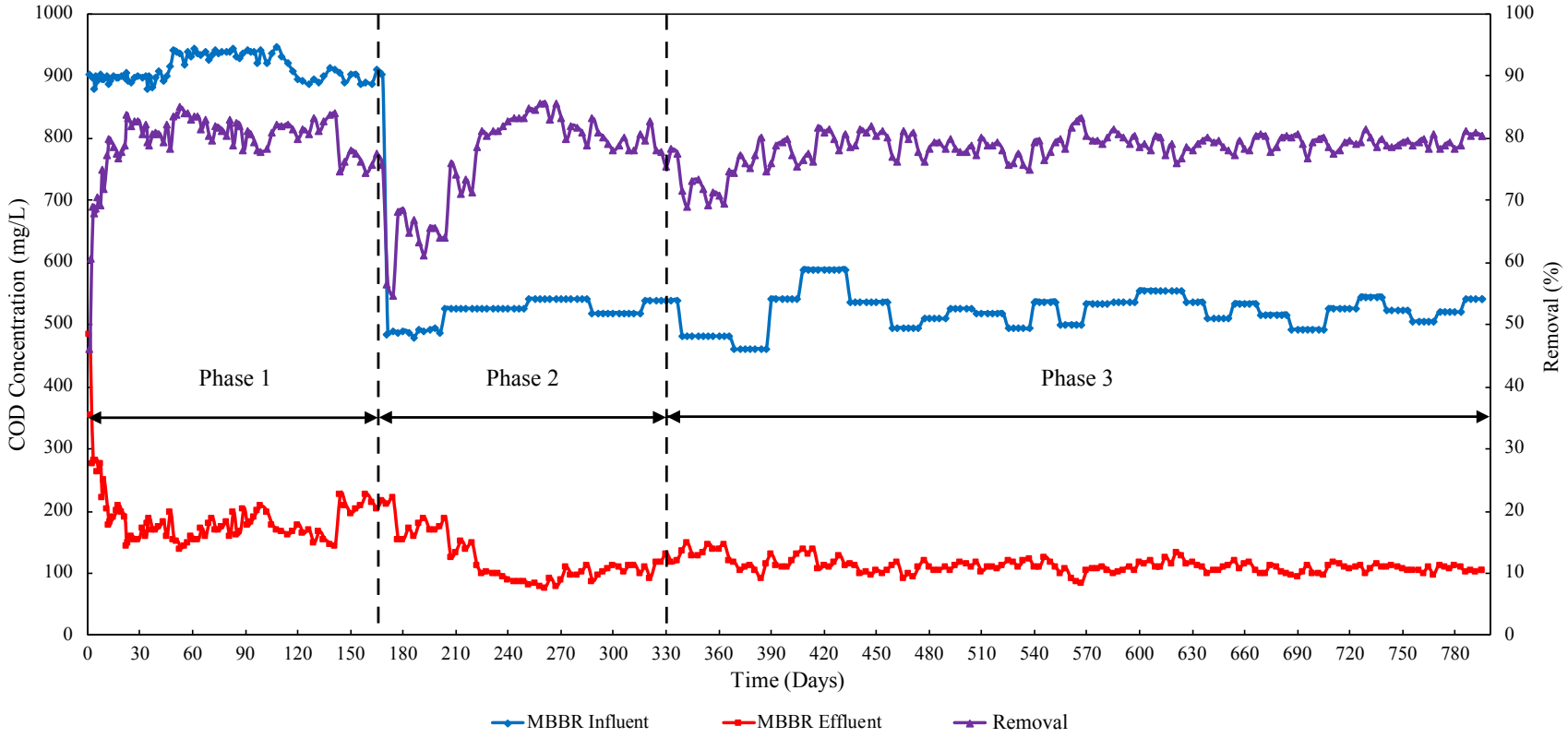

Figure 4-6 COD performance of MBBR during operation at different phases

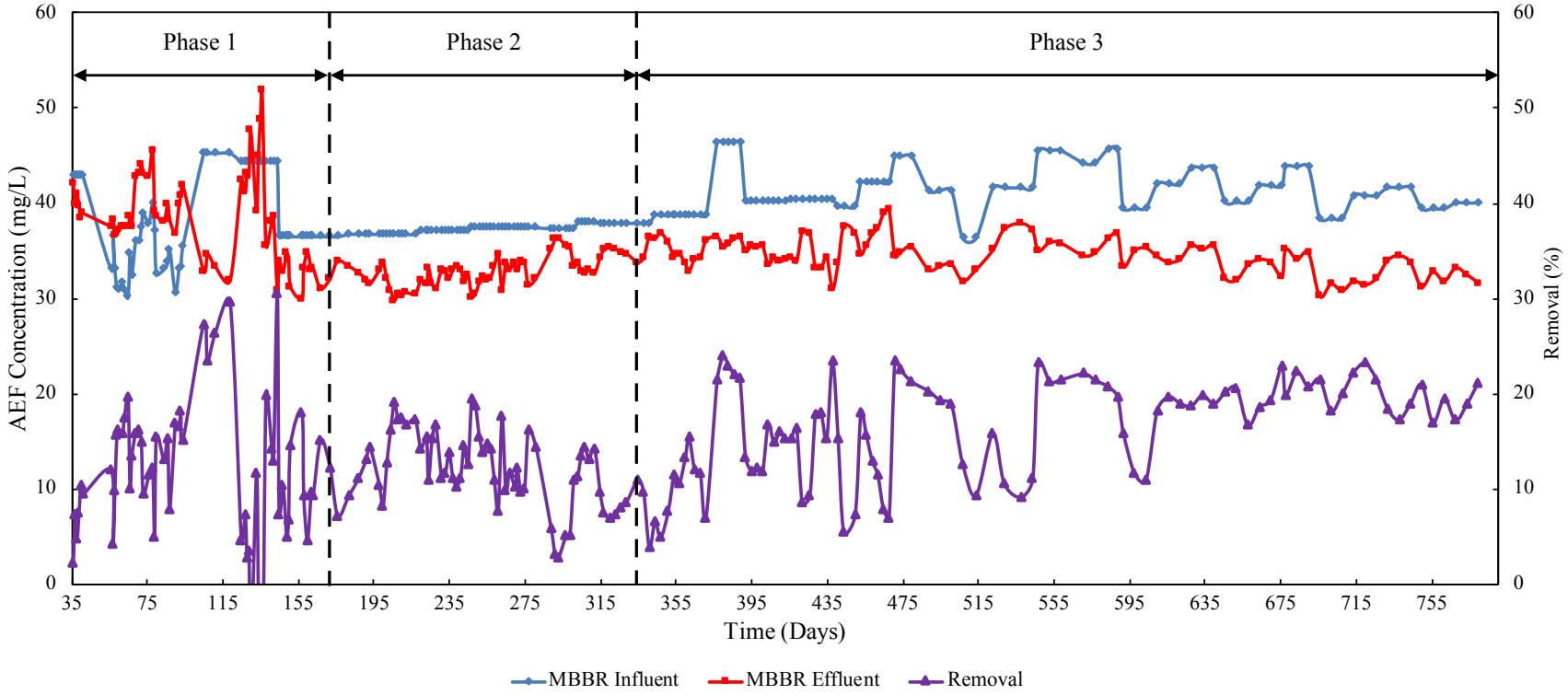

Figure 4-7 AEF performance of MBBR during operation at different phases

4.2 Chemical Oxidation Process

Chemical oxidation process, as the Component 2 in the bioreactor process train, was to decompose the residual recalcitrant organic compounds with complex structure in MBBR effluent into biodegradable organic compounds with simple structure, which would be removed by the following bioreactor. Ozone, as one of the strongest oxidants, was reported to be capable of breaking down highly branched and cyclic fractions of NAs efficiently in OSPW (Dong et al., 2015; Islam et al., 2014). Ozone will produce hydroxyl radical (•OH) and the superoxide radical (O_2•) after a complex chain of reactions when it is added to water (Hoigne, 1998). Those radicals are powerful oxidants for recalcitrant organics oxidation. In this research, ozone will be introduced for NAs decomposition and improving MBBR effluent biodegradability, which is regarded as the pretreatment for the MABR. Batch test was used to determine the optimal dosage of ozone in the following subsections.

4.2.1 Materials and Methods

In this experiment, MBBR effluent was the target water. The ozone generator was Absolute Ozone® ATLAS 30C, bought from Absolute Systems Inc., Edmonton, Canada. The ozone monitor was ATI Model Q45 (Analytical Technology Inc., Collegeville, PA, USA) and the dissolved ozone probe was A10-64-0536-1A (Analytical Technology Inc., Collegeville, PA, USA). COD and AEF analysis method were illustrated in the Section 4.1.2. BOD seed inoculum was POLYSEED® from InterLab™ (Spring, TX, USA) in BOD test. For each batch of samples, the glucose-glutamic acid check was included in BOD test. 6 mL of standard glucose-glutamic acid solution (150 mg/L glucose and 150 mg/L glutamic acid) was added into each of three 300 mL BOD incubation bottles. The average BOD value for the three bottles must fall into the range

of 198 ± 30.5 mg/L, which will make sure the accuracy and precision of the BOD test. For sample analysis, triplicate samples were taken and tested during the experiment.

4.2.2 Ozonation System Setup and Operational Procedure

The schematic drawing of the ozonation system in the lab is shown in Figure 4-8.

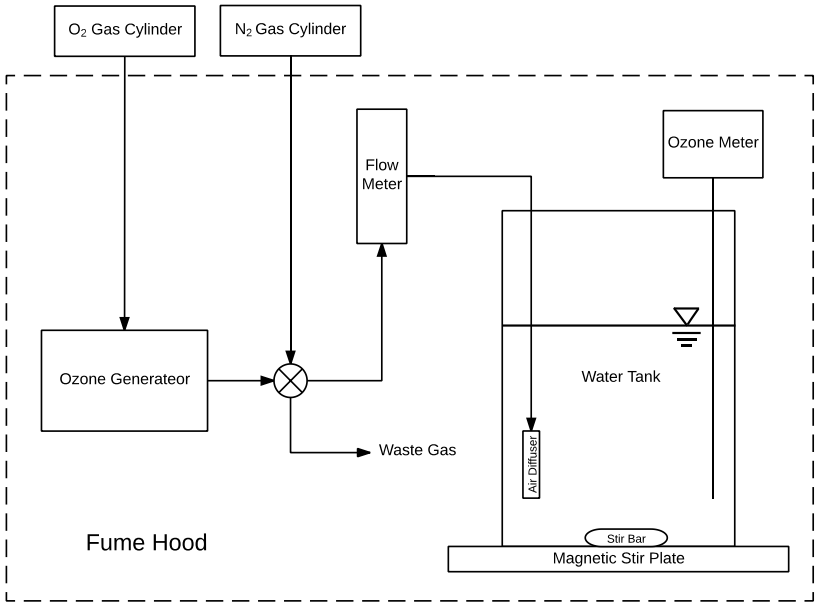

Figure 4-8 Schematic diagram of chemical oxidation system

The procedure of this ozonation system was as follows: 1) put the water tank filled with certain amount of MBBR effluent on the magnetic stir plate; 2) turn on the stir plate and set the speed of stir bar at 300 RPM; 3) turn the 3-way valve to "Waste Gas" direction, open the O_2 gas cylinder at 20 psi and let the O_2 flow through the ozone generator for 1-2 min; 4) turn on the ozone generator and set the "Ozone Output" at 80% and wait for 5 min to get the stable ozone generation; 5) set the flow meter rate at 2 liter per minute (LPM) and turn the 3-way valve to "Flow Meter" direction; 6) ozone generated was introduced into the water tank through air diffuser at the bottom of the water tank for certain time (determined by the following experiment); then turn 3-way valve into "Waste Gas" direction; 7) turn "Ozone Output" dial to

zero and switch off the generator; 8) wait for 5 min before turning off O_2 gas cylinder; 9) After a certain contact time (determined by the following experiment), purge N_2 into the water tank to get rid of the residual ozone until the reading of ozone meter was zero. The ozone concentration was monitored to determine the operation time for purging nitrogen to strip the residual ozone from the water tank. All the above operations were finished inside the fume hood to prevent from ozone exposure.

4.2.3 Batch Test Experiment for Optimal Ozone Dose

It is known that the effectiveness of ozonation highly depends on the ozone dose utilized. Low dose of ozone applied may not sufficiently break down the recalcitrant NAs in OSPW, while high dose of ozone applied will be very costly or even be harmful for biodegradation. In the research by Goi et al. (2006), oil contaminated sand and peat was treated by five hours' ozonation, which did not improve its biodegradability significantly. Amat et al. (2003) also demonstrated that the BOD value of phenolic wastewater during ozonation process would increase sharply at first and slowly decrease with further ozonation. Furthermore, the toxicity of by-products of ozonation may be even higher than that of the parent compounds. The study conducted by Ledakowicz et al. (2006) showed that the toxicity of ozonated resin acid solution would increase when the ozone dose applied was over the range 0.3-0.5 mg O_3/mg COD. From those studies, it is clearly that ozone dosage applied before MABR must be carefully determined.

In this batch test, 5 L Pyrex® bottle (Catalog number: 06-414-1F, Fisher Scientific Company, ON, Canada) was used as the water tank in the ozonation system. The volume of MBBR effluent tested in the bottle was 3.5 L. During the experiment, the amount of ozone generated was determined by the ozone generator performance provided by the manufacture, which is shown in the Figure S-4 in Appendix B. Based on the previous studies (Ledakowicz et

al., 2006; Hwang et al., 2013; Dong et al., 2015), there were five scenarios applied for this batch test, which were 30 seconds, 60 seconds, 90 seconds, 120 seconds and 150 seconds' operations. The ozone amount produced were 47mg, 94mg, 141mg, 188mg and 235mg, respectively. The control group was the MBBR effluent without ozonation. The contact time for ozonation was 5 min. The residual concentration of ozone in the water phase was measured by the ozone monitor. The ozone escaped from the bottle was introduced into 10 L ultra-pure water and measured by the ozone monitor. The applied ozone dosage was the produced ozone deducted the combination of residual ozone and escaped ozone and divided by the water tested volume, which was expressed in the following equation:

$$\Delta O_3 = \frac{M_{in} - M_{out}}{V_L} - C_R \qquad \text{(Eq. 4-1)}$$

where ΔO_3 is the amount of ozone applied (mg/L), M_{in} is the amount of ozone produced by the ozone generator during the operation time (mg), M_{out} is the amount of ozone escaped (mg), V_L is the volume of treated MBBR effluent (L), C_R is the residual ozone concentration in the liquid phase (mg/L).

4.2.4 Results and Discussion

In this batch test, the pH value of MBBR only changed slightly (from 7.9 to 8.2) in the last scenario with the highest ozone dose applied. It means the lower ozone dose has less impact on the pH value. The increase of pH value is due to the formation of OH^- caused by the direct reaction of ozone with some inorganic and organic compounds (Beltran, 2004), which existed in the MBBR effluent.

Table 4-3 summarizes the results of the five scenarios in the batch test. Based on Equation 1, the dose of ozone applied on each scenario were 13mg/L, 27mg/L, 35 mg/L, 44mg/L and 54

mg/L, respectively. It was found that the COD value of each scenario was lower than that of MBBR effluent after ozonation. The COD removal increased constantly as the ozone dose applied increased until the injection time of ozone over 90 seconds. After that, the COD removal was almost leveled up. Similar pattern was observed in AEF reduction during the ozonation process. However, the AEF removal was remarkable higher that the COD removal, which demonstrated the effectiveness of ozone on NAs decomposition, especially on carbonyl group (C=O) in NAs (Han et al., 2008). Some previous studies (Dong et al., 2015; Hwang et al., 2013) also reported the similar phenomenon. Although the smaller organic compounds converted can still contribute to COD, this portion of COD was biodegradable, which was proved by the increase of BOD/COD ratio (from 0.02 to 0.19). It indicates that ozonation can improve the biodegradability of MBBR effluent, which will be beneficial for the following biological treatment process.

Table 4-3 Results for the five scenarios of ozonation in the batch test

Scenario	COD (mg/L)	COD Removal (%)	BOD/COD Ratio	AEF (mg/L)	AEF Removal (%)	Ozone Dose Applied (mg/L)
Control	115 ± 3	0	0.03	32.8 ± 0.3	0	0
T_{30}	102 ± 2	11	0.12	28.9 ± 0.1	12	13
T_{60}	95 ± 3	17	0.14	23.0 ± 0.2	30	27
T_{90}	92 ± 1	20	0.19	18.7 ± 0.1	43	35
T_{120}	90 ± 2	22	0.18	18.4 ± 0.2	44	44
T_{150}	89 ± 3	23	0.19	17.4 ± 0.1	47	54

For the performance of ozonation on AEF reduction, almost 0.4 mg/L of AEF was degraded per mg/L of applied ozone dose when the ozone dose applied was lower than 35 mg/L, while 0.3 mg/L of AEF was oxidized per mg/L of applied ozone dose when higher ozone doses were utilized. Furthermore, the BOD/COD ratio did not change at the applied ozone dose higher than 35 mg/L. These results were consistent with the study by Gamal El-Din, M. et al. (2011), in

which the ultimate ozone dose of 25 mg/L. Therefore, the optimal ozone dose applied in MBBR effluent was 35 mg/L based on the batch test. Accordingly, when I prepared 20 L of MBBR effluent for ozonation, the operational conditions are as follows: 8 min for ozone injection; 20 min for reaction contact time; and 20 min for purging nitrogen to strip the residual ozone.

4.3 Membrane Aerated Biofilm Reactor

In the proposed bioreactor process train, MABR, as the Component 3, was seeded by the sludge from the MBBR to degrade the decomposed organic compounds in MBBR effluent by ozonation process. As illustrated in Chapter 2, the main difference between MBBR and MABR is the biofilm structure, which is known as 'co-diffusional biofilm' and 'counter-diffusional biofilm', respectively (Nerenberg, 2016). Due to this counter diffusion of electron donor and acceptor, microbial community structure developed in the biofilm of MABR is unique, which will bring in more functions for MABR. Previous research has demonstrated that simultaneous nitrification and denitrification can be achieved in MABR (Nerenberg, 2016). In this section, a lab scale MABR was designed, fabricated and operated to investigate its performance on OSPW treatment. The chemical profile and microbial community in the biofilm of MBBR and MABR will be illustrated in Chapter 5.

4.3.1 MABR Design and Fabrication

Considering the operation of the entire bioreactor process train when it is built up, the operational volume of MABR was designed to be 4.6 L, close to that of MBBR. The MABR is made of acrylic glass, whose structure is two cuboids connected together. Figure 4-9 shows the picture of MABR in the lab. The lower cuboid is the working zone for biodegradation while the upper cuboid is used for preventing water from getting out when purging nitrogen to manage biofilm accumulation. The reason for biofilm control in MABR is that flux in counter-diffusional

biofilm will increase up to a point and decrease as the biofilm thickness increases further (Martin and Nerenberg, 2012). Good management of biofilm accumulation is necessary and important to maintain the performance of MABR during operation. A stainless-steel tube with tiny holes near the bottom of MABR is designed for purging nitrogen to meet this requirement.

As mentioned in the beginning of this section, hollow fiber made of gas-transferring membrane is the key part in the MABR. I contacted one Japanese company named NAGAYANAGI Co. LTD to fabricate a hollow fiber membrane module based on our design, which is the white part inside the reactor shown in Figure 4-9. In the membrane module design, the hollow fiber is operated in flow-through mode, in which the distal end is open and the gas is continually introduced. Dead-end membranes mostly are utilized for combustible or expensive gases, like methane and hydrogen (Martin and Nerenberg, 2012). Also, flow-through mode can avoid gas back-diffusion, which can significantly dilute the supply gas and consequently decrease the performance of MABR. For this MABR, high oxygen concentration throughout the entire membrane is needed for the biodegradation of OSPW. Flow-through mode can serve this purpose better than dead-end mode although it has greater consumption of gas and energy and more pressure losses during operation (Martin and Nerenberg, 2012).

The size of the hollow membrane module is 400 mm L × 15 mm W × 200 mm H, which is made of silicone rubber. The inner and outer diameters of fiber are 200 μm and 360 μm. The permeability of different kinds of gases is shown in Table S-2 in Appendix B. There are 4 pieces of membrane modules inside the reactor. The membrane area of each module is 0.38 m^2, which means the specific surface area (330 m^2/m^3) is very high. The schematic graph of the membrane module is shown in Figure 4-10.

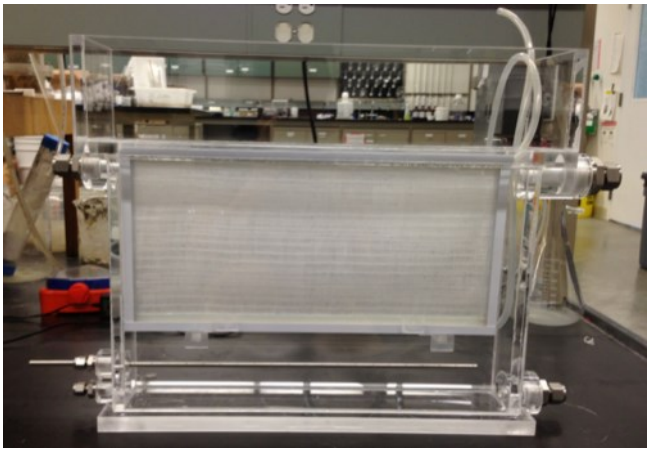

Figure 4-9 Picture of MABR with hollow fiber membrane module (white)

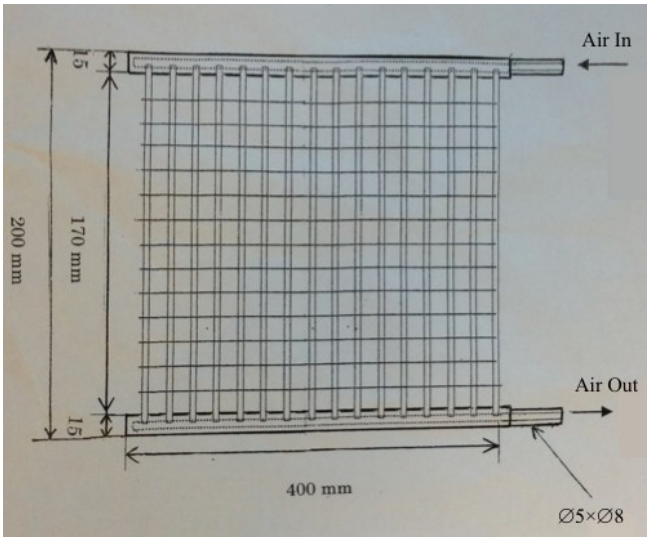

Figure 4-10 Schematic graph of the hollow fiber membrane module

The detailed design of the MABR is shown in Figure B-2 in Appendix B. The accessories in the MABR are listed in the Table A-1 in Appendix A. The MABR fabricated by the machine shop in the Department of Chemical Material Engineering at the University of Alberta based on my design.

The MABR system in the lab is shown in Figure 4-11. A 20 L plastic influent pail was stored in a walk-in cooler under 4°C. The influent was pumped by a peristaltic pump into the MABR ⑪ from the inlet port ①. The water flowed out from outlet port ② and was stored in

the storage bottle ③. The MABR was completely mixed by internal recycle using the recycling pump ⑤ from port ④ to port ⑥. The compressed air was introduced into the hollow fiber membrane module through inlet tubing ⑧ to support biofilm growth while the extra air was released from outlet tubing ⑨. The port ⑩ was used for sampling. The nitrogen was introduced from port ⑦ for biofilm accumulation control periodically. The reactor was covered by foil to prevent algae growth due to the light.

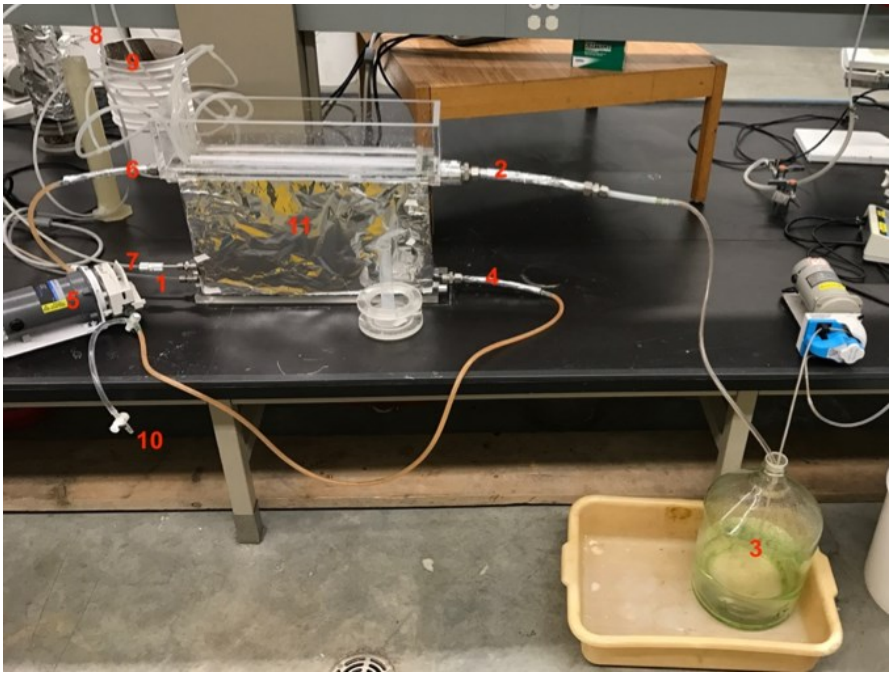

Figure 4-11 MABR system: ① inlet; ② outlet; ③ effluent storage tank; ④ internal recycle outlet; ⑤ recycling pump; ⑥ internal recycle inlet; ⑦ nitrogen inlet; ⑧ compressed air inlet; ⑨ compressed air outlet; ⑩ sampling port; ⑪ MABR reactor

4.3.2 Materials and Methods

4.3.2.1 Influent Preparation for MABR

Although the biodegradability of MBBR effluent increased after ozonation, there was still shortage of nutrients and carbon source for the operation of the MABR. Therefore, the addition of growth medium R2 is necessary for the MABR system as well. The influent of the reactor was composed by the ozonated MBBR effluent and growth medium R2 with different volume ratio at

different operational phases. The details of the volume ratio were described in Section 4.3.3. The same method described in subsection 4.1.2.1 was applied on the evaluation of MABR performance on COD and AEF removal due to growth medium addition for influent preparation.

4.3.2.2 Water Quality Analyses

All the operational monitoring parameters and related testing methods were the same as those illustrated in subsection 4.1.2.2.

4.3.3 Operation and Performance Evaluation

The MABR system was started on Feb 8, 2014 when MBBR system performance was stable after one year's operation. The operation of MABR system lasted fourteen months, which was divided into two phases according to operational conditions. Figure 4-12 shows the operational conditions under each phase for the MABR.

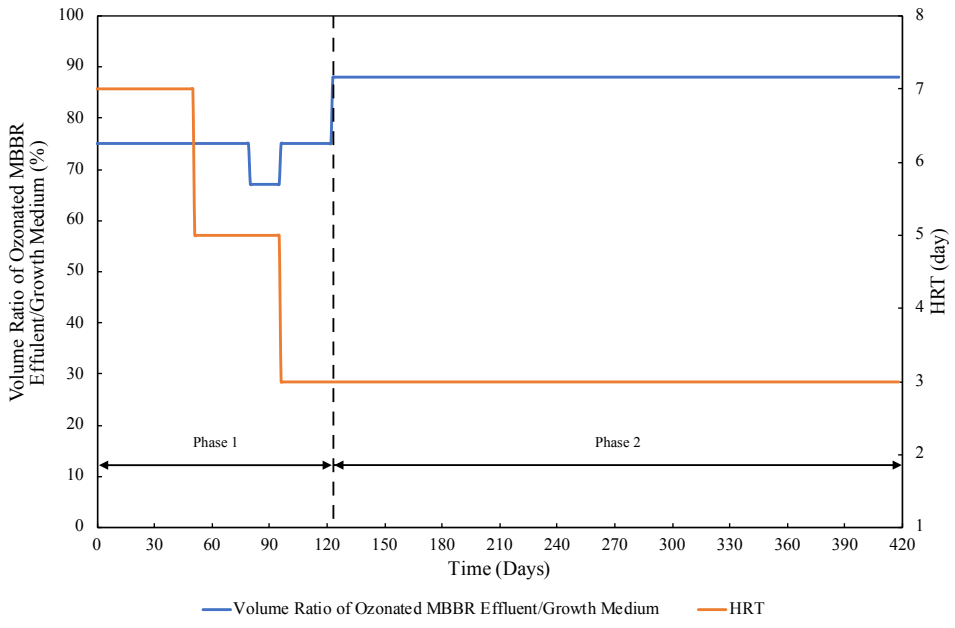

Figure 4-12 Influent composition and HRT of MABR at different phases

In phase 1, the MABR reactor start-up phase, the main purpose was to get the seeding bacteria from MBBR attached and grown on the membrane, which is the white part shown in

Figure 4-9. Bacteria centrifuged from raw OSPW and suspended sludge from MBBR were used as the inoculums for seeding MABR. The influent of the reactor at this phase was composed of ozonated MBBR effluent and growth medium R2 with a volume ratio of 3:1, which will supply sufficient nutrients for inoculum microorganism growth. pH for the influent was in the range of 7.6-7.9. The compressed air in the membrane hollow fiber was maintained at 20 psi to supply oxygen for the attached biofilm during the operation. In order to let inoculated microorganism to attach on the membrane quickly and evenly, a complete mixing generated by internal recycle was applied in the MABR. The HRT was 7 days at the seeding phase. After 15 days' operation, the state of biofilm formation inside MABR was shown in Figure 4-13. Most of the inoculum microorganism was attached on the membrane module and a little suspended sludge settled at the bottom of the reactor.

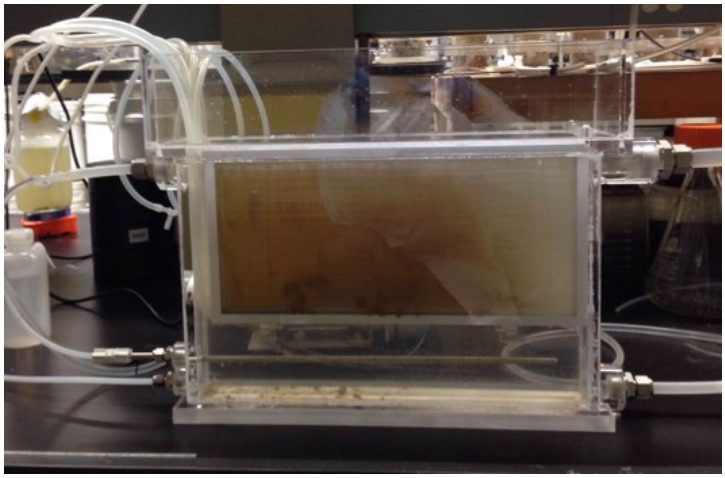

Figure 4-13 The state of biofilm formation inside MABR after 15 days' seeding period

After 50 days' operation, the performance of the MABR was stable with 28% of COD removal, which meant the seeding process was finished. During the seeding period, the unique operational feature of MABR different from that of MBBR was the application of nitrogen

sparging when the reactor performance deteriorated. Those arrows in Figure 4-14 and 4-15 indicate the applications of nitrogen sparging during operation.

Due to the continuous operation with MBBR system, the HRT of MABR would be the same as that of MBBR. Therefore, the HRT of MABR should decrease gradually to 3 days with the flow rate at 1.5 L/day when the whole process train was completely built up.

From Day 51 to Day 79, the HRT of MABR changed from 7 days to 5 days. On Day 51, some deterioration of MABR performance on COD removal was observed like what happened in MBBR. It was recovered after one week. The average COD removal was maintained the same level as before and the biomass inside the reactor increased as the organic loading increased due to short HRT. From Day 80 to Day 95, the portion of growth medium R2 increased from 1/4 to 1/3, which helped the biofilm grow faster to compensate biofilm loss due to a false nitrogen sparging happened on Day 77, which is shown as the red arrow in Figure 4-14. At that time, I realized that the control of biofilm accumulation with careful operation was critical for maintaining MABR performance. When the performance of MABR returned to the stable state, the average COD removal was 37% and AEF removal was 19% (shown in Figure 4-15). From Day 96 to 122, the HRT changed further, from 5 days to 3 days, to match the HRT of MBBR. When the performance of MABR was stable, the COD and AEF removal were 38% and 20%, respectively, at HRT 3 days.

In phase 2, I wanted to investigate the feasibility of MABR for treating OSPW with a higher NAs concentration than that in phase 1. The volume ratio of ozonated MBBR effluent and growth medium R2 changed from 3:1 to 7:1, which means the increase of selection pressure for microorganisms inside MABR due to higher recalcitrant organic compounds existed in the influent. In the first month of the phase 2, the performance of MABR deteriorated and more

biomass was founded at the bottom of the MABR. It indicated that the detachment of biofilm happened inside the MABR. In the study by Liu and Tay (2001), the detachment of biofilm inside MABR is complicated, which varies with biofilm structure, detachment force and environmental conditions. In my case, the biofilm detachment was due to the low organic loading and the increase of toxicity of influent. Therefore, biomass limitation is the reason for low removal performance in the MABR. Fortunately, there was no large biofilm pieces found during that period, which meant no total biomass loss inside the MABR under that harsh environment. It was a disaster if it happened.

As the operation continued for the next two months under closely monitoring, the performance of MABR recovered finally and reached a stable state. The average COD removal and AEF removal were 44% and 24%, respectively, which were even higher than each of those in phase 1. The final COD and AEF concentration were 63 ± 5 mg/L and 10.7 ± 1.2 mg/L accordingly. The detachment of biofilm caused by low organic loading and more toxic environment might make the thickness of biofilm thinner. Base on the Fick's law that is the most commonly utilized to determine the mass transfer coefficients of substances in biofilm (Liu and Tay, 2001), thinner biofilm has a higher diffusivity for substances transfer. As a result, the counter diffusion rate of electron donor and acceptor was improved, which made the performance of MABR increase. This observation emphasized again the importance of biofilm accumulation control in the operation of MABR. Furthermore, microorganism with long generation time accumulated in the biofilm and was protected from serious loss due to long SRT in MABR as mentioned in Chapter 2, which would be illustrated in the microbial community analysis presented in Chapter 5.

In the previous studies, Shi et al. (2015) reported that MBBR inoculated by activated sludge from municipal wastewater treatment plant could remove 14.5% of AEF from ozonated OSPW at HRT 48 h. The ozone dose was 30 mg/L. In the research by Huang et al. (2015), two integrated fixed-film activated sludge (IFAS) reactors, which were seeded by activated sludge from a municipal wastewater treatment plant, could remove 12.2% of COD and 15% of AEF from ozonated OSPW with ozone dose of 30 mg/L. The HRT of the IFAS reactor was 48 h. With a higher ozone does at 80 mg/L, a continuous biofilm reactor reported by Choi et al. (2014) could remove 48% of COD and 51% of AEF from ozonated OSPW at HRT 19 h. The membrane biofilm reactor reported by Xue et al. (2016a) had no substantial removal of COD but achieved 41.8% of classical NAs from ozonated OSPW with ozone does of 30 mg/L. Comparing with those above results, the performance of MABR on ozonated OSPW treatment was competitive.

The promising results indicated that microorganisms inside MABR adopted to the harsh environment and were able to utilize the decomposed organic compounds in the ozonated MBBR effluent as growth substrate. The control of biofilm accumulation with careful operation is critical for optimal MABR performance due to the counter-diffusional biofilm structure. Due to long SRT, MABR can capture some specific microorganisms with long generation time, which will be beneficial for OSPW remediation. In Stage 4, the structure and microbial community inside biofilm will be investigated to explain the performance of MBBR and MABR, which will be described in Chapter 5.

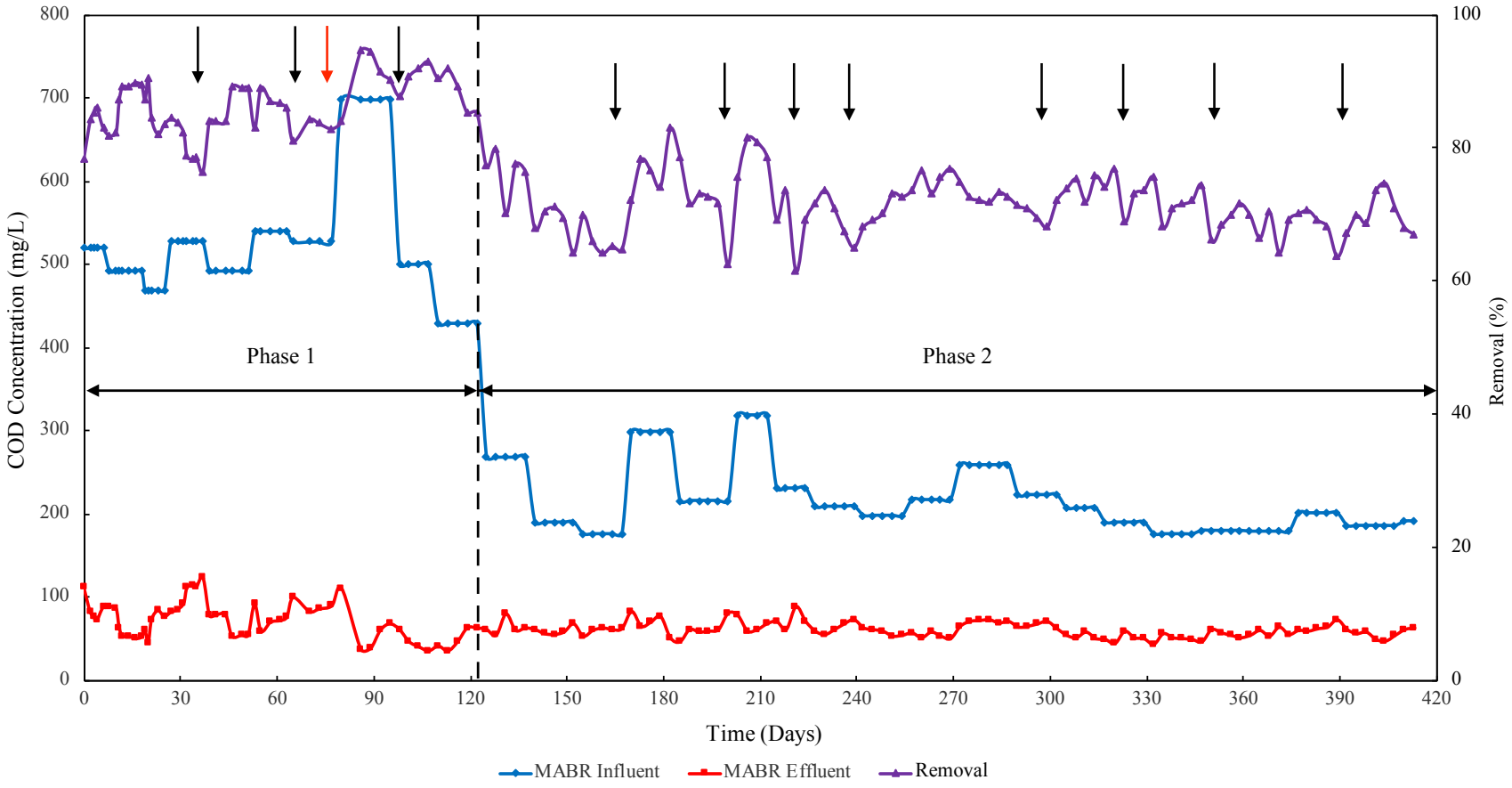

Figure 4-14 COD performance of MABR during operation at different phases

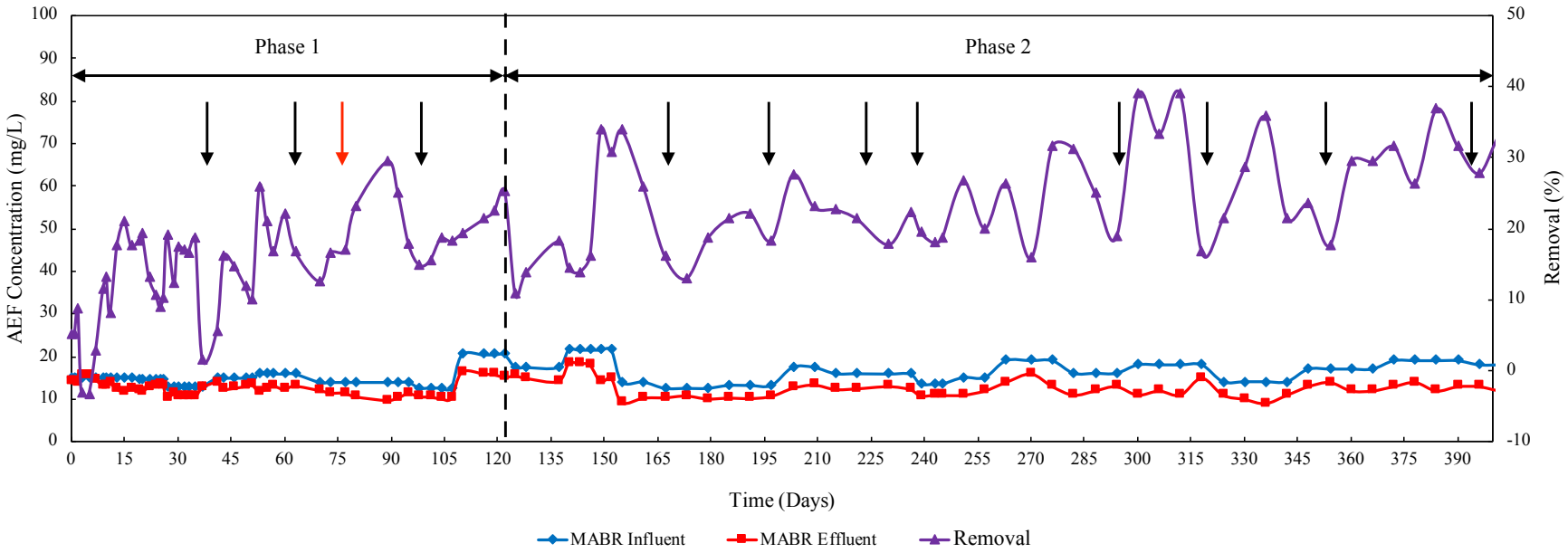

Figure 4-15 AEF performance of MABR during operation at different phases

4.4 Adsorption Process

Adsorption process, the last component of the process train, is widely used in water and wastewater treatment for the purpose of controlling trace hazardous organic compounds (Crittenden et al., 2012). Since there is no widely-accepted safe OSPW discharging limit, the remaining NAs in the MABR effluent were still a concern, although the concentration was much lower than that in raw OSPW after biological and chemical oxidation process. Therefore, an adsorption process was applied to polish the MARB effluent and further improve the water quality of the final effluent. In this section, granular activated carbon (GAC) column was investigated due to its high treatment efficiency and operational convenience.

4.4.1 Materials and Methods

4.4.1.1 Source Water

The adsorption experiments were conducted with MABR effluent. The effluent contains 58 ± 5mg/L of COD and 10.4 ± 0.5mg/L of AEF.

4.4.1.2 Adsorption Isotherm

Adsorption isotherms describe how much adsorbate can be caught by adsorbent at a specific temperature when equilibrium is reached, and they are useful in revealing affinity mechanisms between certain adsorbate and adsorbent. We define C_e as equilibrium aqueous phase of adsorbate (mg/L), V as volume of aqueous (L), C_0 as initial aqueous phase of adsorbate (mg/L), and M as the mass of adsorbent (g). q_e (mg/g), which denotes equilibrium adsorbent-phase of adsorbate, is calculated using Eq. 4-2 (Crittenden et al., 2012):

$$q_e = \frac{V}{M}(C_0 - C_e) \qquad \text{(Eq. 4-2)}$$

An adsorption isotherm can be obtained when we plot q_e vs. C_e.

Langmuir model (Eq. 4-3) and *Freundlich* model (Eq. 4-4) are commonly used to normalize GAC isotherms (Crittenden et al., 2012):

$$q_e = \frac{q_m \cdot K_L \cdot C_e}{1 + K_L \cdot C_e} \quad \text{(Eq. 4-3)}$$

$$q_e = K_F \cdot C_e^{1/n} \quad \text{(Eq. 4-4)}$$

where q_m (mg/g) is the maximum adsorbent-phase concentration of adsorbate when surface sites are saturated with adsorbate. K_L (L/mg) is *Langmuir* adsorption constant of adsorbate. K_F (mg/g)·(L/mg)$^{1/n}$ is *Freundlich* adsorption capacity parameter. 1/n is *Freundlich* intensity parameter, unitless.

For the *Langmuir* model, it assumes that the adsorbed layer is one molecular thick and all sites are equal. It is applicable for modeling adsorption that occurs on homogeneous surface sites. For the *Freundlich* model, it assumes that the adsorption capacity is different at different sites due to energy distribution. It is applicable for modeling adsorption that occurs on heterogeneous surface sites (Cengeloglu et al. 2002).

NORIT™ 12-40 mesh GAC (ACROS Organics™) was used in this experiment. Adsorption isotherm was determined based on EPA GAC isotherm protocol (Dobbs and Cohen, 2002). GAC was firstly powdered with a clean pestle and mortar to allow pass a 230-mesh sieve and was then washed with boiling ultrapure water for 1h. After being washed, it was dried in an oven at 105ºC for 24h and stored in a desiccator until use. To establish equilibrium, accurately weighted amounts of pretreated GAC (0.0050–0.0500 g/L) were continuously and vigorously mixed with MABR effluent in a 25 RPM rotating tumbler for 8 days at 21.1ºC. The mixing of carbon and effluent was in 300 mL bottles that filled with headspace free in order to prevent the volatizing

of organics and the inference of air. Equilibrium COD concentration in each bottle was tested with standard method (APHA, 2005).

4.4.1.3 Column Experiments

In order to have a well-designed adsorption column, some important parameters needed to be determined such as empty bed contact time (EBCT) and breakthrough time. Adsorbate in the fluid needs to travel a certain distance before being adsorbed, and that specific length in the column is defined as mass transfer zone (MTZ) (Crittenden et al., 2012). MTZ will keep moving towards the end of the column, and the adsorbate at the front of MTZ will eventually show up at the effluent. The time point when effluent concentration exceeds treatment target is defined as breakthrough time (t_{bk}). After breakthrough happened, effluent concentration will increase sharply within a short time period. The time when effluent concentration is same as influent concentration is defined as exhaustion time, because all carbon is saturated and the GAC bed cannot remove contaminants any more.

EBCT is used as a measure of how much contact occurs between particles, such as activated carbon, and water as the water flows through a bed of the particles (Crittenden et al., 2012). As the EBCT increases, the time available for adsorbent to adsorb adsorbate from the water also increase, as does the amount of adsorbate removed from the water during its transition through the bed. It equals the volume that occupied by adsorbent media divided by flow rate. For removal of soluble organic compounds from water, the range of EBCTs in fixed-bed adsorption processes often varies from 5 to 30 min for GAC (Crittenden et al., 2012).

If the MTZ is short, the GAC column will be completely saturated when the adsorbate reaches the end of the column. A simple mass balance in the column can be derived as follows:

$$Q \cdot C_{\text{inf}} \cdot t_{\text{bk}} = M_{\text{GAC}} \cdot q_{einf} \qquad \text{(Eq. 4-5)}$$

where Q is flow rate of the column, (L/d); C_{inf} is the adsorbate concentration in the influent, mg/L; t_{bk} is breakthrough time, d; M_{GAC} is the mass of GAC in the column, g; and q_{einf} is adsorbent-phase of adsorbate concentration when it equilibrates with the influent concentration, mg adsorbate/ g adsorbent.

Thus, theoretical breakthrough time can be calculated with the following equation:

$$t_{bk} = \frac{M_{GAC} \cdot q_{einf}}{Q \cdot C_{inf}} \quad \text{(Eq. 4-6)}$$

The same flowrate of bioreactors process train, 1.5 L/day, was used to ensure a synchronous operation. A Cole-Parmer peristaltic pump (Catalog No. S-77800-60, Fisher Scientific Company, ON, Canada) was used to maintain the flowrate. Down-flow pattern was used to avoid potential carbon expansion and floatation of fine carbon particles (U.S. Army Corps of Engineers, 2001). To ensure a stable effluent flowrate, effluent tubing was lifted above the upper surface of GAC bed. Fig 4-16 is a schematic of GAC adsorption column applied in this experiment.

Due to no regulation on OSPW discharge, the water quality of effluent after adsorption would be as best as it can be achieved. Furthermore, the flow rate of influent for GAC column is very low (1.5 L/d). Typical adsorber velocities range from 5 to 15 m/h (Crittenden et al., 2012). Therefore, two GAC columns with EBCT of 30 min and 300 min were tested to determine the optimal one for this adsorption process. Concentrations of COD and AEF were tested to evaluate performances of the adsorption columns. The test method of COD and AEF was the same as those were described in Section 4.2.1.

Table 4-4 shows main properties of two GAC columns. I also tested COD concentration of the 30 min EBCT column effluent every week to develop its breakthrough curve.

Table 4-4 Main properties of two GAC columns

Items	30 min EBCT column	300 min EBCT Column
Bed height(cm)	14.0	32.0
Column diameter(cm)	2.5	4.8
Cross section(cm^2)	4.91	18.09
Mass of GAC (g)	15.0	150.0

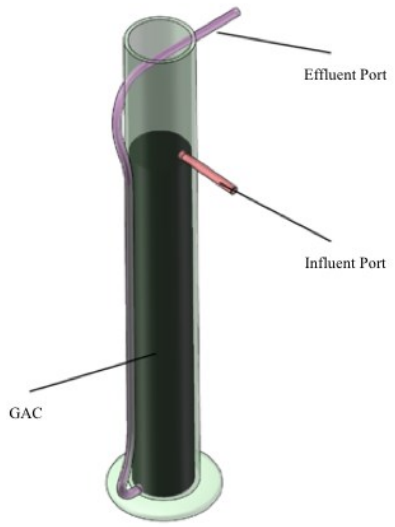

Figure 4-16 Schematic of GAC adsorption column

4.4.2 Results and Discussions

4.4.2.1 Isotherm

As shown in Figure 4-17, COD concentration was used to plot adsorption isotherm. The *Langmuir* and *Freundlich* isotherms models were used to fit the experimental data of the COD adsorption isotherms. The corresponding adsorption parameters were determined and are displayed in Table 4-5. For COD adsorption by GAC, the experimental data is in better agreement with the *Langmuir* model than *Freundlich* model. The correlation coefficient (R^2) is 0.98 for the *Langmuir* model, which suggests that the adsorption of COD onto GAC can be attributed to monolayer adsorption. Fitting results display a relatively high adsorption capacity (K_F=403.4mg COD/g GAC, q_m=833.3mg COD/g GAC) and a high intensity of adsorption (n=5).

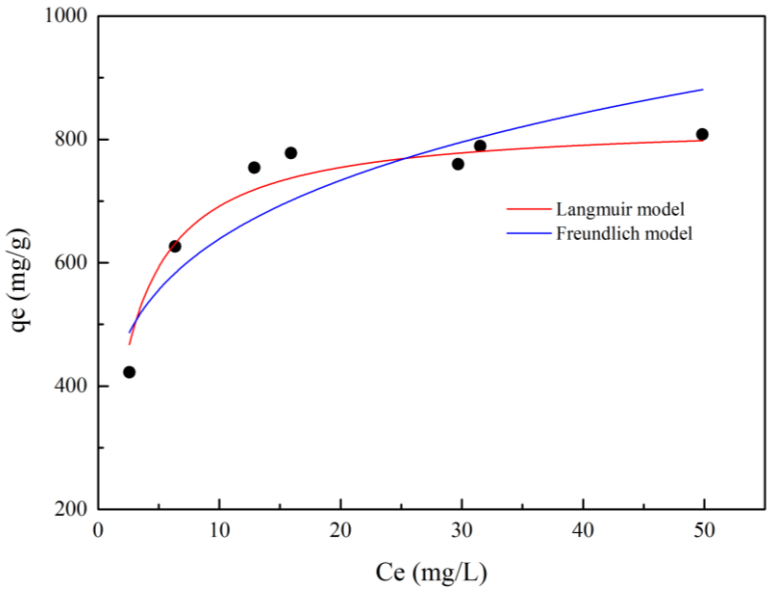

Figure 4-17 Adsorption isotherm of COD in MABR effluent onto GAC at 21°C

Table 4-5 Characteristic parameters of two adsorption isotherm models

***Freundlich* model**			***Langmuir* model**		
K_F (mg/g)	n	R^2	q_m (mg/g)	K_L (L/mg)	R^2
403.4	5.0	0.82	833.3	0.5	0.98

4.4.2.2 Performance of GAC Columns

Table 4-6 is a summary of the performances of two columns. Effluent COD concentrations were both 17 mg/L. 79% of COD removal was achieved, which indicated the high effectiveness of adsorption process on COD removal. In the study by Islam et al. (2015), GAC adsorption process was applied to treat OSPW with an optimal dose of 0.4 g GAC/L OSPW. The GAC adsorption could remove 31.1% of COD from raw OSPW and 30.7% of COD from ozonated OSPW with utilized dose of 20 mg/L after 28 days' batch test. Regardless of the different target OSPW, the big difference of non-adsorbable portion of COD between the study of Islam et al. (2015) and this experiment indicated that GAC adsorption process would be more effective as the post-treatment of OSPW or ozonated OSPW. It indirectly demonstrated the rationality and feasibility of the proposed bioreactor process train for OSPW treatment in this research.

AEF concentrations in two adsorption columns effluent were 3.1 mg/L and 2.6 mg/L, respectively. The removal performances of two columns are 71% and 76%, accordingly. Scott et al. (2008) suggested that effective FT-IR detective limit was 1 mg/L and FT-IR detection tended to overestimate NAs concentrations when the concentration was below 10 mg/L. Moreover, based on several previous studies on bioreactor for OSPW treatment (Hwang et al., 2013; Huang et al., 2016; Islam et al., 2014), the AEF removal was higher than that of COD removal under the same operational condition. Therefore, AEF concentrations in the effluent from both two adsorption columns might be very low.

Table 4-6 Performance of two GAC adsorption columns

	Item	30 min EBCT column	300 min EBCT column
COD	Concentration (mg/L)	17	17
	Removal (%)	79	79
AEF	Concentration (mg/L)	3.1	2.6
	Removal (%)	71	76

When the performances of two columns are compared, it is clearly shown that COD and AEF removals are almost the same. Thus, 30 min EBCT was chosen for this study. If EBCT is much lower (i.e. 10 min), the volume of adsorption column will be excessively small considering the small flow rate of treated MABR effluent. In that case the breakthrough time will be too short to make operators renew GAC frequently. If EBCT is too long, the column will be unnecessarily large, which would cause a waste energy and materials. As a result, I chose to build a GAC column with 30 min EBCT.

4.4.2.3 Theoretical and Tested Breakthrough Time

According to Eq. 4-6, q_{einf} was needed to calculate the theoretical breakthrough time. *Langmuir* model was chosen to estimate q_{einf} based on the result in subsection 4.4.2.1. Thus, the theoretical breakthrough time obtained was 138 days. Figure 4-18 was the breakthrough curve of

the GAC column with 30 min EBCT. It was shown that breakthrough happened at approximately 85 days. Here are two possible reasons for the difference between theoretical and tested breakthrough time. The first possible cause might be the existence of mass transfer zone, which means breakthrough happens before all GAC bed in the column is saturated. The second possible cause is that actual q_{einf} might be lower than the value estimated by *Langmuir* isotherm. Since GAC used in isotherm test was powered with pestle and mortar while GAC used in column was filled without grinding. The effective adsorption area (per gram GAC) in the column might be lower than that used in isotherm test. Therefore, GAC with small diameter utilized in the adsorption process will expand the operational life until breakthrough.

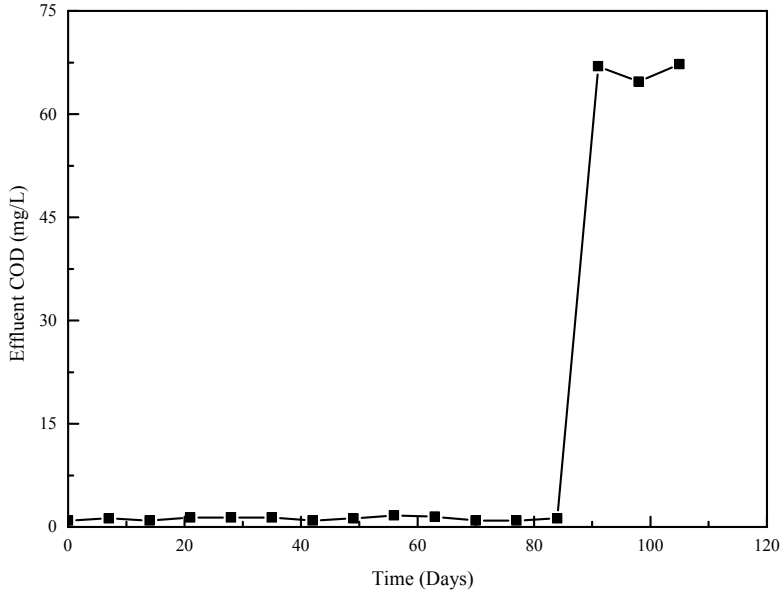

Figure 4-18 Breakthrough curve of the GAC column with 30 min EBCT

From the above analysis, it was found that GAC adsorption column was highly effective on removing COD (79%) and AEF (71%) from the MABR effluent. The COD concentration of the effluent after adsorption was as low as 17 mg/L with 85 days of breakthrough time, which demonstrated the necessity and rationality of adsorption process in the entire bioreactor process train.

4.5 Performance Evaluation of the Process Train and Conclusions

After two years' continuous, careful operation and thousands of troubleshooting, each operation component in the bioreactor process train finally reached a stable state. The stable performance of each component in the entire process train was evaluated and shown in Figure 4-19.

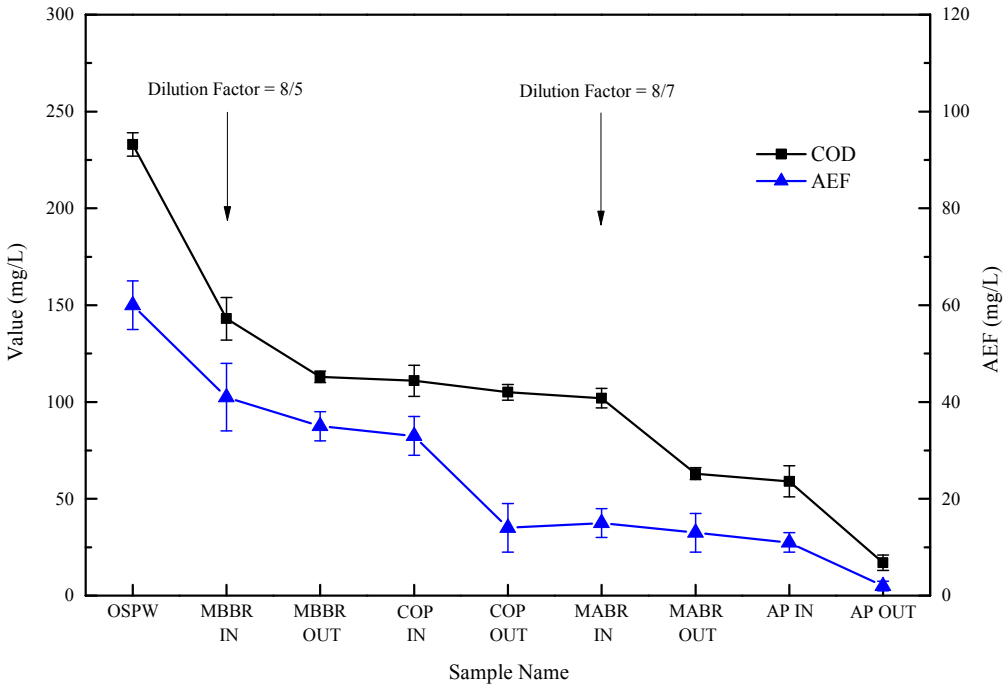

Figure 4-19 Performance evaluation of each operational component when the process train was at stable state

From Figure 4-19, it was illustrated that MBBR could achieve 23% of COD removal and 16% of AEF removal from raw OSPW. For chemical oxidation process, COD decreased from 111 to 105 mg/L while AEF concentration decreased from 32.1 mg/L to 16.2 mg/L. The dosage of ozone at stable state was 35 mg/L. Based on the results shown in Figure 4-20, it was clearly demonstrated that BOD increased from 3 mg/L to 19 mg/L after ozonation, which proved that ozonation was efficient on increasing the biodegradability of MBBR effluent and facilitating the further treatment of OSPW on MABR. The removals of COD and AEF in MABR were 44% and

24%, respectively, which were both higher than those of MBBR. The BOD of the MBBR and MABR effluent were both very low, which demonstrated that biological treatment had a certain capacity of removing recalcitrant organic compounds in OSPW with growth medium addition under alkaline environment. The residual COD inside MABR effluent could be further removed by GAC adsorption process, achieving 79% of COD and 71% of AEF removal. The COD of final effluent was 17 mg/L and AEF of the final effluent was as low as 2.9 mg/L. Therefore, Adsorption process is useful and efficient on elimination of residual non-biodegradable chemicals in MABR effluent, which will be beneficial for OSPW final discharge in the future.

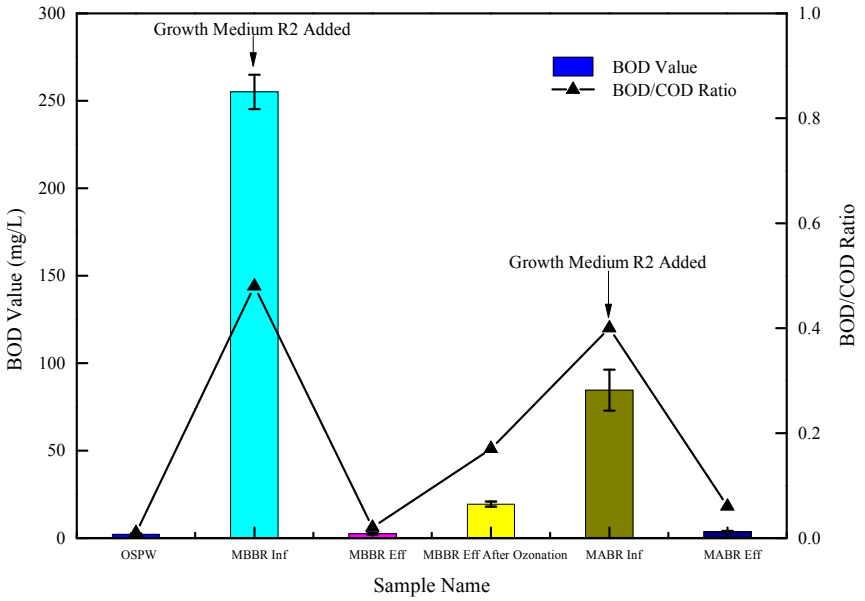

Figure 4-20 BOD value and BOD/COD ratio of each operational component when the process train was at stable state

Based on the above results, the process train combining bioreactors with chemical oxidation and adsorption process was a feasible treatment approach for OSPW treatment, which provided a solution for minimizing environmental and health impacts associated with the recycle and safe release of treated OSPW in the future.

CHAPTER 5 STAGE IV - Microbial Activity and Community Analysis of Biofilms in the Bioreactors

In this chapter, the main focus is to investigate the internal structure and microbial community of the biofilm inside the bioreactors when the performance of the bioreactor process train was stable. It is also the task of Stage 4 in the research approach described in Chapter 1. Microsensor and molecular biological techniques were applied in this Stage. These findings about biofilm internal structure and microbial community analysis inside biofilm provided a better understanding about the performance and function of bioreactors on OSPW treatment, which will further demonstrate the feasibility of the established bioreactor process train in this study and help to optimize engineered bioreactors for OSPW treatment in the future.

5.1 Background

The microsensors are needle-shaped biochemical sensors with a tip diameter of 1-100 μm, which can measure the chemical profiles in microbial communities (Okabe et al, 2011). There are two types of electrochemical microsensors used in this study: (1) amperometric microsensors, including O_2 and H_2S microsensors; (2) potentiometric microsensors. Liquid membrane ion-selective microsensors are the examples of potentiometric sensors, such as NO_3^- and pH microsensors. The working principles for different type of electrochemical microsensors are different. For amperometric microsensors, it measures the current resulting from the electrode reactions, which is proportional to the concentration of electroactive reactants (Revsbech, 2005). For potentiometric microsensors, it measures the membrane potential as a function of ion concentration (Lewandowski and Beynal, 2007). Taking pH microsensor for example, a straight-line calibration curve can be plotted as the potentiometric response of pH microsensor versus logarithms of the H^+ concentrations in a series of standard solutions. The concentration of H^+ in

the unknown sample can be calculated from the calibration curve based on the potential measured by pH microsensor. Generally speaking, amperometric microsensors have longer lifetime and better selectivity but shielding needed for eliminating interference. For potentiometric microsensors, they have shorter lifetime but easier for fabrication (Lewandowski and Beynal, 2007).

Microsensor techniques have been successfully used to determine *in situ* metabolic activities in microbial communities because they are able to probe and quantify the local chemistry at microenvironment with high spatial resolution (Revsbech, 2005). In the last two decades, the remarkable heterogeneity of biofilms has been revealed based on their composition, structure, and *in situ* activity (de Beer et al., 1994). Microsensors have been developed to measure the chemical gradient within a biofilm, which can illustrate the microscale heterogeneity within a biofilm. Taking oxygen distribution in a biofilm for example, it was typically reported that a steady decrease oxygen concentration could be observed as the microsensor progressed from the bulk liquid above the biofilm into the biofilm depths. Oxygen can be consumed by the microorganisms in the upper layer of biofilm, which is called as oxic zone and has dimensions of tens to a few hundred micrometers as mostly reported.

Recently, microsensor techniques were utilized to illustrate concentration gradients of metabolic substrates and products in many studies of wastewater biofilms. Those profiles of metabolic substrates and products will help researchers learn more about the organization and regulation of important metabolic processes inside biofilm. In the study of Revsbech and Jorgensen (1986), microsensors was applied in microbial environments and the potential relevance of microsensor techniques to microbial ecology was addressed. For nitrification process, de Beer *et al*. (1997) applied nitrite, nitrate and oxygen microsensors to illustrate the

conversion of ammonium to nitrite and nitrite to nitrate along the depth of biofilm. It revealed that both nitrification and denitrification occurred simultaneously in a biofilm. Zhang and Bishop (1996) studied the effect of pH and substrate on nitrification in a biofilm sample using pH, ammonium, nitrate and oxygen microsensors. It demonstrated that substrate composition had a great effect on the microbial community and pH change inside the biofilm. Those findings were useful for researchers to better understand the nitrification process in biofilms. For sulfate reduction process, Yu and Bishop (2001) investigated the stratification of sulfate reduction processes by using the oxidation-reduction potential (ORP) and sulfide microsensors on an aerobic and sulfate reducing biofilm. It was observed that aerobic oxidation took place in a surface layer of the biofilm and sulfate reduction occurred in the deeper anoxic zone. For ORP profile inside the biofilm, there was a sharp decrease happening near the interface between aerobic zone and sulfate reduction zone. In the study of Tan and Yu (2007), the production of H_2S in the anoxic zone of the biofilm inside a MABR measured by H_2S microsensor demonstrated the occurrence of active sulfate reduction activity. Furthermore, simultaneous microbial processes including nitrification, denitrification, sulfate reduction, and the stratification of these processes in the biofilm was investigated by a set of microsensors such as oxygen, ORP, nitrate, pH, ammonium and H_2S microsensors (Liu, 2015; Tan, 2012; Yu, 2000). Those above studies demonstrate that microsensor as a useful tool can help us to visualize and understand the function and internal structure of biofilm, which will be beneficial for optimizing bioreactor operation.

Molecular biological techniques can be used to identify specific microbial populations that cannot be detected by traditional microbiology techniques of isolation and cultivation. Comparing with the Sanger sequencing as the first commercialized DNA sequencing techniques,

next-generation sequencing techniques are high-throughput and have robust, low noise data (Buermans and den Dunnen, 2014). It includes Illumina sequencing, Roche 454 sequencing, Ion torrent: Proton™/PGM™ sequencing and SOLiD (Sequencing by Oligonucleotide Ligation and Detection) sequencing (Buermans and den Dunnen, 2014). They have already been widely applied to investigate the distribution of microbial community and functional diversity in the biofilm.

For the analysis of microbial diversity, sequencing data from 16S rRNA genes amplified from environmental samples are used. Firstly, similar 16S rRNA sequences were clustered into operational taxonomic units (OTU) after quality checking. Microbials assigned in one OTU are considered to be from the same taxon (Edgar, 2003). Then, alpha and beta diversity analysis were conducted based on the OTU aligned by certain software platforms, including mothur (https://mothur.org/wiki/Main_Page), Quantitative Insights Into Microbial Ecology (Qiime; http://qiime.org) and Ribosomal Database Project (RDP; http://rdp.cme.msu.edu/). Alpha diversity defines the diversity of microbial community within one sample while beta diversity defines the diversity of microbial community between several samples. The number of OTUs, Chao 1 and Shannon index can be used to measure α diversity. Principal coordinate analysis (PCoA) is performed to investigate the correlation among microbial communities from different samples, which was one of analysis for measuring β diversity.

For OSPW treatment, it was found that NAs can be degraded by indigenous microorganisms in oil sands tailings ponds (Han et al., 2009). However, the estimated time for *in situ* biodegradation of NAs in tailings ponds could be decades (Han et al., 2009). Therefore, the application of engineered bioreactors will be necessary for accelerating the biodegradation process for OSPW reclamation. Recent studies including this study have demonstrated the

capacity of bioreactors inoculated by indigenous microorganisms to accelerate the biodegradation of NAs in OSPW (Choi et al., 2014; Clemente et al., 2004; Han et al., 2008; Holowenko et al., 2001; Hwang et al., 2013; Islam et al., 2013; Xue et al., 2016b). Based on the published studies, the phylum *Proteobacteria* is commonly found to be the dominating microbial consortium in bioreactors for treating OSPW (Xue et al., 2018). Several microbial species like *Rhizobiales*, *Pseudomonads* and *Flavobacterium* have been reported to have the capacity of degrading organic compounds in OSPW (Headley and McMartin, 2004; Xue et al., 2016b; Xue et al., 2017). In nitrification process, ammonia oxidizing bacteria (AOB) involved can generate ammonia monooxygenase (AMO) enzyme, which are able to degrade aliphatic and aromatic hydrocarbons (Chang et al., 2003). In denitrification process, Gunawan et al. (2014) found that NAs removal coupled with denitrification was two times faster than that under aerobic conditions. However, in the study of Misiti et al. (2013), it was reported that commercial NAs were not degraded by denitrifiers but by aerobic heterotrophs. For sulfate reduction process, Clothier and Gieg (2016) reported that simple surrogate NAs could be biodegraded under anoxic condition with sulfate amendment. It was also found that sulfate reduction was driven by complex NAs in OSPW, in which an increase in the relative abundance of the genera *Desulfobulbus* and *Desulfomicrobium* were observed.

With the application of molecular biological techniques, it will be feasible for us to investigate the shift of bacterial communities under different bioreactor operational conditions and to qualify and quantity those functional bacteria groups. Combining the related chemical profiles by microsensor, the linkage between related functional bacteria groups and functions performed by bioreactors could be established, which will be beneficial for the design and operation of bioreactors in the future. In this study, the molecular biological technique Illumina

MiSeq sequencing combined with a set of microsensors were at the first time utilized together to investigate the chemical profiles and the distribution of microbial community inside the biofilm from MBBR and MABR for OSPW treatment.

5.2 Chemical Profiles inside Biofilms from MBBR and MABR Measured by Using Microsensor Techniques

In this section, biofilms from MBBR and MABR were studied by using a set of microsensors including pH, ORP, NO_3^-, O_2 and H_2S microsensors to get the corresponding profiles, which are related to biological processes existed in the biofilm such as nitrification, denitrification and sulfate reduction process.

5.2.1 Microsensors and Microsensor Measurements

Microsensors applied in this research are electrochemical microsensors which are divided into amperometric and potentiometric microsensors. The amperometric microsensors include combined O_2 microsensor and combined H_2S microsensor. The potentiometric microsensors include pH, NO_3^- and ORP microsensors.

Combined O_2 microsensor (OX-10) with a tip diameter of 10 μm, combined H_2S microsensor (H_2S-25) with a tip diameter of 25 μm and Picoammeter (PA2000) used in this study were bought from Unisense (http://www.unisense.com), Denmark. Before measurement, the O_2 microsensor was polarized according to the method described in the study by Tan (2012). The calibration was conducted by using nitrogen gas (0% O_2) and compressed air (21% O_2, DO = 8.90 mg/L at 21°C), which is suitable for the measuring range in this study. The calibration curve is shown in Figure C-1 (a) in Appendix C. For the H_2S microsensor, the calibration curve was obtained by plotting a serial dilution (0 to 500 μM) of H_2S standard solution at pH 8.0 versus current (Tan and Yu, 2007), which is shown in Figure C-1 (b) in Appendix C.

Liquid membrane ion-selective microsensors such as pH and NO_3^- consist of an ion-selective electrode with liquid membrane and a half-cell reference electrode with liquid junction (Tan, 2012). The membrane solution for pH and NO_3^- microsensors are commercially available: Hydrogen ionophore I - cocktail B (Catalog No. 95293, Fluka, Sigma-Aldrich, Canada) for pH microsensor. Nitrate ionophore - cocktail A (Catalog No. 72549, Fluka, Sigma-Aldrich, Canada). In this study, pH and NO_3^- microsensors with a tip diameter of about 15 μm were fabricated and calibrated by following the method described by Tan (2012). The calibration curves for each liquid membrane ion-selective microsensor could be found in Figure C-1 (c) and (d) in the Appendix C.

ORP microsensor is used to measure the potential drop between the working electrode and the reference electrode when both electrodes are immersed in the same solution. The fabrication and calibration of ORP microsensor was detailed described in the study by Tan (2012). Figure C-1 (e) shows the calibration curve of ORP microsensor used in this study. The slopes of both curves are 0.99 and 0.98, respectively, which are quite close to the theoretical value of 1.00. It means the quality of ORP microsensor is good. The tip diameter of the ORP microsensor in this study was around 15 μm.

When each of the bioreactors reached steady state, biofilm was taken out of the bioreactor and placed into a measuring setup in which the condition of biofilm was as close as possible to that in the operational bioreactor. An illustration of microsensor measurement setup in the lab is shown in the following Figure 5-1. The measuring setup for each bioreactor will be described in the Section 5.2.2.

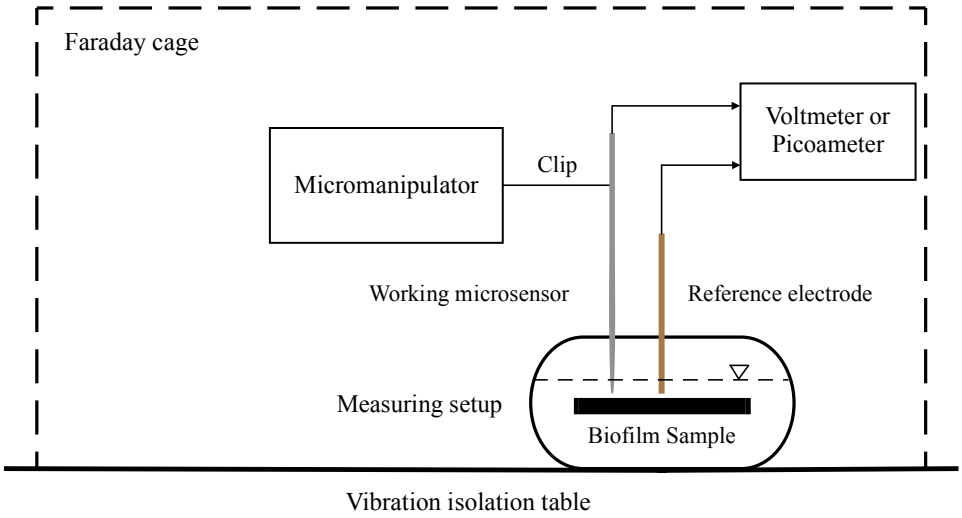

Figure 5-1 An illustration diagram of microsensor measurement setup

Each microsensor was calibrated with the procedure described in those above paragraphs before and after the measurements. The measuring setup with biofilm inside was placed on a vibration isolation table (TMC^{TM} Vibration Control, MA, USA) to avoid the interference by vibration on measurement. All measurements were conducted inside a Faraday cage to reduce the electrical noise. During measurements, each microsensor was mounted on a micromanipulator (Model M3301R, World Precision Instruments, Inc., Sarasota FL, USA). The microsensor tip was advanced into the biofilm placed in the measuring setup. When the tip touched biofilm surface, the microsensor penetrated the biofilm by moving the micromanipulator at the interval of 50 μm. The movement was viewed through a horizontal dissection microscope (Model: Stemi SV11, Carl Zeiss, Jena, Germany). An illuminator was used to enhance the view of movement area. A zero reading in the biofilm was the same as the reading in the N_2-saturated water for O_2 microsensor and in H_2S-free water for the H_2S microsensor. For pH, ORP and NO_3^- measurement, a commercially purchased Ag/AgCl micro-reference electrode (Catalog No. MI-409, Microelectrodes Inc., USA) was used as the separate reference electrode. For O_2 and H_2S

measurement, there was no separate reference electrode because the reference electrode was combined into the microsensor (i.e., combined microsensor).

In order to link the performance of bioreactors and chemical profiles in the biofilms illustrated by microsensors, water samples from bioreactors were taken simultaneously with the collection of biofilm samples. The concentration measurement of nitrate nitrogen, ammonium nitrogen, nitrite nitrogen and sulfate were conducted by ion chromatography (IC). In this chapter, total nitrogen (TN) was defined as the sum of nitrate nitrogen, ammonium nitrogen and nitrite nitrogen. The IC test of each sample was conducted in duplicate.

5.2.2 Results and Discussion

5.2.2.1 Chemical Profiles in Biofilm from MBBR

For MBBR biofilm measurements, one piece of packing material was taken out of MBBR when the performance was stable. It was cut into half and held in a petri dish filled with solution from MBBR. During the measurement, DO concentration was maintained 2-3 mg/L and pH value was 7.5-8.0 in the bulk water, which were the same as the operational conditions in MBBR.

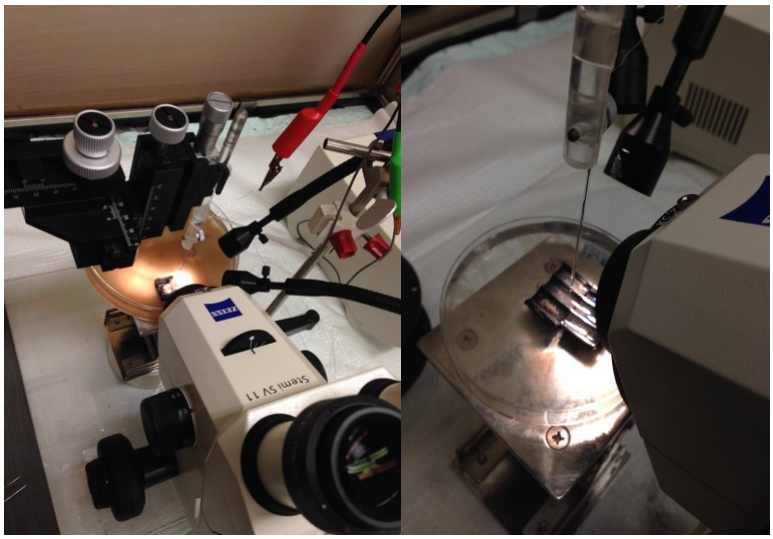

Figure 5-2 Pictures of microsensor measurement setup for MBBR biofilm

Figure 5-2 shows part of the set up for microsensor measurements. The red electrical clip in the left picture was connected to the working microsensor while the green electrical clip was connected to the reference electrode. The profiles of pH, ORP, O_2, NO_3^- and H_2S along the depth of MBBR biofilm were shown in Figure 5-3.

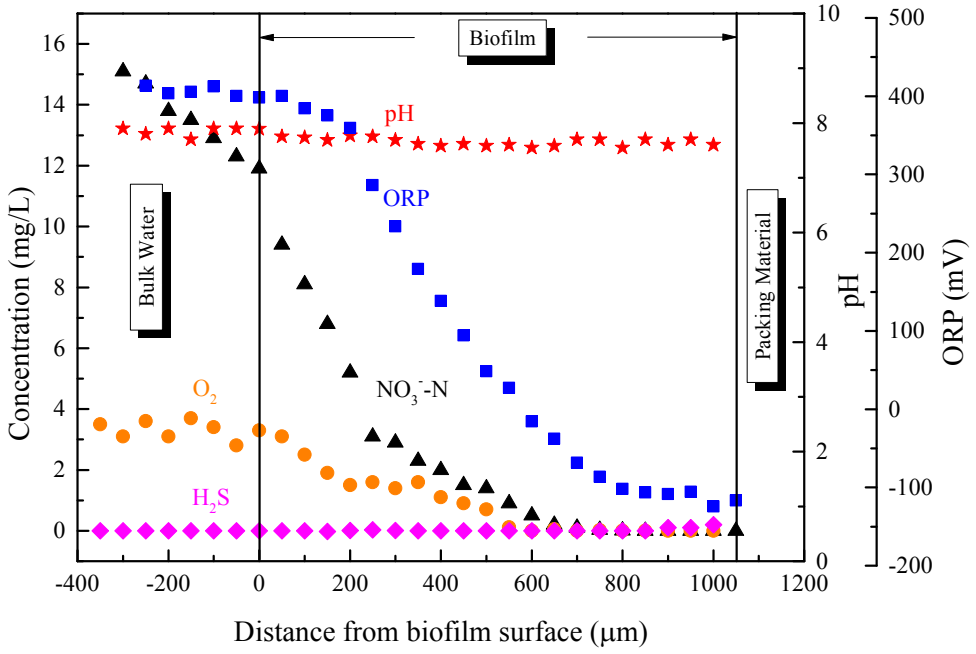

Figure 5-3 Chemical profiles inside MBBR biofilm

From Figure 5-3, the thickness of the biofilm measured was around 1050 μm. The pH profile showed that pH inside the biofilm was almost the same with that in the bulk water, which was around 7.8. pH profile inside the biofilm is necessary to determine the H_2S concentration due to the relationship of H_2S concentration with pH.

The O_2 concentration profile revealed that O_2 was gradually consumed and then depleted at 550 μm below the biofilm/bulk water interface, indicating oxic and anoxic zone in the MBBR biofilm. The penetration depth of oxygen in most wastewater biofilms is within 50~150 μm (Syron and Casey, 2008). From the bulk liquid to the biofilm, nitrate concentration decreased and was depleted at 750 μm below the interface. In the anoxic zone, located from 550 μm below

the interface to the packing material wall, denitrification process occurred. It was consistent with 40% of TN removal in MBBR. The TN concentration for influent and effluent of MBBR were 26.6 ± 1.5 mg/L and 15.9 ± 1.1 mg/L, respectively.

ORP measurement can be used to verify the ability or potential of wastewater to permit the occurrence of specific biological reactions, including nitrification, denitrification and sulfate reduction (Gerardi, 2007). Nitrification is performed by nitrifying bacteria when the ORP is +100 to +350 mV. Denitrification is performed by denitrifying bacteria with the ORP in the range of +50 to -50 mV. Sulfate reduction occurs when the ORP is -50 to -250 mV (Gerardi, 2007). Along the entire biofilm depth, the redox potential changed from +419 to -125 mV. It means the existence of nitrification, denitrification and sulfate reduction process is possible in MBBR biofilm. In the studies of Yu (2000) and Tan (2012), the ORP value for sulfate reduction process inside biofilm was around -150 mV. In this experiment, there was only a narrow zone, from 900 μm below the interface to the wall of packing material, suitable for sulfate reduction process.

Furthermore, the profile of H_2S concentration in MBBR biofilm revealed that H_2S accumulated in the deeper section of the biofilm closed to the packing material wall where the ORP value was around -100 mV. It was consistent with results reported by Yu (2000) and Tan (2012). The very small H_2S concentration implied the rare existence of sulfate reduction process in MBBR biofilm, which also explained the poor performance of MBBR on sulfate removal. The sulfate removal was around 5% with the influent concentration of 64.5 ± 4.5 mg/L.

5.2.2.2 Chemical Profiles in Biofilm from MABR

For MABR biofilm measurements, one piece of membrane module was taken out of MABR and put into a wide-open plastic tray. In order to simulate the condition of biofilm inside the tray

as the same of that in the operational MABR, a temporal measuring system was setup, which is shown in Figure 5-4 (a). A 10 L Pyrex® bottle (Catalog No. 06-414-1G, Fisher Scientific Company, ON, Canada) was used as a reservoir for solution from MABR, in which nitrogen gas was purged to get rid of dissolved oxygen. Two sets of pump and controller were utilized to recycle the solution, which maintained DO inside the tray as low as possible and reduced the interference caused by air diffusion from the atmosphere. The compressed air was supplied by the red gas cylinder on the left side of the figure and introduced into the membrane module by a flow meter to keep the same flow rate used in the operational MABR. Figure 5-4 (b) and (c) show the microsensor measurement when the temporal measuring system was setup. Due to the space limitation in the Faraday cage and the size of the tray, a portable 15 times magnifier instead of a horizontal dissection microscope was used to locate the biofilm/bulk water interface initially for microsensor measurement.

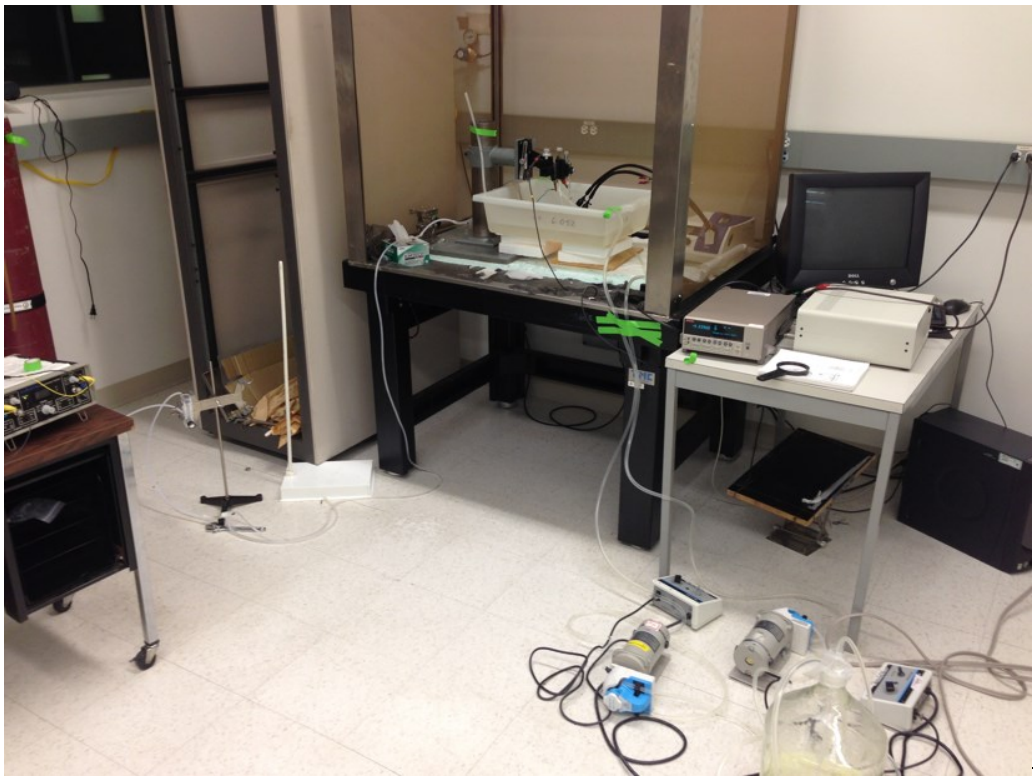

(a)

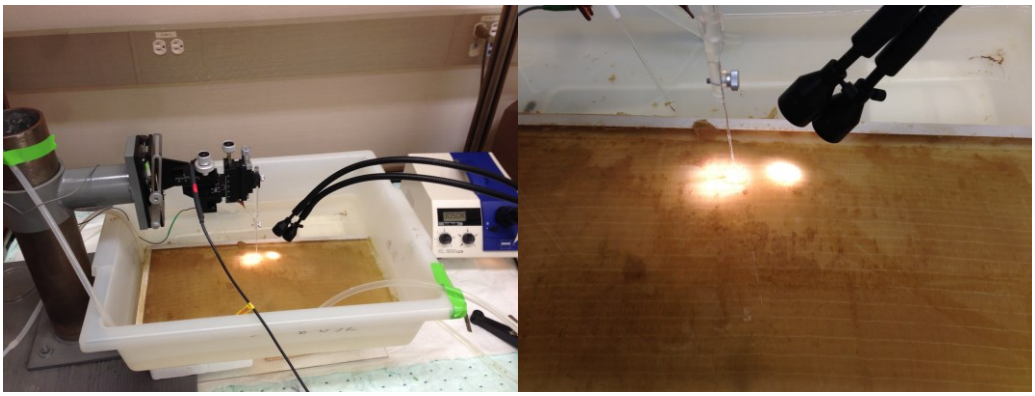

(b) (c)

Figure 5-4 Pictures of microsensor measurement setup for MABR biofilm

The profiles of O_2 concentration, NO_3^- concentration, H_2S concentration, ORP and pH as a function of distance from the surface of the biofilm were plotted in Figure 5-5.

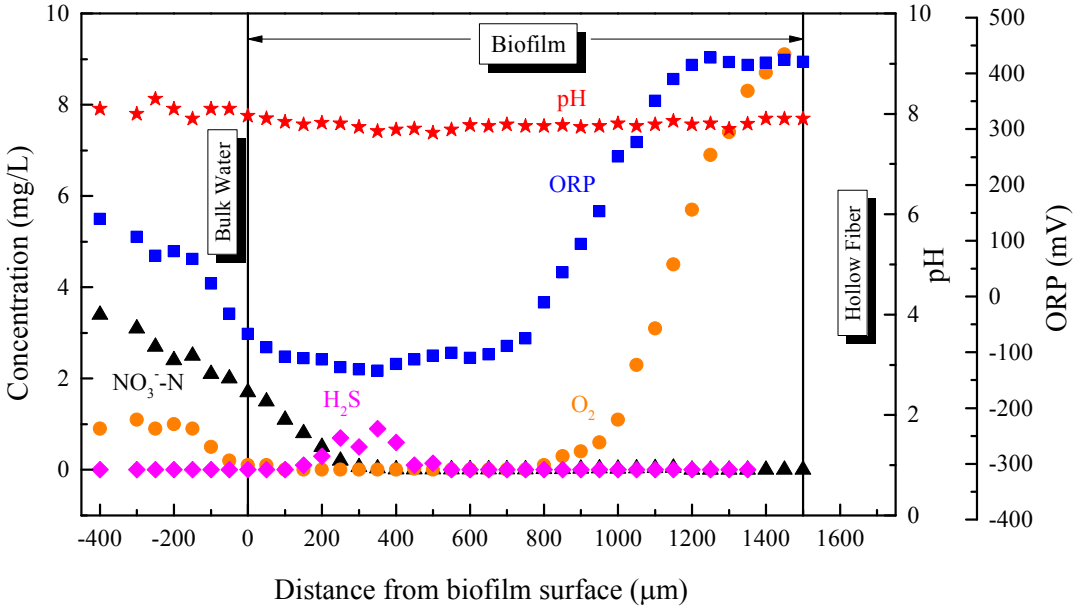

Figure 5-5 Chemical profiles inside MABR biofilm

The biofilm thickness is determined by the distance traveled by the micromanipulator. From Figure 5-5, the thickness of MABR biofilm was around 1500 μm. It was clearly found that oxygen and nutrients (such as NO_3^-) were provided from opposite directions in MABR biofilm, which was 'counter-diffusional biofilm' mentioned in Chapter 4. From the oxygen concentration

profile in Fig. 5-5, oxygen penetrating through the membrane was depleted at about 650 μm below the biofilm/bulk liquid interface in the upper biofilm, which was the anoxic zone inside MABR biofilm. The existence of oxygen concentration was observed near the biofilm/bulk water interface and in the bulk water, which should not happen when the membrane module placed in MABR. Considering the feasibility of microsensor measurement, this interference caused by air diffusion from the atmosphere cannot be eliminated. The measurement results were acceptable for supporting the related discussion. Therefore, the oxic zone inside MABR biofilm was from the surface of membrane to 650 μm below the biofilm/bulk liquid interface.

pH profile along the depth of biofilm changed slightly (within 0.2 unit), which was around 7.9. The H_2S concentration profile showed that H_2S production was restricted to the upper layer (250~350 μm below the biofilm/bulk liquid interface) of the anoxic zone where the ORP value was -140 mV. Tan et al. (2014) reported that the highest H_2S production rate was found about 400 to 450 μm below the biofilm/bulk liquid interface in a MABR. In the aerobic zone, H_2S produced was oxidized. Due to the oxygen diffused from the atmosphere, H_2S was also non-detected near the biofilm/bulk liquid interface where the ORP value was back to -40 mV. The sulfide detected in the MABR biofilm indicated the existence of sulfate reduction process, which was evidenced by the performance of MABR on sulfate removal. The sulfate removal was 20%, with the influent concentration of 53.4 ± 3.7 mg/L.

For ORP profile, the value of redox potential changed from +410 mV to -140 mV. It was found that the redox potential changed dramatically near the interface of aerobic and anoxic zone. The same phenomenon was observed in the previous studies (Tan et al., 2014, Yu and Bishop, 1998). The NO_3^- concentration decreased along the depth of biofilm from the bulk water side and was depleted at 300 μm from the interface, indicating that denitrification process took place in

the anoxic ozone of MABR biofilm. It was consistent with the result reported by Tan et al. (2014). Furthermore, the removal of TN in MABR was achieved around 84% with the influent concentration of 22.3 ± 2.0 mg/L, which could ensure the occurrence of denitrification process inside the biofilm.

5.3 Analysis of Microbial Community inside MBBR and MABR by Using Molecular Biological Techniques

In this section, microbial community inside biofilm from MBBR and MABR were investigated by using molecular biological techniques. The main focus is to find out the microbial community diversity and dynamic shift inside each bioreactor under different operational conditions. Combined with the chemical profiles illustrated in Section 5.2, it gave us a comprehensive insight about performance and function of bioreactors on OSPW treatment, which demonstrated the necessity and feasibility of the established bioreactor process train in this study.

5.3.1 Illumina MiSeq Sequencing

The microbial diversity of inoculum and enriched microbial consortia through our novel bioreactor process train was analyzed via Illumina MiSeq sequencing, utilizing the capacity in The Applied Genomics Core (TAGC) at University of Alberta. Genomic DNA was first extracted from bioreactor samples by using the PowerSoil® DNA Isolation Kit (MO BIO Laboratories, Inc., CA, USA) according to the manufacture's manual.

Sequencing amplicon libraries were generated by PCR following the "16S Metagenomic Sequencing Library Preparation - Preparing 16S Ribosomal RNA Gene Amplicons for the Illumina MiSeq System" protocol (Illumina Part # 15044223 Rev. B, https://support.illumina.com). Internal parts of the 16S ribosomal RNA (rRNA) gene, covering

variable regions V3 and V4, were PCR-amplified with the KAPA HiFi HotStart ReadyMix (Catalog No. KK2602, KAPA Biosystems, MA, USA) and the primers 5′-TCGTCGGCAGCGTCAGATGTGTATAAGAGACAGCCTACGGGNGGCWGCAG-3′ and 5′-GTCTCGTGGGCTCGGAGATGTGTATAAGAGACAGGACTACHVGGGTATCTAATCC-3′ and purified with the Agencourt AMPure XP kit (Catalog No. A63880, Beckman Coulter Inc., CA, USA).

The PCR process was conducted as follows: 95°C for 3 min, followed by 25 cycles at 95°C for 30 s, 55°C for 30 s, 72°C for 30 s and a final extension at 72°C for 5 min. PCR reactions were performed in triplicates. Each 25 μL PCR reaction mixture contained 12.5 ng of microbial DNA, 5 μL of each primer (1 μM), and 12.5 μL 2x KAPA HiFi HotStart ReadyMix.

Purified amplicons were pooled in equimolar and sequenced on an Illumina MiSeq platform using the MiSeq Reagent Kit v3 in the 2 x 300bp Paired-End mode.

The sequencing data analysis was conducted by mothur (Schloss et al., 2009) following MiSeq SOP (http://www.mothur.org/wiki/MiSeq_SOP). Firstly, the raw paired-end reads were assembled to reduce sequencing and PCR errors of the reads, and then the reads containing ambiguous bases, incorrect barcode or primer sequences, or longer than 275 bp were excluded from further analysis. Putative chimeras were detected and excluded from previously treated sequences with UCHIME algorithm within mothur. Taxonomy was assigned with Silva database using k-mer searching method with cutoff of 80%. The sequences classified in Chloroplast, Mitochondria, Archaea, and Eukaryota were excluded from further analysis. The remaining reads were clustered into OTUs at 97% identity. Rarefaction and diversity statistics including library coverage, Chao 1, and Shannon index were calculated for each sample after OTUs clustered. PCoA was conducted with thetayc distance. Finally, the raw reads were deposited into the

National Center for Biotechnology Information Sequence Read Archive database under accession.

5.3.2 Sample Description

There were six samples collected from MBBR and MABR for Illumina MiSeq sequencing analysis. Table 5-1 provides description of these samples.

Table 5-1 Description of six samples for Illumina MiSeq sequencing

Sample Name	Sample Description
S_0	Raw OSPW extraction
SA_{B1}	MBBR biofilm when seeding period was just completed
SA_{S2}	MBBR suspended solid in phase 3 when MBBR was at the stable state
SA_{B2}	MBBR biofilm in phase 3 when MBBR was at the stable state
SB_0	MABR inoculum sludge
SB_{B1}	MABR biofilm in phase 2 when MABR was at the stable state

The microbial community analysis of S_0 can tell us the indigenous microorganisms existed in OSPW. The influence of operation conditions on microbial community inside biofilm of MBBR can be revealed by the difference between SA_{B1} and SA_{B2}. The feature of biofilm can be illustrated by comparing the microbial community in SA_{S2} (suspended solid in MBBR) and SA_{B2} (biofilm in MBBR). As described in subsection 4.1.3 and 4.3.3, S_0 was a source of seed for inoculating MBBR and MABR. The comparation of S_0, SA_{B2} and SB_{B1} can explicate the function of engineered bioreactor on selecting and enriching some specific microorganisms. Based on those comparisons, we can have an insight about the influence on microbial communities inside bioreactors at different operational conditions, which makes us interpret the performance of bioreactor process train on OSPW treatment comprehensively.

5.3.3 Results and Discussion

5.3.3.1 Diversity Indices

A total of 3,608,551 16S rRNA sequences obtained were selected for classification. To compare the diversity indices, the sequences number of each sample was normalized to 544,425 reads. To examine α diversity of each sample and evaluate the performance of test method, Chao 1, OTU number, coverage, and Shannon indices were computed through rarefaction at a cutoff 3%. The results are shown in Table 5-2.

Table 5-2 Alpha diversity parameters of microbial communities for all six samples

Sample	**Parameters** (N = 544425 sequences/sample)			
	OTU number	**Coverage (%)**	**Chao 1**[a]	**Shannon**[b]
S_0	7077	99.1	43532	4.30
SA_{B1}	7637	99.3	33714	4.59
SA_{S2}	5471	99.3	28986	4.12
SA_{B2}	6185	99.4	30564	4.20
SB_0	6427	99.5	33340	4.19
SB_{B1}	4372	99.4	17969	4.60

a. Chao 1 index is used to estimate the total number of species within a sample;
b. Shannon index indicates the evenness that combines species richness and abundance to describe how different species are numerically distributed within a sample.

From the above table, the coverage of each sample was higher than 99%, which demonstrated that the obtained sequences reasonably represented the overall microbial communities. The Chao 1 value of S_0 were the highest in all six samples while OTU number and Chao 1 value of SB_{B1} were the lowest in all six samples. It means the richness of microbial species inside raw OSPW extraction was the highest among all six samples. Some microbial species might not survive or be washed out of bioreactors due to the different environmental conditions inside bioreactors from that in OSPW. However, MABR, with demonstrated good performance on AEF removal, had the lowest richness of microbial species in all six samples. It indicated that those non-survival or washed-out microbials, which largely affected the species richness of the community, might not contribute to NAs degradation. The same observation was also reported in the previous study (Xue et al., 2017).

The OTU value of SA_{B1} was the highest among all six samples. Because I used two more sources of seed other than extraction from raw OSPW for seeding MBBR, which made the diversity of microbial community in this bioreactor higher than that in raw OSPW. The advantage of choosing diverse sources for seeding bioreactor will be further illustrated in the following section.

Comparing SA_{S2} and SA_{B2}, it was found that the OTU number and Chao 1 value in the biofilm sample SA_{B2} were higher than those in the suspended solid sample SA_{S2}, which demonstrated the microbial richness in the biofilm was higher than that in the suspended solid in MBBR. This result is accordance to previous study (Huang et al., 2017). Furthermore, the oxygen profile in the biofilm of MBBR described in subsection 5.2.2.1 also illustrated that there were oxic and anoxic zone in the biofilm, where could supply two kinds of microenvironment for aerobic and anaerobic microorganisms. Therefore, these results demonstrated the advantageous of biofilm comparing with the suspended sludge in the bioreactor.

Shannon index is used to reflect both species richness and evenness in the microbial community. A higher value of Shannon index indicates higher diversity of the microbial community. For SA_{B1} and SA_{B2}, these two biofilm samples were taken from different phase of MBBR operation. The decreased Shannon index value (from 4.59 for SA_{B1} to 4.20 for SA_{B2} in Table 5-2) may be caused by the chronic toxicity of NAs in MBBR due to the different influent composition at different phases. The portion of raw OSPW in phase 1 (when SA_{B1} was taken) was lower than that in phase 3 (when SA_{B2} was taken) as described in Chapter 4. It means only bacteria with high tolerance on the toxicity of NAs can survive. Xue et al. (2017) also reported the same trend in MBR for treating OSPW. Comparing with SA_{S2}, the higher Shannon index value of SA_{B2} also demonstrated that biofilm had the capacity for providing different

microenvironments from that in the bulk water for microorganisms to survive due to the diffusion limit. More kinds of microorganisms mean more possible existence of metabolic processes, which will be further explained in the following section.

The Shannon index value of SB_{B1} was the highest in all six samples. There were two main reasons: (1) the toxicity of MABR influent was lower than that of MBBR influent due to the chemical oxidation process in the bioreactor process train. The capability of ozone on reducing toxicity of NAs was well studied by the previous researches (Dong et al., 2015; Gamal El-Din, M. et al., 2011; He et al., 2012; Hwang et al., 2013; Martin et al, 2010). (2) the long SRT described in Chapter 2 made MABR capture the bacteria with slow growing rate from being washed out, which increased the diversity of the microbial community in MABR biofilm. In the study by Wittebolle et al. (2009), it was found that the evenness of a microbial community had a strong influence on the resistance of microorganisms to environmental stresses such as high salinity and toxicity. The higher evenness of the microbial community, the higher probability that the microbial community tolerant to an environmental stress is present. In this study, the higher value of Shannon index for SB_{B1} than that of SA_{B2} explained the better performance of MABR on AEF removal than that in MBBR when both reactors were at stable state, which was illustrated in Chapter 4.

5.3.3.2 Bacterial Community Structure Analysis

Figure 5-6 shows the top 10 most abundant phyla of each sample, indicating that *Proteobacteria*, *Bacteroidetes*, *Firmicutes*, and *Chloroflexi* were the dominant phyla of the microbial communities, accounting for over 80% of the total abundance. *Proteobacteria* was the most dominant phylum in all six samples (21.6-78.1%), which is known as the commonly predominate phylum in sediment of reservoirs and lakes (Chen et al., 2014; Haller et al., 2011)

and play an important role on the performance of degradation of organic compounds and nutrients removal in an ecosystem (Yang et al., 2014). It was reported that *Bacteroidetes* have an import role in the mineralization of complex organic compounds in the marine realm (Kabisch et al., 2014). The relative abundance (RA) of *Bacteroidetes* in the suspended solid (21.7% in SA_{S2}) was higher than that in MBBR biofilm (7.2% in SA_{B2}). Comparing to raw OSPW, the RA of *Acidobacteria* in the bioreactors increased, which was found to be able to degrade the carbohydrate in the peatland. It meant the bioreactor enriched the specific microorganisms for carbohydrate degradation. *Nitrospirae*, which was involved in nitrification and denitrification, was only detected in both bioreactors. Because there were other sources like activated sludge from CASR in Chapter 3 than extraction of OSPW for seeding bioreactor. The diversity of seeds gave us the diversity of microbial community in the bioreactor, which also was demonstrated by the highest OTU value of SA_{B1} in Table 5-2. Due to the addition of other sources, bioreactors in the process train had the capacity of nitrification and denitrification related to *Nitrospirae*, which was not detectable in S_0 (extraction of raw OSPW). It indicated that seeding bioreactor with non-OSPW-origin sources was a wise and advantageous decision in this study.

The RA of *Nitrospirae* in MABR biofilm (4.8% in SB_{B1}) was higher than that in MBBR biofilm (2.9% in SA_{B2}), which matched the higher removal of TN in MABR than that in MBBR mentioned in Chapter 4. Furthermore, the RA of *Chloroflexi* that can participate in carbon oxidation and nitrification (Kragelund et al., 2007) increased in the biofilm samples (17.1% in SA_{B2}; 13.9% in SB_{B1}) were also higher than that in the inoculums (2.2% in SA_{B1} and 1.5% in SB_0) for both bioreactors. These findings were consistent with the nitrate profiles described in the Section 5.2.2. for both bioreactors.

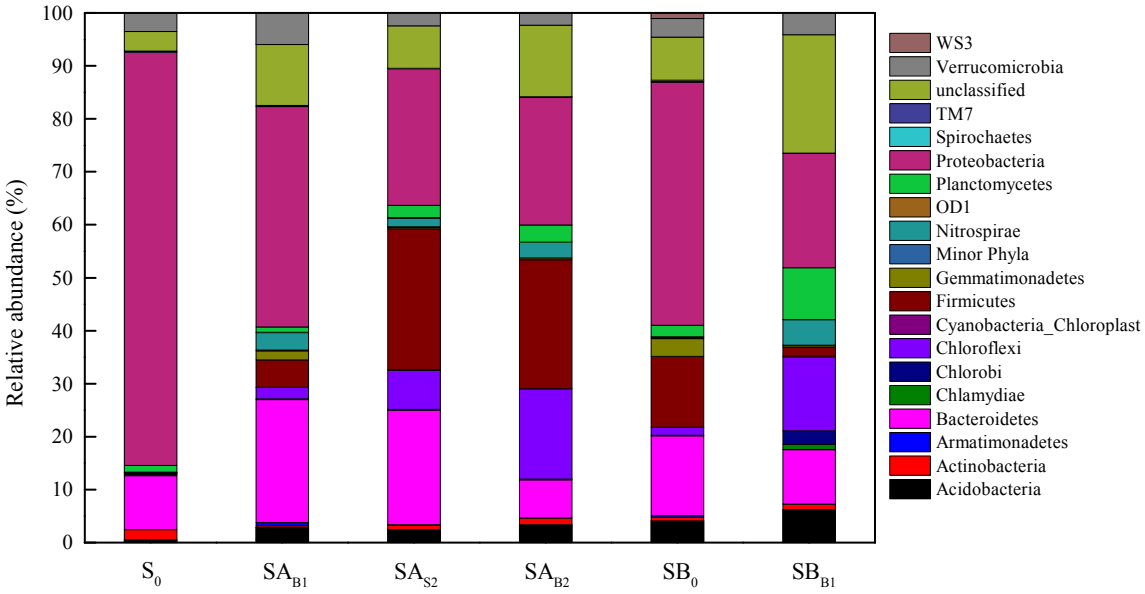

Figure 5-6 The top 10 most relative abundance of the bacteria at the phylum level

In order to further investigate the structure of microbial communities of all six samples, the dominant classes were identified, which were shown in Figure 5-7. More difference can be observed at the class level.

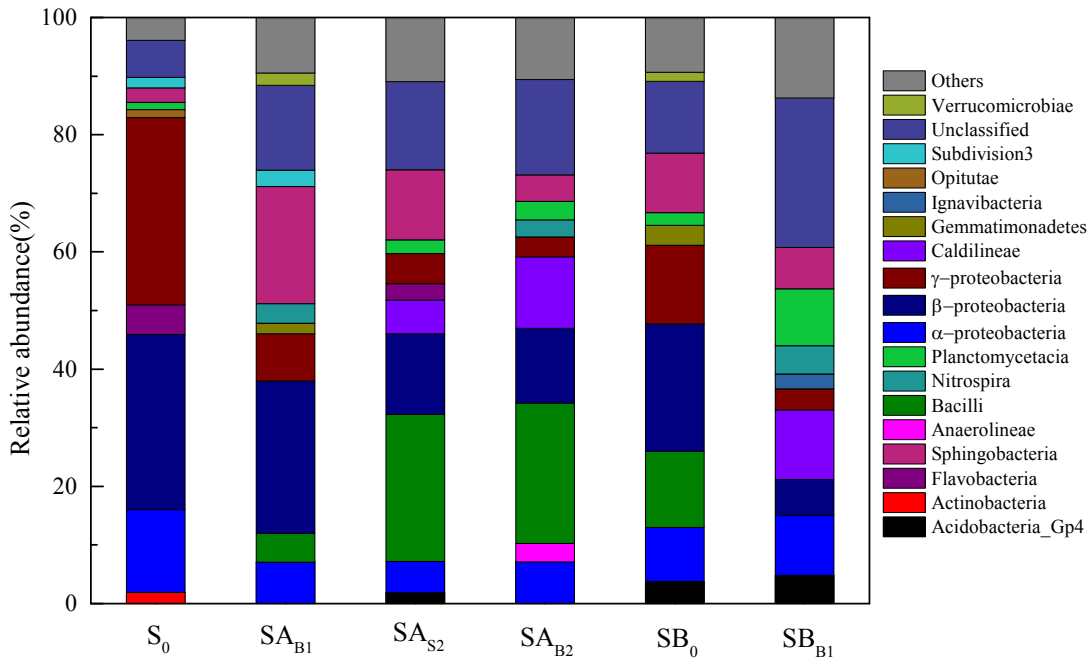

Figure 5-7 The top 10 most relative abundance of the bacteria at the class level

Among *Proteobacteria* the dominant phylum, *alpha*-, *beta*-, and *gamma-Proteobacteria* were the dominant classes in all six samples. The *delta-Proteobacteria* populations in all samples were relatively small (<2%). The similar observation was also reported by Huang et al. (2017), in which fixed-film activated sludge systems were utilized for OSPW treatment. In raw OSPW sample (S_0), *β-Proteobacteria* and *γ-Proteobacteria* were dominant, whose RA were 29.9% and 31.9%, respectively. After inoculating extraction of raw OSPW into the bioreactor, the proportion of *γ-Proteobacteria* was remarkably declined due to the different circumstance in the bioreactors from tailings pond while *β-Proteobacteria* was still the dominant class in the samples from bioreactors. In the study of Yergeau et al. (2012), it was found that the *β-Proteobacteria* existed in oil sands tailings ponds had the capacity of degradation of naphthenic acids and aromatic hydrocarbons. The RA of *β-Proteobacteria* in SA_{S2}, SA_{B2} and SB_{B2} were comparable, which were 13.7%, 12.7% and 6.1%, respectively. It explained the degradability of NAs in MBBR and MABR demonstrated in Chapter 4.

Regarding to the *Bacteroidetes* phylum, *Sphingobacteria* showed a relative high abundance in both bioreactors after inoculation, which was demonstrated to be responsible for degradation of recalcitrant organic compounds (Drury et al., 2013). The increase of populations of *Sphingobacteria* in both bioreactors proved that bioaugmentation happened in MBBR and MABR after inoculation. The RA of *Sphingobacteria* in SA_{S2} (12%) was higher than that in SA_{B2} (4.5%) and SB_{B2} (7%) due to its characteristics of aerobic living.

By comparing SA_{B2} and SB_{B2}, the relative abundance of *Nitrospira* and *Planctomycetacia* were 2.9% and 3.2% in SA_{B2}, while 4.8% and 9.7% in SB_{B2}, respectively. It was reported by Schmidt et al. (2003) that anaerobic ammonium oxidation belongs to phylum *Planctomycetes*,

which may explain the better TN removal in MABR than that in MBBR due to the relative high abundance of *Planctomycetacia*.

Figure 5-8 was the heat map for top 50 most abundant genera for all six samples. There were nine common genera for all six samples, which were *3_genus_incertae_sedis*, *Caldilinea*, *Falvobacterium*, *Gp4*, *Hydrogenophaga*, *Opitutus*, *Prosthecobacter*, *Pseudomonas*, and *Rhodobacter* in different abundances. It was reported that some *Pseudomonas* and *Falvobacterium* species had the capacity of degrading recalcitrant organic compounds, including polycyclic aromatic hydrocarbons (Cao et al. 2009, Van den Tweel et al. 1988) and NAs (Whitby, 2010; Zhang et al., 2015). *Rhodobacter* were believed to show great resistance to the harsh environment and capability of degrading carboxylic group on the main carbon chain (Loy et al. 2005). For *Pseudomonas*, the RA in S_0, SA_{A2}, SA_{B2} and SB_{B2} were 0.55%, 1.3%, 1.04% and 0.87%, respectively. For *Rhodobacter*, the RA in S_0, SA_{A2}, SA_{B2} and SB_{B2} were 0.36%, 0.51%, 0.72% and 0.6%. For *Falvobacterium*, the RA in S_0, SA_{A2}, SA_{B2} and SB_{B2} were 0.82%, 2.17%, 0.53% and 0.3%. Based on those data, it was easily found that the RA of *Pseudomonas*, *Rhodobacter* and *Falvobacterium* in bioreactors were almost double of those in raw OSPW. It indicated that MBBR and MABR enriched specific microorganisms capable of degradation of recalcitrant organic compounds, which accelerated the reclamation of OSPW. It helped explain the performance of bioreactors on NAs removal on such a short HRT (3 days) comparing years of natural biodegradation of NAs in OSPW illustrated in Chapter 4. The high population of *Nitrospira* in SA_{B2} (2.93%) and SB_{B2} (4.81%) also explained the performance of nitrogen removal in both bioreactors when they were at stable state, which was mentioned in Section 5.2. The RA of *Ignavibacterium* in SB_{B1} was 2.58%, which was reported to be the cultured member of the phylum Chlorobi and related to sulfur metabolism (Liu et al., 2012). It explained the

sulfate reduction happened in MABR, which was also demonstrated by H_2S profile in MABR biofilm illustrated in Section 5.2.

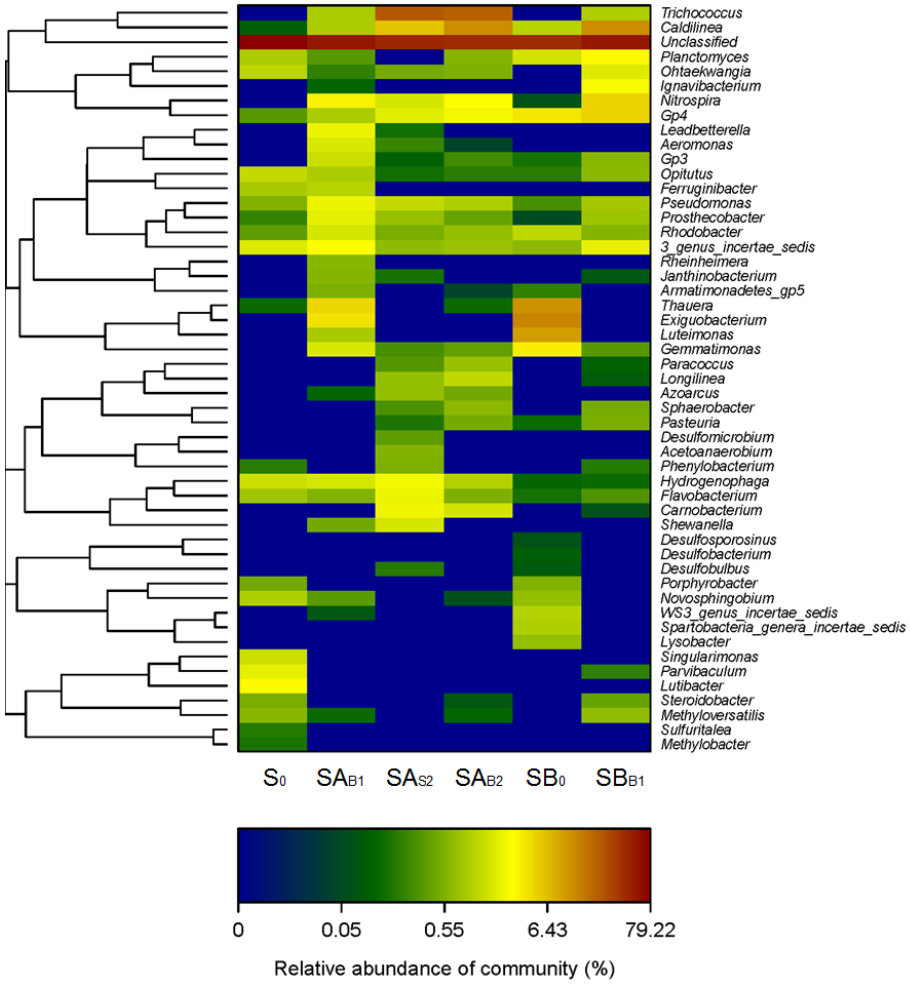

Figure 5-8 Heat map for top 50 most abundant bacteria at genus level

5.3.3.3 Comparative Analysis of Microbial Communities

To investigate the relationship between all six samples, PCoA was performed with thetayc distance to examine the correlation among microbial communities from different samples. In PCoA analysis, samples ordinated closer to one another are more similar than those ordinated further away. Figure 5-9 shows the PCoA analysis results.

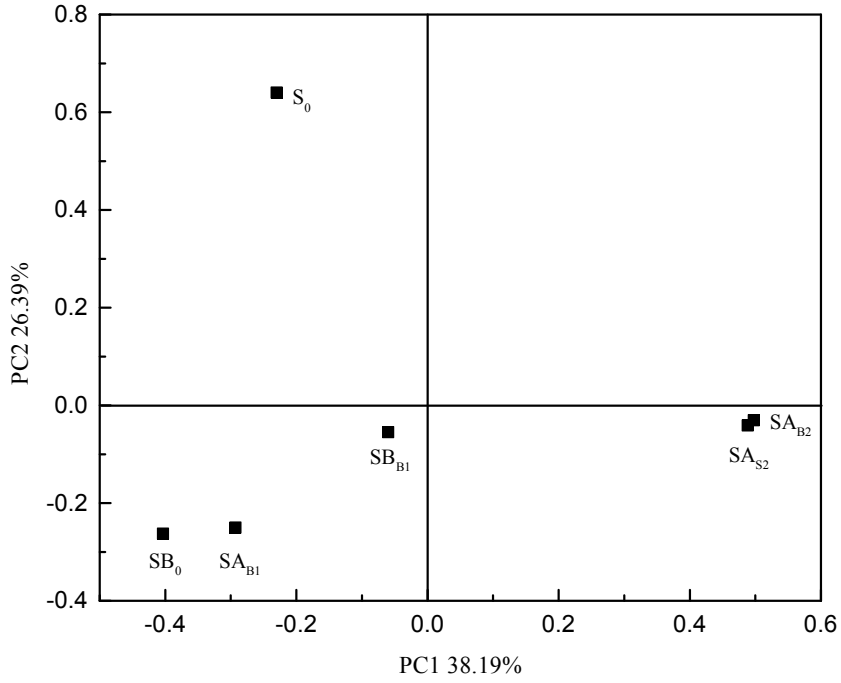

Figure 5-9 PCoA analysis

Based on the above figure, principal component 1 and 2 explained 38.19% and 26.39% of the total community variations, respectively. Overall, the PC1 and PC2 showed 64.58% variation between the different communities for all six samples. It was clearly found that significant differences of microbial communities were present between Raw OSPW sample and samples from bioreactors. That was because the operation conditions inside bioreactors were totally different from the water quality condition of OSPW. For samples in MBBR, SA_{A2} and SA_{B2} were clustered together and well separated from SA_{B1} despite the fact they shared the same source of microbial consortia. To identify the crucial factor resulting in microbial community structure change, we analyzed the operational conditions in MBBR when those samples were taken. In the description in Section 4.1.3, it was known that the influent composition and HRT as two main operational conditions were different at Phase 1 for SA_{B1} and Phase 3 for SA_{A2} and SA_{B2}. pH and DO were almost the same at Phase 1 and 3. The same reason was found for explaining the clear distinction of microbial community between SB_0 and SB_{B1}. Based on the

above discussion, the influent composition and HRT might be factors affecting the abundance and diversity of microbial communities.

5.4 Conclusions

In this chapter, microsensor and molecular biological techniques were utilized together to investigate the internal structure and microbial communities inside biofilms from MBBR and MABR. The oxygen and NO_3^- profiles inside MBBR and MABR indicated the existence of nitrification and denitrification process, which was verified by the high relative abundance of *Nitrospira* in biofilms from both bioreactors. High level of H_2S was found in a narrow band about 250 μm to 350 μm below the interface of MABR biofilm, in which the ORP lower than -140 mV. Both H_2S and ORP profiles proved that sulfate reduction process existed inside MABR biofilm. *Ignavibacteria* belonging to *Chlorobi* phylum which relates to sulfur metabolism was also found in MABR biofilm. The comprehensive analysis in this chapter indicated that results from Illumina MiSeq sequencing in terms of microbial community structures corresponded well with those from microsensor measurements in terms of their metabolic functions in biofilm.

Although the richness of raw OSPW was the highest among all six sample, some microbial species only existed in OSPW might not contribute to NAs degradation in bioreactors. Because the OTU number and Chao 1 value of biofilm in MABR were the lowest while the performance of MABR on NAs removal was good. The highest value of Shannon index for biofilm in MABR explained the good performance on NAs degradation. Seeding bioreactor with non-OSPW-origin microbial consortia was beneficial for the application of bioreactor on OSPW treatment due to new capacity introduced into bioreactor caused by new microbial consortia seeded. Because bioreactors in the process train had the capacity of nitrification and denitrification related to *Nitrospirae*, which was not coming from the extraction of raw OSPW.

By analyzing the microbial communities of each sample at phylum, class and genus level, it was found that high relative abundance of bacteria involved in removing nitrogen (*Nitrospira* and *Planctomycetacia*), aromatic compounds (*β-Proteobacteria*), and hydrocarbons (*Sphingobacteria*) in bioreactors accounted for the good performance of the bioreactor process train on nitrification, denitrification and effective removal of OSPW NAs. Bioreactors selected and enriched specific microorganisms (i.e., *Pseudomonas*, *Falvobacterium* and *Rhodobacter*) which showed great resistance to the harsh environment and the capacity of degrading carboxylic group of the main carbon chain. It was clearly indicated that bioaugmentation happened inside bioreactors, which made the biodegradation of recalcitrant organic chemicals in OSPW faster and the acceleration of OSPW reclamation promising. Also, PCoA analysis of all six samples illustrated that influent composition and HRT of bioreactor were the two main factors affecting the abundance and diversity of microbial communities.

Therefore, seeding with non-OSPW-origin microbial consortia and nutrient addition are highly recommended for biodegradation of recalcitrant organics in OSPW. With the understanding of microbial community and biofilm structure, it is believed that the results obtained in this chapter can help to optimize engineered bioreactors for OSPW treatment in the future.

CHAPTER 6 Conclusions and Recommendations

6.1 Conclusions

This research aims to establish a proper and feasible bioreactor process train for treating OSPW. The foremost part of this research is to develop this process train and test it for OSPW treatment continuously and effectively. The following conclusions are based on the results of this research.

Based on the development and performance evaluation of this new bioreactor process train:

(1) The bioreactor process train composed of bioreactors, chemical oxidation and adsorption processes was effective on enhancing biodegradation of recalcitrant organic chemicals and reducing the toxicity of OSPW;

(2) Each component of this process train played a critical and indispensable role in OSPW treatment. To be specific,

   a) Bioreactors especially for biofilm reactors had more resistance for toxic OSPW, in which biofilm could supply a suitable microenvironment for bacteria growth. At HRT=3 days, MBBR achieved 23% of COD removal and 16% of AEF removal from raw OSPW; MABR removed 44% of COD and 24% of AEF from raw OSPW.

   b) Chemical oxidation process increased the biodegradability of OSPW for further biological treatment. With the applied dosage of 35 mg/L of ozone, BOD increased from 3 mg/L to 19 mg/L, which enlarged the ratio of BOD/COD.

   c) Adsorption process polished the effluent to make the final discharge possible in the future. 79% of COD and 71% of AEF was removed from MABR effluent by

adsorption column. The average final effluent's COD and AEF was 17 mg/L and 2.9 mg/L, respectively.

When the performance of this process train was demonstrated, the focus of this research shifted to biofilm internal structure and microbial community change during operation. A suite of microsensors were used to investigate the chemical profiles inside biofilms, which could tell the internal structure of biofilms. Illumina MiSeq sequencing analysis illustrated the community diversity, abundance and dynamic shift inside bioreactors at different operation phases. Based on those results, it was found that:

(3) Nitrification and denitrification processes existed in MBBR and MABR biofilm. Firstly, DO profiles inside both biofilm samples showed the existence of oxic and anoxic zone. The NO_3^- profile showed the degradation of NO_3^- inside biofilm sample. Secondly, *Nitrospira* that were related to nitrification process existed in biofilms. Lastly, the performance of TN removal in MBBR and MARB could verify the existence of nitrification and denitrification processes.

(4) High level of H_2S was found in a narrow band about 250 μm to 350 μm below the interface of MABR biofilm, in which the ORP lower than -140 mV. Both H_2S and ORP profiles proved that sulfate reduction process existed inside MABR biofilm, which also could explain the removal of sulfate in MABR. Furthermore, *Ignavibacteria* belonging to *Chlorobi* phylum was found in MABR biofilm, which relates to sulfur metabolism.

(5) As a source of seeding, microbial community in raw OSPW had the highest richness compared to the samples from bioreactors based on the Chao 1 value. However, the rare microbial communities which largely affect the richness of microbial community

may not contribute to NAs degradation in the bioreactor. The Shannon index of biofilm from MABR was higher than that in biofilm from MBBR, which may explain the better performance on NAs removal in MABR. Seeding bioreactor with non-OSPW-origin microbial consortia could benefit the application of bioreactor on OSPW treatment due to new capacity of bioreactor caused by new microbial consortia introduced (e.g., *Nitrospira*).

(6) Raw OSPW provided some valuable specific microorganisms showing great resistance to the harsh environment and capability of degrading carboxylic group of main carbon chain. Bioreactors could select and enrich those microorganisms during operation, which would be beneficial for OSPW treatment. The details were as follows:

a) The number of common OTUs in MBBR and MABR biofilm samples decreased during operation. However, the Shannon index value of biofilm from MABR was the highest, suggesting the increase of evenness and diversity inside the microbial community. Given the good performance of MBBR and MABR on NAs removal, it was indicated that bioreactor could capture and select some specific microorganism related to degradation of NAs in OSPW.

b) Nine common genra, *3_genus_incertae_sedis*, *Caldilinea*, *Falvobacterium*, *Gp4*, *Hydrogenophaga*, *Opitutus*, *Prosthecobacter*, *Pseudomonas*, *Rhodobacter*, were founded in all tested samples. *Pseudomonas* and *Falvobacterium* were reported to exhibit great resistance under toxic and alkaline environment like OSPW. *Rhodobacter* had been demonstrated to exhibit metabolic capability of the carboxylic group of the main carbon chain.

c) The relative abundance of those three genera (*Pseudomonas*, *Rhodobacter* and *Rhodobacter*) in biofilm samples were higher than that in raw OSPW, which demonstrated bioaugmentation happening inside bioreactors.

(7) PCoA analysis revealed the correlation between tested samples. For samples in bioreactors, it was found that sample from different phase were well separated from each other despite the fact they shared the same source of microbial consortia. It was observed that operational conditions including the influent composition and HRT might be the two main factors for affecting the abundance and diversity of microbial communities.

6.2 Environmental Implications

As far as we know, there is no government regulations or standards about OSPW management officially launched until now, which is critical and necessary for this environmental challenge in Alberta. The novel bioreactor process train established in this research provides an option for minimizing environmental and health impacts associated with the recycle and/or safe release of treated OSPW. The performance evaluation of this process train could be used to elucidate the feasibility of biological treatment for OSPW. The same principles of bioreactor applications are applicable as well for addressing the issue of end-pit lakes in oil sands tailings' reclamation. Therefore, the operational conditions and performance results of bioreactors in this research could be a reference in the development of regulations or standards for OSPW treatment.

It is the first time to introduce MABR into OSPW biological treatment, which will expand the application of MABR and accumulate experience of running MABR. Also, this research is one of the few studies using microsensors and molecular biological techniques together to investigate the microbial processes in the biofilm, such as nitrification, denitrification and sulfate

reduction process. The comprehensive analysis of microbial community inside biofilm and operational performance of bioreactors could be beneficial for the design, operation and modelling of bioreactors for OSPW treatment in the future.

REFERENCES

Afzal, A., Drzewicz, P., Perez-Estrada, L. A., Chen, Y., Martin, J. W., and Gamal El-Din, M. (2012). Effect of molecular structure on the relative reactivity of naphthenic acids in the UV/H_2O_2 advanced oxidation process. *Environmental Science and Technology*, 46(19), 10727-10734.

Allen, E. W. (2008a). Process water treatment in Canada's oil sands industry: I. Target pollutants and treatment objectives. *Journal of Environmental Engineering and Science*, 7(2), 123-138.

Allen, E. W. (2008b). Process water treatment in Canada's oil sands industry: II. A review of emerging technologies. *Journal of Environmental Engineering and Science*, 7(5), 499-524.

Amat, A.M., Arques, A., Beneyto, H., García, A., Miranda, M.A. and Seguí, S. (2003). Ozonisation coupled with biological degradation for treatment of phenolic pollutants: a mechanistically based study. *Chemosphere*, 53, 79-86.

APHA. (2005). Standard methods for the examination of water and waste water, 21st edn. American Public Health Association, Washington, DC, New York.

Araya, R., Tani, K., Takagi, T., Yamaguchi, N. and Nasu, M. (2003). Bacterial activity and community composition in stream water and bio lm from an urban river determined by uorescent in situ hybridization and DGGE analysis. *FEMS Microbiology Ecology*, 43(1), 111-119.

AWWARF. (1998). Effect of biocarbonate alkalinity on performance of advanced oxidation processes. American Water Works Association Research Foundation, Denver.

Barrow, M. P., Headley, J. V., Peru, K. M., and Derrick, P. J. (2004). Fourier transform ion cyclotron resonance mass spectrometry of principal components in oil sands naphthenic acids. *Journal of Chromatography A*, 1058, 51-59.

Bassin, J. P., Dezotti, M., and Sant'Anna, G. L. (2011). Nitrification of industrial and domestic saline wastewaters in moving bed biofilm reactor and sequencing batch reactor. *Journal of Hazardous Materials*, 185(1), 242-248.

Bell, T. H., Yergeau, E., Maynard, C., Juck, D., Whyte, L. G. and Greer, C. W. (2013). Predictable bacterial composition and hydrocarbon degradation in arctic soils following diesel and nutrient disturbance. *The ISME Journal*, 7(6), 1200-1210.

Beltran, F. J. (2003). Ozone reaction kinetics for water and wastewater systems. CRC, Boca Raton, FL.

Brindle, K., and Stephenson, T. (1996). The application of membrane biological reactors for the treatment of wastewaters. *Biotechnology and Bioengineering*, 49(6), 601-610.

Buermans, H. P. J. and den Dunnen, J. T. (2014). Next generation sequencing technology: *Advances and applications. Biochimica et Biophysica Acta*, 1842(10), 1932-1941.

Cao, B., Nagarajan, K. and Loh, K. C. (2009). Biodegradation of aromatic compounds: current status and opportunities for biomolecular approaches. *Applied Microbiology and Biotechnology*, 85(2), 207-228.

Casey, E., Glennon, B., Hamer, G. (1999). Review of membrane aerated biofilm reactors. Resources, *Conservation and Recycling*, 27, 203-215.

Chang, S. W., Hyman, M. R., and Williamson, K. J. (2002). Cooxidation of naphthalene and other polycyclic aromatic hydrocarbons by the nitrifying bacterium, *Nitrosomonas europaea*. *Biodegradation*, 13(6), 373-381.

Chen, C., Ren, N. Q., Wang, A. J., Yu, Z. G., and Lee, D. J. (2008). Simultaneous biological removal of sulfur, nitrogen and carbon using EGSB reactor. *Applied Microbiology and Biotechnology*, 78(6), 1057-1063.

Cheng, W., Zhang, J. X., Wang, Z., Wang, M. and Xie, S. G. (2014). Bacterial communities in sediments of a drinking water reservoir. *Annals of Microbiology*, 64(2), 875-878.

Choi, J., Hwang, G., Gamal El-Din, M. and Liu, Y. (2014). Effect of reactor configuration and microbial characteristics on biofilm reactors for oil sands process-affected water treatment. *International Biodeterioration and Biodegradation*, 89, 74-81.

Clapp, L. W., Regan, J. M., Ali, F., Newman, J. D., Park, J. K., and Noguera, D. R. (1999). Activity, structure, and stratification of membrane-attached methanotrophic biofilms cometabolically degrading trichloroethylene. *Water Science and Technology*, 39(7), 153-161.

Clemente, J. S., and Fedorak, P. M. (2005). A review of the occurrence, analyses, toxicity, and biodegradation of naphthenic acids. *Chemosphere*, 60(5), 585-600.

Clemente, J. S., MacKinnon, M. D. and Fedorak, P. M. (2004). Aerobic biodegradation of two commercial naphthenic acids preparations. *Environmental Science and Technology*, 38(4), 1009-1016.

Collins, A. G., Theis, T. L., Kilambi, S., He, L., and Pavlostathis, S. G. (1998). Anaerobic treatment of low-strength domestic wastewater using an anaerobic expanded bed reactor. *Journal of Environmental Engineering*, 124(7), 652-659.

Collins, G., Foy, C., McHugh, S., and O'Flaherty, V. (2005). Anaerobic treatment of 2,4,6-trichlorophenol in an expanded granular sludge bed-anaerobic filter (EGSB-AF) bioreactor at 15 degrees C. *FEMS Microbiology Ecology*, 53(1), 167-178.

Collins, G., Mahony, T., and O'Flaherty, V. (2006). Stability and reproducibility of low-temperature anaerobic biological wastewater treatment. *FEMS Microbiology Ecology*, 55(3), 449-458.

Connaughton, S., Collins, G., and O'Flaherty, V. (2006). Development of microbial community structure and activity in a high-rate anaerobic bioreactor at 18°C. *Water Research*, 40(5), 1009-1017.

Crittenden, J. C., Trussell, R. R., Hand, D. W., Howe, K. J., and Tchobanoglous, G. (2012). Adsorption. In Water Treatment: Principles and Design (pp.1245-1358). Hoboken, New Jersey: John Wiley and Sons, Inc.

de Beer, D., Stoodley, P., Roe, F. and Lewandowski, Z. (1994). Effects of biofilm structures on oxygen distribution and mass-transport. *Biotechnology and Bioengineering*, 43(11), 1131-1138.

de Beer, D., Schramm, A., Santegoeds, C. M. and Kuhl, M. (1997). A nitrite microsensor for profiling environmental biofilms. *Applied and Environmental Microbiology*, 63(3), 973-977.

Debus, O., Baumgartl, H., and Sekoulov, I. (1994). Influence of fluid velocities on the degradation of volatile aromatic-compounds in membrane bound biofilms. *Water Science and Technology*, 29(10-11), 253-262.

Debus, O., and Wanner, O. (1992). Degradation of xylene by a biofilm growing on a gas-permeable membrane. *Water Science and Technology*, 26(3-4), 607-616.

De Gusseme, B., Pycke, B., Hennebel, T., Marcoen, A., Vlaeminck, S.E., Noppe, H., Boon, N. and Verstraete, W. (2009). Biological Removal of 17 Alpha-Ethinylestradiol by a Nitrifier Enrichment Culture in a Membrane Bioreactor. *Water Research*, 43(9), 2493-2503.

de la Rosa, C. and Yu, T. (2006). Development of an automation system to evaluate the three-dimensional oxygen distribution in wastewater biofilms using microsensors. *Sensors and Actuators B-Chemical*, 113(1), 47-54.

Del Rio, L. F., Hadwin, A. K. M., Pinto, L. J., MacKinnon, M. D., and Moore, M. M. (2006). Degradation of naphthenic acids by sediment micro-organisms. *Journal of Applied Microbiology*, 101(5), 1049-1061.

Deni, J. and Penninckx, M. J. (1999). nitrification and autotrophic nitrifying bacteria in a hydrocarbon-polluted soil. *Applied and Environmental Microbiology*, 65(9), 4008-4008.

Dobbs, R. and Cohen, J. (2002). Carbon adsorption isotherms for toxic organics. U.S. Environmental Protection Agency, Washington, D. C., EPA/600/8-80/023 (NTIS PB80197320).

Dollerer, J. and Wilderer, P. A. (1996). Biological treatment of leachates from hazardous waste landfills using SBBR technology. *Water Science and Technology*, 34(7-8), 437-444.

Dong, T., Zhang, Y. Y, Islam, M. S., Liu, Y. and Gamal El-Din, M. (2015). The impact of various ozone pretreatment doses on the performance of endogenous microbial communities for the remediation of oil sands process-affected water. *International Biodeterioration and Biodegradation*, 100, 17-28.

Drury, B., Rosi-Marshall, E. and Kelly, J. J. (2013). Wastewater treatment effluent reduces the abundance and diversity of benthic bacterial communities in urban and suburban rivers. *Applied and Environmental Microbiology*, 79(6), 1897-1905.

Edgar, R. C. (2013). UPARSE: highly accurate OTU sequences from microbial amplicon reads. *Nature Methods*, 10, 996.

Eiler, A. and Bertilsson, S. (2004). Composition of freshwater bacterial communities associated with cyanobacterial blooms in four Swedish lakes. *Environmental Microbiology*, 6(12), 1228-1243.

Enright, A. M., Collins, G., and O'Flaherty, V. (2007). Low-temperature anaerobic biological treatment of toluene-containing wastewater. *Water Research*, 41(7), 1465-1472.

Enright, A. M., McHugh, S., Collins, G., and O'Flaherty, V. (2005). Low-temperature anaerobic biological treatment of solvent-containing pharmaceutical wastewater. *Water Research*, 39(19), 4587-4596.

Fang, H. H. P., Chen, T., Li, Y. Y., and Chui, H. K. (1996). Degradation of phenol in wastewater in an upflow anaerobic sludge blanket reactor. *Water Research*, 30(6), 1353-1360.

Farhadian, M., Duchez, D., Vachelard, C., and Larroche, C. (2008). Monoaromatics removal from polluted water through bioreactors-A review. *Water Research*, 42(6-7), 1325-1341.

Flint, L. (2005). Bitumen recovery technology: A review of long term R and D opportunities. Calgary, Alberta.

Frankin, R. J. (2001). Full-scale experiences with anaerobic treatment of industrial wastewater. *Water Science and Technology*, 44(8), 1-6.

Gamal El-Din, M., Fu, H. J., Wang, N., Chele-Ayala, P., Perez-Estrada, L., Drzewicz, P., Martin, J. W., Zubot, W. and Smith, D. W. (2011). Naphthenic acids specitation and removal during pertroleum-coke adsorption and ozonation of oil sands process-affected water. Science of Total Environment, 409(2011), 5119-5125.

Gerardi, M. H. (2007). ORP management in wastewater as an indicator of process efficiency. Retrieved from https://www.ysi.com/File%20Library/Documents/Application%20Notes/A567-ORP-Management-in-Wastewater-as-an-Indicator-of-Process-Efficiency.pdf

Goi, A., Kulik, N., Trapido, M. (2006). Combined chemical and biological treatment of oil contaminated soil. *Chemosphere*, 63, 1754-1763.

Grewer, D. M., Young, R. F., Whittal, R. M., and Fedorak, P. M. (2010). Naphthenic acids and other acid-extractables in water samples from Alberta: What is being measured? *Science of the Total Environment*, 408(23), 5997-6010.

Gunawan, Y., Nemati, M. and Dalai, A. (2014). Biodegradation of a surrogate naphthenic acid under denitrifying conditions. *Water Research*, 51(2014), 11-24.

Haller, L., Tonolla, M., Zopfi, J., Peduzzi, R., Wildi, W. and Pote, J. (2011). Composition of bacterial and archaeal communities in freshwater sediments with different contamination levels (Lake Geneva, Switzerland). *Water Research*, 45(3), 1213-1228.

Han, X., MacKinnon, M. D. and Martin, J. W. (2009). Estimating the in situ biodegradation of naphthenic acids in oil sands process waters by HPLC/HRMS. *Chemosphere*, 76(1), 63- 70.

Han, X., Scott, A. C., Fedorak, P. M., Bataineh, M. and Martin, J. W. (2008). Influence of molecular structure on the biodegradability of naphthenic acids. *Environmental Science and Technology*, 42(4), 1290-1295.

Headley, J. V., and McMartin, D. W. (2004). A review of the occurrence and fate of naphthenic acids in aquatic environments. *Journal of Environmental Science and Health. Part A, Toxic/Hazardous Substances and Environmental Engineering*, 39(8), 1989-2010.

Headley, J. V., Du, J. L., Peru, K. M. and McMartin, D. W. (2009). Electrospray ionization mass spectrometry of the photodegradation of naphthenic acids mixtures irradiated with titanium dioxide. *Journal of Environmental Science and Health. Part A, Toxic/Hazardous Substances and Environmental Engineering*, 44(4), 591-597.

Hoigne, J. "Chemistry of Aqueous Ozone and Transformation of Pollutants by Ozonation and Advanced Oxidation Processes" in *The Handbook of Environmental Chemistry*, Vol. 5 Part C, *Quality and Treatment of Drinking Water II*. Ed. J. Hrubec. Berlin: Springver-Verlag, 1998. 83-141. Print.

Holowenko, F. M., MacKinnon, M. D., and Fedorak, P. M. (2000). Methanogens and sulfate-reducing bacteria in oil sands fine tailings waste. *Canadian Journal of Microbiology*, 46(10), 927-937.

Holowenko, F.M., Mackinnon, M. D. and Fedorak, P. M. (2001). Naphthenic acids and surrogate naphthenic acids in methanogenic microcosms. *Water Research*, 35(11), 2595-2606.

Huang, C., Shi, Y., Gamal El-Din, M. and Liu, Y. (2015). Treatment of oil sands process-affected water (OSPW) using ozonation combined with integrated fixed-film activated sludge (IFAS). *Water Research*, 85, 167–176.

Huang, J., Nemati, M., Hill, G., and Headley, J. (2012). Batch and continuous biodegradation of three model naphthenic acids in a circulating packed-bed bioreactor. *Journal of Hazardous Materials*, 201, 132-140.

Hwang, G., Dong, T., Islam, M. S., Sheng, Z. Y., Perez-Estrada, L. A., Liu, Y., and Gamal El-Din, M. (2013). The impacts of ozonation on oil sands process-affected water biodegradability and biofilm formation characteristics in bioreactors. *Bioresource Technology*, 130, 269-277.

Ibrahim, M. D. (2018). Oil sands process-affected water characterization and application of adsorption process for the removal of naphthenic acids (Doctoral dissertation). Retrieved from https://era.library.ualberta.ca/items/33cb87b3-1e0c-4120-b626-34a7f220d2fe

Islam, M. S., Dong, T., Sheng, Z., Zhang, Y., Liu, Y. and Gamal El-Din, M. (2013). Microbial community structure and operational performance of a fluidized bed biofilm reactor treating oil sands process-affected water. *International Biodeterioration and Biodegradation*, 91, 111-118.

Islam, M. S., Moreira, J., Chelme-Ayala, P. and Gamal El-Din, M. (2014). Prediction of naphthenic acid species degradation by kinetic and surrogate models during the ozonation of oil sands process-affected water. *Science of the Total Environment*, 493, 282-290.

Islam, M. S., Zhang, Y., McPhedran, K. N., Liu, Y. and Gamal El-Din, M. (2015). Granular activated carbon for simultaneous adsorption and biodegradation of toxic oil sands process affected water organic compounds. *Journal of Environmental Management*, 152, 49-57.

Jeroschewski, P., Steuckart, C. and Kuhl, M. (1996). An amperometric microsensor for the determination of H_2S in aquatic environments. *Analytical Chemistry*, 68(24), 4351-4357.

Kabisch, A., Otto, A., Konig, S., Becher, D., Albrecht, D., Schuler, M., Teeling, H., Ammann, R. I. and Schweder, T. (2014). Functional characterization of polysaccharide utilization loci in the marine Bacteroidetes 'Gramella forsetii' KT0803. *International Seociety for Microbial Ecology*, 8, 1492-1502.

Kannel, P. R., and Gan, T. Y. (2012). Naphthenic acids degradation and toxicity mitigation in tailings wastewater systems and aquatic environments: A review. *Journal of Environmental Science and Health. Part A, Toxic/Hazardous Substances and Environmental Engineering*, 47(1), 1-21.

Kasperski, K. L. (1992). A review of properties and treatment of oil sands tailings. *AOSTRA Journal of Research*, 8(1), 11-53.

Kato, M. T., Field, J. A., Versteeg, P., and Lettinga, G. (1994). Feasibility of expanded granular sludge bed reactors for the anaerobic treatment of low-strength soluble wastewaters. *Biotechnology and Bioengineering*, 44(4), 469-479.

Kennedy, E. J. and Lentz, E. M. (2000). Treatment of landfill leachate using sequencing batch and continuous flow upflow anaerobic sludge blanket (UASB) reactors. *Water Research*, 34(14), 3640-3656.

Kindaichi, T., Okabe, S., Satoh, H. and Watanabe, Y. (2004). Effects of hydroxylamine on microbial community structure and function of autotrophic nitrifying biofilms determined by in situ hybridization and the use of microelectrodes. *Water Science and Technology*, 49(11-12), 61-68.

Kragelund, C., Levantesi, C., Borger, A., Thelen, K., Eikelboom, D., Tandoi, V., Kong, Y. H., van der Waarde, J., Krooneman, J., Rossetti, S., Thomsen, T. R. and Nielsen, P. H. (2007). Identity, abundance and ecophysiology of filamentous *Chloroflexi* species present in activated sludge treatment plants. *FEMS Microbiology Ecology*, 59 (3), 671-682.

Lettinga, G. (1995). Anaerobic-digestion and waste-water treatment systems. *Antonie Van Leeuwenhoek International Journal of General and Molecular Microbiology*, 67(1), 3-28.

Liu, H. (2015). Community structure and microbial activity of sulfate reducing bacteria in wastewater biofilms and mature fine tailings analyzed by microsensors and molecular biology techniques (Doctoral dissertation). Retrieved from https://era.library.ualberta.ca/items/3d971e34-1a5e-41ba-9e7e-17b87e7ee4cd

Liu, Z. F., Frigaard, N.-U., Vogl, K., Iino, T., Ohkuma, M., Overmann, J. and Bryant, D. (2012). Complete genome of *Ignavibacterium album*, a metabolically versatile, flagellated, facultative anaerobe from the phylum Cholrobi. *Frontiers in Microbiology*, 3(185).

Loy, A., Schulz, C., Lücker, S., Stoecker, K., Baranyi, C., Lehner, A., Wagner, M., Lu, S. and Scho, A. (2005). Microarray for environmental monitoring of the betaproteobacterial order 16s rrna gene-based oligonucleotide microarray for environmental monitoring of the betaproteobacterial order "Rhodocyclales". *Applied and Environmental Microbiology*, 71(3), 1373-1373.

Ma, J. X., Wang, Z. W., Yang, Y., Mei, X. J. and Wu, Z. C. (2013). Correlating microbial community structure and composition with aeration intensity in submerged membrane bioreactors by 454 high-throughput pyrosequencing. *Water research*, 47(2), 859-869.

Marchal, R., Penet, S., Solano-Serena, F., and Vandecasteele, J. P. (2003). Gasoline and diesel oil biodegradation. *Oil and Gas Science and Technology-Revue d'IFP Energies nouvelles*, 58(4), 441-448.

Martin, K. J. and Nerenberg, R. (2012). The membrane biofilm reactor (MBfR) for water and wastewater treatment: principles, applications, and recent developments. *Bioresource Technology*, 122, 83-94.

McMartin, D. W., Headley, J. V., Friesen, D. A., Peru, K. M. and Gillies, J. A. (2004). Photolysis of naphthenic acids in natural surface water. *Journal of Environmental Science and Health. Part A, Toxic/Hazardous Substances and Environmental Engineering*, 39(6), 1361-1383.

McQuarrie, J. P., and Boltz, J. P. (2011). Moving bed biofilm reactor technology: process applications, design, and performance. *Water Environment Research*, 83(6), 560-575.

Mishra, S., Meda V., Dalai, A. K., McMartin, D. W., Headley, J. V. and Peru, K. M. (2010). Photocatalysis of naphthenic acids in water. *Journal of Water Resource and Protection*, 2(7), 645-650.

Misiti, T., Tandukar, M., Tezel, U. and Pavlostathis, S. G. (2013). Inhibition and Biotransformation Potential of Naphthenic Acids under Different Electron Accepting Conditions. *Water Research*, 47(1), 406-418.

Moussavi, G., Mahmoudi, M., and Barikbin, B. (2009). Biological removal of phenol from strong wastewaters using a novel MSBR. *Water Research*, 43(5), 1295-1302.

Nerenberg R. (2016). The membrane-biofilm reactor (MBfR) as a counter-diffusional biofilm process. *Current Opinion in Biotechnology*, 38, 131-136.

Ohandja, D. G. and Stuckey, D. C. (2007). Biodegradation of PCE in a hybrid membrane aerated biofilm reactor. *Journal of Environmental Enginnering*, 133(1), 20-27.

Okabe, S., Satoh, H., and Kindaichi, T. (2011). A polyphasic approach to study ecophysiology of complex multispecies nitrifying biofilms. In M. G. Klotz and L. Y. Stein (Eds.), Methods in Enzymology, Vol 46: Research on Nitrification and Related Processes, Pt B (Vol. 496, pp. 163-184). San Diego: Elsevier Academic Press Inc.

Penner, T. J., and Foght, J. M. (2010). Mature fine tailings from oil sands processing harbour diverse methanogenic communities. *Canadian Journal of Microbiology*, 56(6), 459-470.

Quagraine, E. K., Peterson, H. G., and Headley, J. V. (2005). In situ bioremediation of naphthenic acids contaminated tailing pond waters in the Athabasca oil sands region-demonstrated field studies and plausible options: A review. *Journal of Environmental Science and Health. Part A, Toxic/Hazardous Substances and Environmental Engineering*, 40(3), 685-722.

Quinlan, P. J., and Tam, K. C. (2015). Water treatment technologies for the remediation of naphthenic acids in oil sands process-affected water. *Chemical Engineering Journal*, 279, 696-714.

Reasoner, D. J. and Gelderich, E. E. (1985). A new medium for the enumeration and subculture of bacteria from potable water. *Applied and Environmental Microbiology*, 49(1), 1-7.

Rebac, S., van Lier, J. B., Lens, P., Stams, A. J. M., Dekkers, F., Swinkels, K. T. M., and Lettinga, G. (1999). Psychrophilic anaerobic treatment of low strength wastewaters. *Water Science and Technology*, 39(5), 203-210.

Revsbech, N. P. (2005). Analysis of microbial communities with electrochemical microsensors and microscale biosensors. *Environmental Microbiology*, 397, 147-166.

Revsbech, N. P. and Jorgensen, B. B. (1986). Microelectrodes: their use in microbial ecology. *Advances in Microbial Ecology*, 9, 293-352.

Rincon, N., Chacin, E., Marin, J., Torrijos, M., Moletta, R., and Fernandez, N. (2003). Anaerobic biodegradability of water separated from extracted crude oil. *Environmental Technology*, 24(8), 963-970.

Rinzema, A. (1993). Anaerobic digestion of long-chain fatty acids in UASB and expanded granular sludge bed reactors. *Process Biochemistry*, 28, 527-537.

Rudzinski, W. E., Oehlers, L., Zhang, Y., and Najera, B. (2002). Tandem mass spectrometric characterization of commercial naphthenic acids and a Maya crude oil. *Energy and Fuels*, 16(5), 1178-1185.

Salloum, M. J., Dudas, M. J., and Fedorak, P. M. (2002). Microbial reduction of amended sulfate in anaerobic mature fine tailings from oil sand. *Waste Management and Research*, 20(2), 162-171.

Schloss, P. D., Westcott, S. L., Ryabin, T., Hall, J. R., Hartmann, M., Hollister, E. B., Lesniewski, R. A., Oakley, B. B., Parks, D. H., Robinson, C. J., Sahl, J. W., Stres, B., Thallinger, G. G., Van Horn, D. J., Weber, C.F. (2009). Introducing mothur: Open-Source,

Platform-Independent, Community-Supported Software for Describing and Comparing Microbial Communities. *Applied and Environmental Microbiology*, 75(23), 7537-7541.

Schneider, E. E., Cerqueira, A., and Dezotti, M. (2011). MBBR evaluation for oil refinery wastewater treatment, with post-ozonation and BAC, for wastewater reuse. *Water Science and Technology*, 63(1), 143-148.

Scott, A. C., Young, R. F., and Fedorak, P. M. (2008). Comparison of GC-MS and FTIR methods for quantifying naphthenic acids in water samples. *Chemosphere*, 73(8), 1258-1264.

Siddique, T., Fedorak, P. M., and Foght, J. M. (2006). Biodegradation of short-chain *n*-alkanes in oil sands tailings under methanogenic conditions. *Environmental Science and Technology*, 40(17), 5459-5464.

Syron, E. and Casey, E. (2008). Membrane-aerated biofilms for high rate biotreatment: Performance appraisal, engineering principles, scale-up, and development requirements. *Environmental Science and Technology*, 42(6), 1833-1844.

Tan, S. Y. (2012). Multiple microbial processes in membrane aerated biofilms studied using microsensors (Doctoral dissertation). Retrieved from https://era.library.ualberta.ca/items/68670d42-b0c4-4590-96e6-2344ad207653

Tan, S. Y. and Yu, T. (2007). Fabrication of an amperometric H_2S microsensor and its application in wastewater biofilms. Proceedings of International Workshop on Monitoring and Sensors for Water Pollution Control, Beijing, China.

Tan, S. Y., Yu, T., and Shi, H. C. (2014). Microsensor determination of mutiple microbial processes in an oxygen-based membrane aerated biofilm. *Water Science and Technology*, 69(5), 909-914.

Toor, N. S., Franz, E. D., Fedorak, P. M., MacKinnon, M. D., and Liber, K. (2013). Degradation and aquatic toxicity of naphthenic acids in oil sands process-affected waters using simulated wetlands. *Chemosphere*, 90(2), 449-458.

U. S. Army Corps of Engineers. (2001). Engineering and design: Adsorption design guide. Retrieved from http://www.dtic.mil/dtic/tr/fulltext/u2/a403095.pdf

Van den Tweel, W. J. J., Smits, J. P. and de Bont, J. A. M. (1988). Catabolism of DL-α-phenylhydracrylic, phenylacetic and 3-and 4-hydroxyphenylacetic acid via homogentisic acid in a *Flavobacterium* sp. *Archives of Microbiology*, 149(3), 207-213.

Vieira, D. S., Servulo, E. F. C., and Cammarota, M. C. (2005). Degradation potential and growth of anaerobic bacteria in produced water. *Environmental Technology*, 26(8), 915-922.

Wang, X., Chen, M., Xiao, J., Hao, L., Crowley, D.E., Zhang, Z., Yu, J., Huang, N., Huo, M. and Wu, J. (2015). Genome sequence analysis of the naphthenic acid degrading and metal resistant bacterium *Cupriavidus gilardii* CR3. *PLOS ONE*, 10(8), e0132881.

Whitby, C. (2010). Microbial naphthenic acid degradation. In A. I. Laskin, S. Sariaslani, and G. M. Gadd (Eds.), Advances in Applied Microbiology, Vol 70 (Vol. 70, pp. 93-125). San Diego: Elsevier Academic Press Inc.

Wittbolle, L., Marzorati, M., Clement, L., Balloi, A., Daffonchio, D., Heylen K., De Vos, P., Verstraete, W. and Boon, N. (2009). Initial community evenness favours functionality under selective stress. *Nature*, 458, 623-626.

Wobus, A., and Roske, I. (2000). Reactors with membrane-grown biofilms: their capacity to cope with fluctuating inflow conditions and with shock loads of xenobiotics. *Water Research*, 34(1), 279-287.

Wobus, A., Ulrich, S., and Roske, I. (1995). Degradation of chlorophenols by biofilms on semi-permeable membranes in two types of fixed bed reactors. *Water Science and Technology*, 32(8), 205-212.

Woolard, C. R., and Irvine, R. L. (1995). Response of a periodically operated halophilic biofilm reactor to changes in salt concentration. *Water Science and Technology*, 31(1), 41-50.

Xue, J. K, Zhang, Y., Liu, Y. and Gamal El-Din, M. (2016a). Treatment of oil sands process-affected water (OSPW) using a membrane bioreactor with a submerged flat-sheet ceramic microfiltration membrane. *Water Research*, 88, 1-11.

Xue, J. K., Zhang, Y., Liu, Y. and Gamal El-Din, M. (2016b). Treatment of raw and ozonated oil sands process-affected water under decoupled denitrifying anoxic and nitrifying aerobic conditions: a comparative study. *Biodegradation*, 27(4-6), 247-264.

Xue, J. K., Zhang, Y. Y., Liu, Y. and Gamal El-Din, M. (2017). Dynamics of naphthenic acids and microbial community structures in a membrane bioreactor treating oil sands process-affected water: impacts of supplemented inorganic nitrogen and hydraulic retention time. *RSC Advances*, 7 (29), 17670-17681.

Xue, J. K., Huang, C. K., Zhang, Y. Y., Liu, Y. and Gamal El-Din, M. (2018). Bioreactors for oil sands process-affected water (OSPW) treatment: A critical review. *Science of the Total Environment*, 627, 916-933.

Yang, Y., Quensen, J., Mathieu, J., Wang, Q., Wang, J., Li, M. Y., Tiedje, M. J. and Alvarez, J. J. P. (2014). Pyrosequencing reveals higher impact of silver nanoparticles than Ag^{+} on the microbial community stucture of activated sludge. *Water Research*, 48(1), 317-325.

Yergeau, E., Lawrence, J. R., Sanschagrin, S., Waiser, M. J., Korber, D. R. and Greer, C. W. (2012). Next-generation sequencing of microbial communities in the Athabasca River and its tributaries in relation to oil sands mining activities. *Applied and Environmental Microbiology*, 78(21), 7626-7637.

Yu, M. (2014). Biodegradation of organic compounds in OSPW with microbial community indigenous to MFT (Masteral dissertation). Retrieved from https://era.library.ualberta.ca/files/vd66w023x

Yu, T. (2000). Stratification of microbial process and redox potential changes in biofilms. PhD Thesis. University of Cincinnati. Cincinnati, USA.

Yu, T., and Bishop, P. L. (1998). Stratification of microbial metabolic processes and redox potential change in an aerobic biofilm studied using microelectrodes. *Water Science and Technology*, 37(4-5), 195-198.

Zhang, T. C. and Bishop, P. L. (1996). Evaluation of substrate and pH effects in a nitrifying biofilm. *Water Environment Research*, 68(7), 1107-1115.

Zhang, Y., McPhedran, K. N. and Gamal El-Din, M. (2015). Pseudomonads biodegradation of aromatic compounds in oil sands process-affected water. *Science of the total environment*, 521-522(2015), 59-67.

APPENDICES

Appendix A

Table A-1 Accessories information of MBBR and MABR biological treatment system

Name	Catalogue NO.	Capacity	Dimensions	Quality	Description
Refrigerator	Western Refrigeration SAKT-48-FA	51 Cubic ft. 2 Solid Doors 8 Shelves	34" D x 56.5" L x 76.5" H	1	Influent container
Stir- Pak Heavy-Duty Mixer System	S-50007-22	9-900 RPM	115, 50/60	6	For reactor mixing CP
L/S variable-Speed Modular Drives	S-07553-80	1-100 RPM	90-130 VAC	4	Influent pump
L/S Easy-Load 3 Pump Heads	S-77800-60			10	Pump water
L/S variable-Speed Modular Drives with wall-mount controller	S-07552-70	6-600 rpm		8	Pump process water
Tubing influent	S-06424-14	7.6 m	1.6 mm	3	For influent NO O_2 permeability
Tubing for recycle water	S-96420-16	7.6 m	3.1 mm	3	For recycling water NO O_2 permeability Acid and base resistant

Appendix B

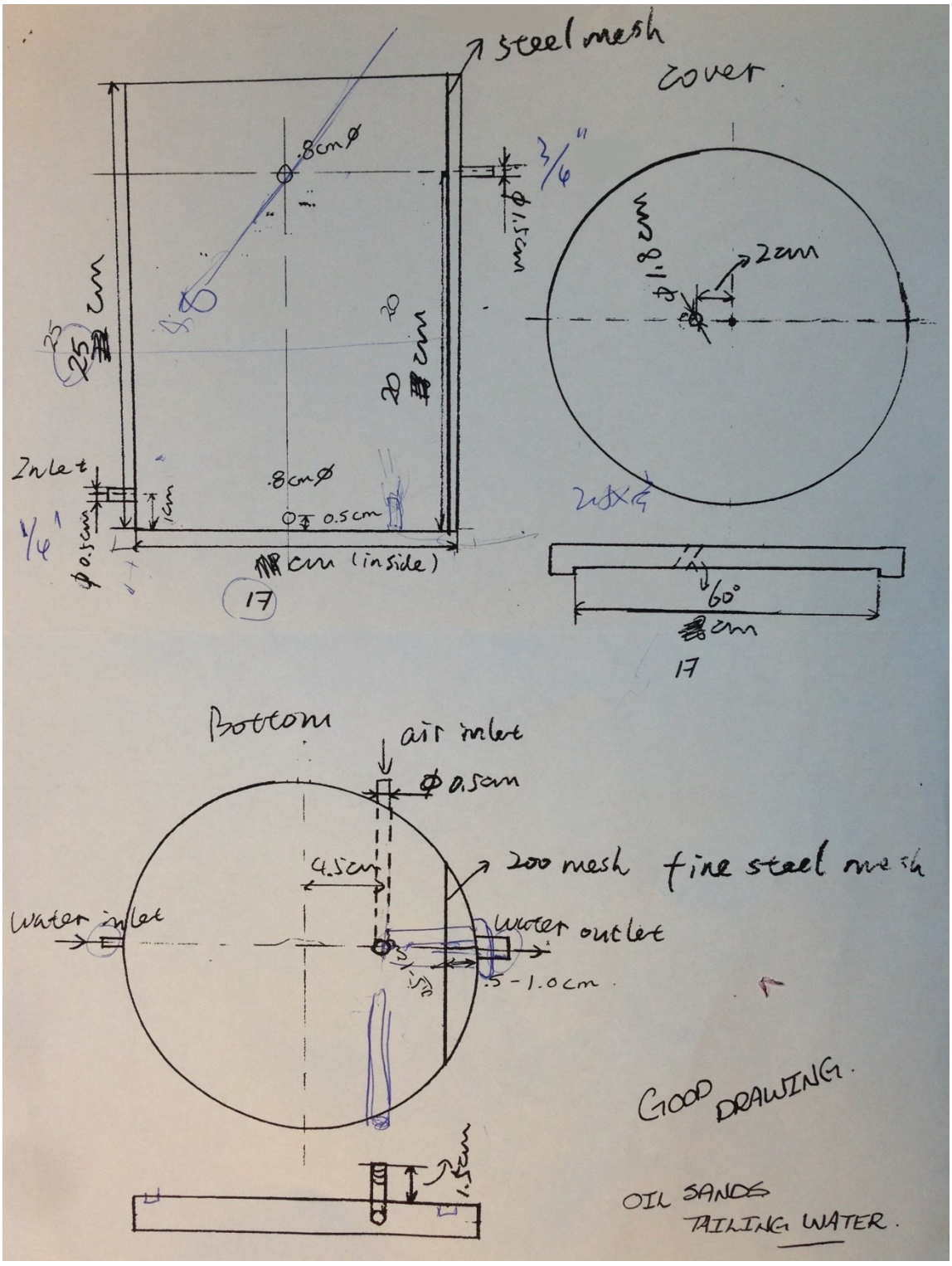

Figure B-1 Handwriting of MBBR design draft

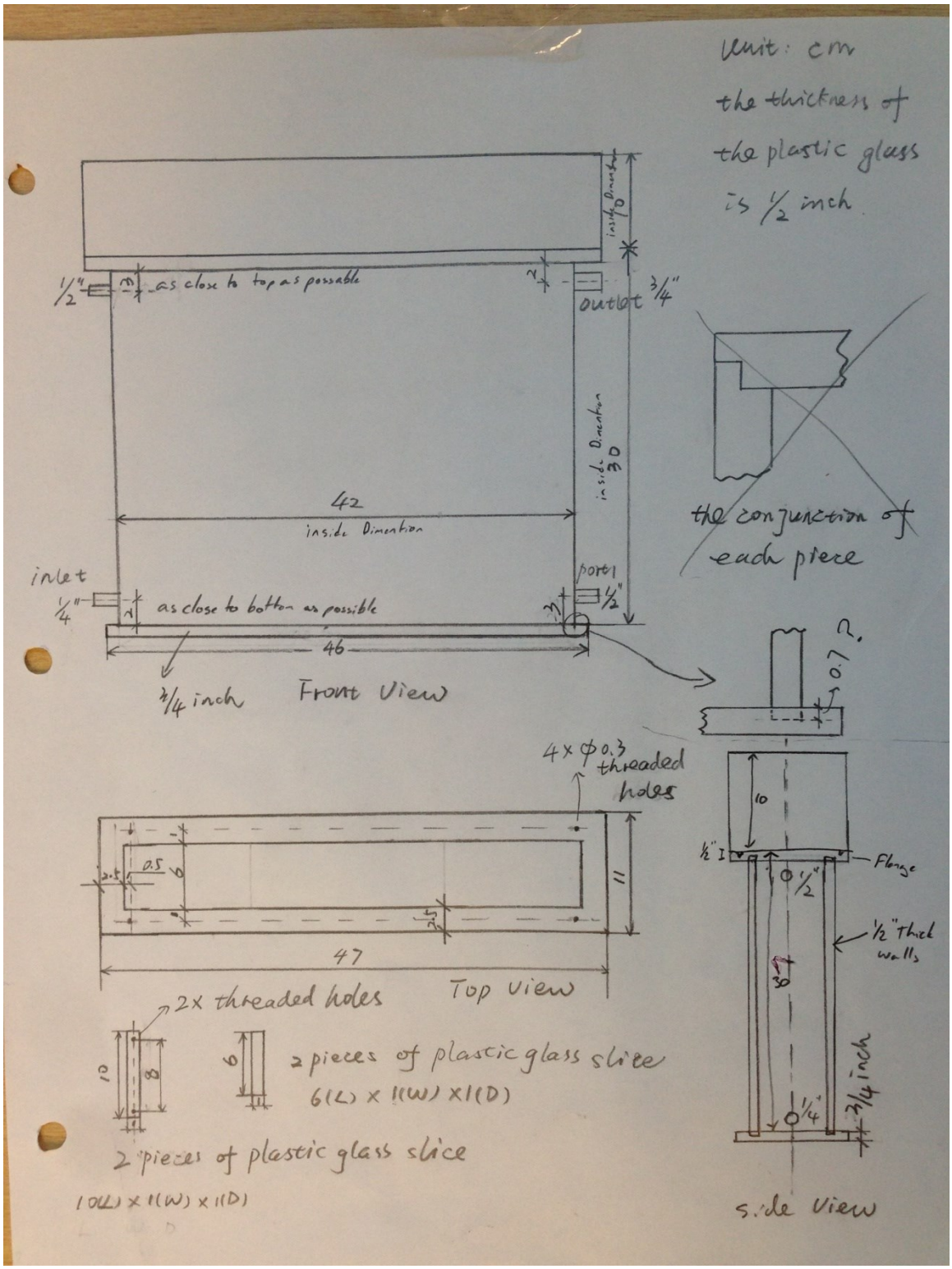

Figure B-2 Handwriting of MABR design draft

Figure B-3 Remote control mixer 04561-50 with universal clamp mounting and analog speed controller

Table B-1 The permeability of different kinds of gases in the hollow fiber

Gas	Permeability $(\frac{10^{-8}cm^3 \cdot cm}{cm^2 \cdot s \cdot cmHg})$
N_2	2.5
CO	3
Ne	3.1
He	3.2
O_2	5
NO	5.3
Ar	5.3
H_2	5.7
CH_4	8.3
Kr	10
C_2H_4	13.3
CO_2	15.3
C_2H_6	16
NH_3	20.9
Xe	22.8
C_3H_8	25
H_2S	88.4
NO_2	133
H_2O (steam)	318
CS_2	793

Appendix C Data for Figures in Each Chapter

Table C-1 Data for Figure 3-2 Ammonium, nitrite and nitrate concentration changes in the SBR on Day 1

Time	NH_4^+ (mg/L)			NO_3^- (mg/L)			NO_2^- (mg/L)			PO_4^{3-} (mg/L)		
Influent	23.4	24.4	23.9	0.0	0.0	0.0	0.0	0.0	0.0	0.0	0.0	0.0
0.5h	22.0	22.3	22.2	24.3	24.8	24.6	0.0	0.0	0.0	4.9	4.8	4.9
1h	20.2	20.1	20.2	25.0	24.9	25.0	6.0	5.9	6.0	6.5	6.8	6.7
2h	18.2	17.5	17.9	25.8	25.4	25.6	9.2	9.7	9.5	6.7	6.9	6.8
3h	15.7	14.2	15.0	28.9	29.7	29.3	12.0	12.4	12.2	6.5	6.4	6.5
4h	9.3	9.7	9.5	31.0	32.1	31.6	16.3	16.4	16.4	5.8	5.8	5.8
5h	0.0	0.0	0.0	34.7	34.6	34.7	20.0	19.4	19.7	7.7	7.9	7.8
6h	0.0	0.0	0.0	48.9	48.2	48.6	20.4	20.6	20.5	4.9	5.1	5.1
8h	0.0	0.0	0.0	45.8	46.4	46.1	22.1	22.2	22.2	9.3	8.6	9.0
9h	0.0	0.0	0.0	55.4	54.8	55.1	15.0	15.2	15.1	7.4	7.8	7.6
10h	0.0	0.0	0.0	64.0	64.6	64.3	11.0	10.8	10.9	7.9	7.4	7.7
12h	-	-	-	68.7	70.1	69.4	0.0	0.0	0.0	8.1	8.8	8.5
24h	-	-	-	75.0	73.7	74.4	0.0	0.0	0.0	7.8	8.2	8.0
30h	-	-	-	-	-	-	0.0	0.0	0.0	8.9	9.0	9.0

Table C-2 Data for Figure 3-3 Profile of COD concentrations of the SBR over the operation time

Time (Day)	Influent COD (mg/L)			Effluent COD (mg/L)			Removal (%)
	Rep 1	Rep 2	Mean	Rep 1	Rep 2	Mean	
1	299	320	310	225	229	227	27
2	248	261	254	226	235	231	9
3	243	251	248	206	219	213	14
4	253	268	261	206	212	209	20
5	251	263	257	198	208	203	21
6	263	278	270	206	224	215	20
7	256	280	268	212	214	213	21
8	256	261	259	208	211	210	19
9	266	276	271	214	227	220	19
10	261	263	263	199	223	211	20
11	253	265	259	191	210	201	22
12	258	275	267	204	219	212	21
13	255	261	258	197	219	208	19

14	246	263	254	197	206	201	21
15	245	254	249	192	204	198	20
16	256	270	263	219	222	220	16
17	252	270	261	201	209	205	21
18	266	269	268	202	219	210	22
19	273	280	276	219	221	220	20
20	275	287	281	212	227	219	22
21	268	270	269	203	211	207	23
22	260	268	264	202	218	210	20
23	268	283	275	225	232	228	17
24	260	278	269	219	218	218	19
25	267	276	271	207	212	209	23
26	268	280	274	204	235	220	20
27	274	289	281	208	224	216	23
28	250	276	263	196	203	199	24
29	257	261	259	192	210	201	22
30	260	271	265	208	219	213	20
31	266	280	273	207	223	215	21
32	264	272	268	208	213	210	22
33	253	265	259	203	214	208	20

Table C-3 Data for Figure 3-5 Profile of pH and DO of the CASR over the operation time

Time (Day)	pH	DO (mg/L)	Time	pH	DO (mg/L)	Time (Day)	pH	DO (mg/L)
0	7.29	1.56	25	8.04	3.1	117	7.85	3.1
1	7.58	1.36	30	7.89	2.8	124	8.12	2.7
2	7.28	0.8	35	7.98	3.2	131	8.01	2.9
4	7.35	3	40	8.02	2.6	136	7.98	2.8
6	7.75	2.5	45	8.04	2.8	142	7.68	2.7
7	7.67	3.5	50	7.85	3.1	150	8.1	2.6
8	7.93	2.8	57	7.86	2.9	157	7.94	2.9
9	7.65	2.7	77	7.9	3.1	164	7.89	3.2
12	7.89	2.4	83	7.8	2.7	170	7.92	2.6
15	7.98	2.7	90	8.1	2.8	177	7.91	3.2
18	7.91	2.6	100	8.2	2.6	182	8.14	2.7
21	8.02	2.8	110	7.93	2.9			

Table C-4 Data for Figure 3-6 Profile of COD for the CASR over the operation time

Time (Day)	Influent COD (mg/L)			Effluent COD (mg/L)			Removal (%)
	Rep 1	Rep 2	Mean	Rep 1	Rep 2	Mean	
0	303	317	310	243	234	239	23
5	-	-	310	214	206	210	32
10	-	-	310	181	198	190	39
15	-	-	310	197	191	194	37
23	-	-	310	185	193	189	39
43	281	299	290	199	181	190	34
49	-	-	290	184	162	173	40
56	-	-	290	177	190	184	37
66	-	-	290	189	171	180	38
83	310	316	313	200	190	195	38
90	-	-	313	194	179	187	40
97	-	-	313	191	191	191	39
104	-	-	313	195	183	189	40
119	287	305	296	194	172	183	38
126	-	-	296	173	168	171	42
133	-	-	296	191	173	182	39
139	-	-	296	181	168	175	41
151	351	370	361	191	177	184	49

Table C-5 Data for Figure 4-6 COD performance of MBBR during operation at different phases

Time (Day)	Influent COD (mg/L)			Effluent COD (mg/L)			Removal (%)
	Rep 1	Rep 2	Mean	Rep 1	Rep 2	Mean	
1	914	894	904	497	475	486	46
2	906	896	901	370	340	355	61
3	906	890	898	289	265	277	69
4	889	871	880	293	271	282	68
5	912	888	900	290	274	282	69
6	904	882	893	277	249	263	71
7	914	896	905	293	263	278	69
8	917	877	897	234	212	223	75
9	909	881	895	265	239	252	72
11	908	894	901	213	197	205	77

12	897	879	888	188	166	177	80
13	902	886	894	196	168	182	80
15	912	892	902	203	181	192	79
17	907	889	898	211	193	202	78
18	905	893	899	223	193	208	77
19	913	887	900	212	188	200	78
21	917	881	899	200	180	190	79
22	917	895	906	153	137	145	84
23	912	872	892	160	138	149	83
25	911	871	891	167	151	159	82
27	906	890	898	168	142	155	83
29	919	885	902	163	145	154	83
31	912	886	899	186	158	172	81
33	913	887	900	170	148	159	82
34	895	867	881	189	171	180	80
35	912	892	902	198	180	189	79
37	892	872	882	178	160	169	81
39	906	890	898	185	155	170	81
41	928	890	909	187	163	175	81
43	905	879	892	193	173	183	79
45	916	888	902	170	148	159	82
47	927	909	918	210	188	199	78
49	951	937	944	167	143	155	84
51	950	932	941	164	140	152	84
53	943	933	938	150	130	140	85
55	931	909	920	157	133	145	84
57	959	921	940	160	138	149	84
59	945	921	933	173	145	159	83
61	954	936	945	168	142	155	84
63	955	919	937	165	143	154	84
65	954	916	935	186	158	172	82
67	951	931	941	172	146	159	83
69	940	916	928	189	171	180	81
71	943	925	934	198	180	189	80
73	955	929	942	180	158	169	82

75	947	929	938	178	162	170	82
77	955	923	939	189	161	175	81
79	959	921	940	197	169	183	81
81	954	924	939	174	144	159	83
83	953	939	946	208	190	199	79
85	945	919	932	175	149	162	83
87	941	921	931	182	154	168	82
89	945	931	938	217	193	205	78
91	953	931	942	185	169	177	81
93	957	921	939	190	174	182	81
95	946	934	940	203	181	192	80
97	939	903	921	210	194	202	78
99	960	924	942	223	193	208	78
102	938	906	922	211	189	200	78
105	956	920	938	190	168	179	81
108	969	929	949	180	158	169	82
111	946	918	932	177	157	167	82
114	926	916	921	175	149	162	82
117	922	894	908	178	158	168	81
120	915	879	897	188	170	179	80
123	908	876	892	179	149	164	82
126	899	875	887	178	162	170	81
129	910	884	897	161	137	149	83
132	906	874	890	177	157	167	81
135	917	885	901	168	142	155	83
138	919	907	913	162	134	148	84
141	922	900	911	159	131	145	84
144	919	893	906	240	216	228	75
147	907	873	890	221	199	210	76
150	915	891	903	207	187	197	78
153	921	889	905	213	193	203	78
156	897	877	887	222	198	210	76
159	910	872	891	238	216	227	75
162	901	877	889	224	206	215	76
165	920	902	911	218	192	205	77

168	916	892	904	228	208	218	76
171	490	480	485	219	203	211	56
174	499	481	490	227	217	222	55
177	504	470	487	161	149	155	68
180	501	481	491	161	147	154	69
183	494	482	488	180	164	172	65
186	491	469	480	165	153	159	67
189	498	486	492	188	172	180	63
192	507	471	489	199	179	189	61
195	501	483	492	174	164	169	66
198	505	485	495	180	160	170	66
201	504	472	488	183	167	175	64
204	535	517	526	194	184	189	64
207	-	-	526	132	120	126	76
210	-	-	526	141	129	135	74
213	-	-	526	161	143	152	71
216	-	-	526	144	136	140	73
219	-	-	526	159	141	150	71
222	-	-	526	118	106	112	79
225	534	524	529	106	92	99	81
228	-	-	529	110	96	103	80
231	-	-	529	104	94	99	81
234	-	-	529	104	94	99	81
237	-	-	529	105	85	95	82
240	-	-	529	96	84	90	83
243	-	-	529	93	83	88	83
246	-	-	529	96	80	88	83
249	-	-	529	96	78	87	83
252	548	534	541	90	74	82	85
255	-	-	541	91	75	83	85
258	-	-	541	82	74	78	86
261	-	-	541	84	70	77	86
264	-	-	541	98	86	92	83
267	-	-	541	86	70	78	86
270	-	-	541	99	81	90	83

273	-	-	541	116	102	109	80
276	-	-	541	103	91	97	82
279	-	-	541	107	89	98	82
282	-	-	541	109	97	103	81
285	-	-	541	122	106	114	79
288	524	514	519	96	78	87	83
291	-	-	519	107	89	98	81
294	-	-	519	109	95	102	80
297	-	-	519	112	104	108	79
300	-	-	519	121	107	114	78
303	-	-	519	117	101	109	79
306	-	-	519	110	96	103	80
309	-	-	519	121	107	114	78
312	-	-	519	119	109	114	78
315	-	-	519	110	90	100	81
318	548	530	539	117	103	110	80
321	-	-	539	99	87	93	83
324	-	-	539	122	114	118	78
327	-	-	539	128	110	119	78
330	-	-	539	139	125	132	76
333	-	-	539	122	112	117	78
336	-	-	539	127	113	120	78
339	500	462	481	144	130	137	72
342	-	-	481	158	140	149	69
345	-	-	481	138	120	129	73
348	-	-	481	135	121	128	73
351	-	-	481	141	129	135	72
354	-	-	481	152	144	148	69
357	-	-	481	145	131	138	71
360	-	-	481	146	134	140	71
363	-	-	481	157	137	147	69
366	-	-	481	130	114	122	75
369	468	454	461	127	107	117	75
372	-	-	461	114	94	104	77
375	-	-	461	118	102	110	76

378	-	-	461	118	110	114	75
381	-	-	461	110	98	104	77
384	-	-	461	95	87	91	80
387	-	-	461	121	111	116	75
390	562	522	542	139	121	130	76
393	-	-	542	122	106	114	79
396	-	-	542	116	106	111	80
399	-	-	542	113	105	109	80
402	-	-	542	128	116	122	77
405	-	-	542	141	123	132	76
408	606	574	590	147	129	138	77
411	-	-	590	140	124	132	78
414	-	-	590	147	133	140	76
417	-	-	590	114	100	107	82
420	-	-	590	121	103	112	81
423	-	-	590	119	99	109	82
426	-	-	590	122	114	118	80
429	-	-	590	138	120	129	78
432	-	-	590	121	105	113	81
435	552	522	537	124	106	115	79
438	-	-	537	117	109	113	79
441	-	-	537	107	91	99	82
444	-	-	537	111	93	102	81
447	-	-	537	104	90	97	82
450	-	-	537	113	97	105	80
453	-	-	537	107	95	101	81
456	-	-	537	114	98	106	80
459	507	483	495	123	103	113	77
462	-	-	495	127	107	117	76
465	-	-	495	98	88	93	81
468	-	-	495	103	95	99	80
471	-	-	495	100	88	94	81
474	-	-	495	119	99	109	78
477	522	498	510	128	114	121	76
480	-	-	510	118	102	110	78

483	-	-	510	109	101	105	79
486	-	-	510	113	97	105	79
489	-	-	510	120	100	110	78
492	544	508	526	110	102	106	80
495	-	-	526	117	109	113	79
498	-	-	526	124	110	117	78
501	-	-	526	123	109	116	78
504	-	-	526	117	105	111	79
507	524	514	519	127	109	118	77
510	-	-	519	107	99	103	80
513	-	-	519	119	99	109	79
516	-	-	519	115	105	110	79
519	-	-	519	111	103	107	79
522	-	-	519	118	108	113	78
525	499	489	494	125	115	120	76
528	-	-	494	128	108	118	76
531	-	-	494	120	100	110	78
534	-	-	494	126	114	120	76
537	-	-	494	133	113	123	75
540	557	519	538	119	101	110	80
543	-	-	538	115	103	109	80
546	-	-	538	132	120	126	77
549	-	-	538	126	112	119	78
552	-	-	538	120	100	110	80
555	506	496	501	107	95	101	80
558	-	-	501	114	102	108	78
561	-	-	501	95	87	91	82
564	-	-	501	90	82	86	83
567	-	-	501	88	78	83	83
570	551	517	534	111	97	104	81
573	-	-	534	112	104	108	80
576	-	-	534	113	103	108	80
579	-	-	534	119	103	111	79
582	-	-	534	112	100	106	80
585	556	516	536	109	89	99	82

588	-	-	536	111	95	103	81
591	-	-	536	115	97	106	80
594	-	-	536	121	101	111	79
597	-	-	536	111	97	104	81
600	561	551	556	126	110	118	79
603	-	-	556	126	106	116	79
606	-	-	556	129	113	121	78
609	-	-	556	119	99	109	80
612	559	549	554	116	102	109	80
615	-	-	554	132	120	126	77
618	-	-	554	120	112	116	79
621	-	-	554	141	125	133	76
624	-	-	554	135	121	128	77
627	547	527	537	120	110	115	79
630	-	-	537	128	108	118	78
633	-	-	537	118	106	112	79
636	-	-	537	118	100	109	80
639	527	493	510	106	96	101	80
642	-	-	510	112	98	105	79
645	-	-	510	108	100	104	80
648	-	-	510	114	104	109	79
651	-	-	510	117	107	112	78
654	547	523	535	126	116	121	77
657	-	-	535	115	101	108	80
660	-	-	535	120	112	116	78
663	-	-	535	123	111	117	78
666	-	-	535	110	100	105	80
669	525	509	517	110	90	100	81
672	-	-	517	110	92	101	80
675	-	-	517	124	104	114	78
678	-	-	517	114	106	110	79
681	-	-	517	109	95	102	80
684	-	-	517	108	94	101	80
687	503	483	493	101	93	97	80
690	-	-	493	105	85	95	81

693	-	-	493	109	95	102	79
696	-	-	493	124	104	114	77
699	-	-	493	108	94	101	80
702	-	-	493	104	94	99	80
705	-	-	493	102	92	97	80
708	533	521	527	118	106	112	79
711	-	-	527	128	108	118	78
714	-	-	527	120	110	115	78
717	-	-	527	113	105	109	79
720	-	-	527	111	103	107	80
723	-	-	527	120	100	110	79
726	553	539	546	116	108	112	79
729	-	-	546	106	96	101	82
732	-	-	546	114	102	108	80
735	-	-	546	122	110	116	79
738	-	-	546	119	99	109	80
741	540	506	523	119	101	110	79
744	-	-	523	120	104	112	79
747	-	-	523	114	106	110	79
750	-	-	523	116	98	107	80
753	-	-	523	111	101	106	80
756	525	487	506	115	97	106	79
759	-	-	506	114	94	104	79
762	-	-	506	107	95	101	80
765	-	-	506	113	105	109	78
768	-	-	506	106	90	98	81
771	532	510	521	121	105	113	78
774	-	-	521	119	101	110	79
777	-	-	521	115	99	107	79
780	-	-	521	117	107	112	79
783	-	-	521	115	105	110	79
786	551	531	541	107	97	102	81
789	-	-	541	111	99	105	81
792	-	-	541	111	95	103	81
795	-	-	541	115	95	105	81

Table C-6 Data for Figure 4-7 AEF performance of MBBR during operation at different phases

Time (Day)	Influent COD (mg/L)			Effluent COD (mg/L)			Removal (%)
	Rep 1	Rep 2	Mean	Rep 1	Rep 2	Mean	
36	43.3	42.7	43.0	42.8	41.4	42.1	2.1
37	-	-	43.0	40.5	39.1	39.8	7.4
38	-	-	43.0	41.2	40.8	41.0	4.8
39	43.7	42.6	43.2	40.0	39.6	39.8	7.9
40	-	-	43.2	39.0	38.0	38.5	10.9
41	-	-	43.2	39.6	38.2	38.9	10.0
56	34.3	31.9	33.1	37.8	37.4	37.6	12.0
57	37.4	35.8	36.6	38.8	37.6	38.2	4.2
58	33.8	32.4	33.1	37.7	35.7	36.7	9.8
59	31.6	30.6	31.1	37.0	36.8	36.9	15.6
60	31.7	30.5	31.1	37.8	36.4	37.1	16.3
62	32.0	31.2	31.6	38.0	37.2	37.6	15.8
63	31.9	30.3	31.1	38.2	37.0	37.6	17.4
65	31.6	28.8	30.2	37.8	37.4	37.6	19.7
66	36.2	33.2	34.7	39.3	37.9	38.6	10.0
67	33.6	31.4	32.5	38.0	37.2	37.6	13.4
69	36.6	35.6	36.1	42.9	42.9	42.9	15.9
71	37.6	34.6	36.1	43.2	43.0	43.1	16.3
72	37.6	37.4	37.5	45.1	43.1	44.1	14.9
73	40.5	37.5	39.0	43.6	42.6	43.1	9.5
76	39.2	36.8	38.0	43.0	42.8	42.9	11.4
78	41.1	38.9	40.0	45.6	45.6	45.6	12.2
79	37.7	36.7	37.2	40.0	38.2	39.1	4.9
80	33.7	31.7	32.7	39.6	37.8	38.7	15.4
84	33.7	32.5	33.1	38.7	37.5	38.1	13.1
86	34.2	33.4	33.8	40.6	39.4	40.0	15.4
87	36.0	34.6	35.3	39.2	37.4	38.3	7.9
90	31.3	30.1	30.7	37.4	36.4	36.9	16.8
92	34.4	32.2	33.3	40.9	38.9	39.9	16.6
93	34.3	32.5	33.4	41.6	40.2	40.9	18.2
94	36.2	34.8	35.5	42.2	41.6	41.9	15.2
105	45.6	45.0	45.3	33.4	32.4	32.9	27.4
107	-	-	45.3	35.6	33.8	34.7	23.5

111	-	-	45.3	34.3	32.5	33.4	26.3
119	-	-	45.3	32.9	30.9	31.9	29.7
125	45.2	43.6	44.4	42.4	42.4	42.4	4.5
127	45.4	43.2	44.3	41.2	41.0	41.1	7.3
128	-	-	44.3	43.3	43.1	43.2	2.8
129	45.4	43.4	44.4	43.4	42.4	42.9	3.4
130	-	-	44.4	48.2	47.2	47.7	-7.3
133	-	-	44.4	39.3	39.1	39.2	11.7
134	-	-	44.4	45.4	44.8	45.1	-1.4
135	-	-	44.4	49.1	48.5	48.8	-9.8
136	-	-	44.4	52.4	51.2	51.8	-16.7
138	-	-	44.4	35.6	35.6	35.6	19.8
141	-	-	44.4	38.6	37.6	38.1	14.3
142	-	-	44.4	39.6	37.8	38.7	12.8
144	-	-	44.4	31.5	30.1	30.8	30.6
145	36.8	36.4	36.6	34.5	33.3	33.9	7.3
147	-	-	36.6	33.6	32.0	32.8	10.3
149	-	-	36.6	35.6	34.0	34.8	4.9
150	-	-	36.6	34.4	33.8	34.1	6.8
151	-	-	36.6	32.2	30.2	31.2	14.6
157	-	-	36.6	30.6	29.2	29.9	18.1
158	-	-	36.6	33.9	32.5	33.2	9.3
160	-	-	36.6	35.8	34.0	34.9	4.7
162	-	-	36.6	34.0	32.0	33.0	9.8
163	-	-	36.6	33.5	32.9	33.2	9.3
167	-	-	36.6	31.9	30.1	31.0	15.2
172	-	-	36.6	32.4	31.8	32.1	12.2
176	-	-	36.6	34.9	32.9	33.9	7.2
182	36.9	36.7	36.8	34.0	32.8	33.4	9.3
187	-	-	36.8	33.3	32.1	32.7	11.1
191	-	-	36.8	32.8	31.2	32.0	13.1
193	-	-	36.8	32.4	30.6	31.5	14.4
198	-	-	36.8	33.6	32.2	32.9	10.5
200	-	-	36.8	34.3	33.3	33.8	8.2
202	-	-	36.8	32.3	31.9	32.1	12.7

204	-	-	36.8	31.0	30.6	30.8	16.2
206	-	-	36.8	30.1	29.5	29.8	19.1
208	-	-	36.8	31.0	29.8	30.4	17.3
210	-	-	36.8	30.6	30.0	30.3	17.5
212	-	-	36.8	31.6	29.6	30.6	16.8
217	-	-	36.8	30.6	30.4	30.5	17.3
220	37.4	37.0	37.2	32.1	31.7	31.9	14.3
223	-	-	37.2	31.7	31.3	31.5	15.4
224	-	-	37.2	33.4	33.0	33.2	10.9
226	-	-	37.2	31.5	31.5	31.5	15.2
228	-	-	37.2	31.5	30.5	31.0	16.7
231	-	-	37.2	33.5	32.5	33.0	11.2
233	-	-	37.2	33.5	32.3	32.9	11.7
235	-	-	37.2	32.6	31.6	32.1	13.8
237	-	-	37.2	33.4	32.8	33.1	11.1
239	-	-	37.2	33.4	33.4	33.4	10.3
241	-	-	37.2	33.8	32.4	33.1	11.1
243	-	-	37.2	31.8	31.8	31.8	14.6
245	-	-	37.2	32.8	32.2	32.5	12.6
247	37.9	37.1	37.5	30.6	29.8	30.2	19.5
249	-	-	37.5	30.8	30.2	30.5	18.7
251	-	-	37.5	31.7	31.7	31.7	15.5
253	-	-	37.5	33.0	31.6	32.3	13.8
255	-	-	37.5	32.7	31.3	32.0	14.7
257	-	-	37.5	32.5	31.9	32.2	14.2
259	-	-	37.5	34.3	32.5	33.4	10.9
261	-	-	37.5	34.7	34.5	34.6	7.7
263	37.1	38.3	37.7	31.7	30.1	30.9	18.0
265	-	-	37.7	34.3	33.3	33.8	10.4
267	-	-	37.7	33.6	32.6	33.1	12.2
270	-	-	37.7	34.1	33.3	33.7	10.7
271	-	-	37.7	33.7	32.1	32.9	12.7
273	-	-	37.7	34.5	33.3	33.9	10.1
275	-	-	37.7	33.9	33.7	33.8	10.5
277	-	-	37.7	32.0	30.8	31.4	16.7

281	-	-	37.7	32.8	31.4	32.1	14.9
289	37.9	36.9	37.4	35.7	34.7	35.2	5.9
291	-	-	37.4	36.6	35.8	36.2	3.2
293	-	-	37.4	36.4	36.2	36.3	2.8
297	-	-	37.4	36.4	34.6	35.5	5.1
299	-	-	37.4	36.0	35.0	35.5	5.2
301	-	-	37.4	33.3	33.3	33.3	10.9
303	38.5	37.5	38.0	34.1	33.3	33.7	11.3
305	-	-	38.0	33.3	32.5	32.9	13.5
307	-	-	38.0	33.5	31.7	32.6	14.4
309	-	-	38.0	33.6	32.4	33.0	13.1
312	-	-	38.0	33.2	32.0	32.6	14.3
315	-	-	38.0	34.9	33.7	34.3	9.6
317	38.7	38.0	38.4	36.0	34.2	35.1	7.6
320	-	-	38.4	36.1	34.7	35.4	6.9
323	-	-	38.4	35.2	35.2	35.2	7.3
326	-	-	38.4	35.1	34.7	34.9	8.1
329	-	-	38.4	35.5	33.9	34.7	8.6
335	-	-	38.4	34.4	33.2	33.8	11.0
338	-	-	38.4	34.3	34.3	34.3	9.7
341	-	-	38.4	37.1	35.9	36.5	3.8
344	39.8	37.8	38.8	36.6	36.0	36.3	6.5
347	-	-	38.8	37.8	36.0	36.9	4.9
351	-	-	38.8	36.7	34.9	35.8	7.6
354	-	-	38.8	34.5	34.3	34.4	11.5
355	-	-	38.8	35.3	33.9	34.6	10.9
357	-	-	38.8	34.9	34.5	34.7	10.6
360	-	-	38.8	34.7	32.7	33.7	13.2
362	-	-	38.8	32.9	32.7	32.8	15.5
365	-	-	38.8	34.2	34.0	34.1	12.0
368	-	-	38.8	35.3	33.3	34.3	11.7
371	-	-	38.8	36.7	35.5	36.1	7.0
377	47.1	45.9	46.5	36.8	36.2	36.5	21.5
380	-	-	46.5	36.3	34.5	35.4	24.0
383	-	-	46.5	36.1	35.5	35.8	23.0

386	-	-	46.5	36.4	36.2	36.3	22.0
389	-	-	46.5	37.1	35.9	36.5	21.6
392	40.4	40.2	40.3	35.4	34.4	34.9	13.3
395	-	-	40.3	35.8	35.2	35.5	11.9
398	-	-	40.3	36.3	34.5	35.4	12.2
401	-	-	40.3	36.0	35.0	35.5	11.9
404	-	-	40.3	34.4	32.6	33.5	16.8
407	40.7	40.2	40.5	35.2	33.4	34.3	14.8
410	-	-	40.5	34.9	32.9	33.9	16.0
413	-	-	40.5	34.8	33.6	34.2	15.2
416	-	-	40.5	34.6	34.0	34.3	15.3
419	-	-	40.5	34.8	33.0	33.9	16.4
422	-	-	40.5	37.7	36.5	37.1	8.5
426	-	-	40.5	36.9	36.7	36.8	9.2
429	-	-	40.5	34.2	32.4	33.3	17.9
432	-	-	40.5	33.5	32.9	33.2	18.0
435	-	-	40.5	35.1	33.5	34.3	15.3
438	-	-	40.5	31.1	30.9	31.0	23.5
441	40.1	39.5	39.8	34.7	32.7	33.7	15.2
444	-	-	39.8	37.8	37.4	37.6	5.4
450	-	-	39.8	36.9	36.9	36.9	7.2
453	42.5	41.9	42.2	34.8	34.6	34.7	18.0
456	-	-	42.2	36.2	35.0	35.6	15.6
459	-	-	42.2	36.9	36.7	36.8	12.9
462	-	-	42.2	38.2	36.6	37.4	11.5
465	-	-	42.2	39.8	38.0	38.9	7.8
468	-	-	42.2	39.6	39.0	39.3	7.0
471	46.2	43.8	45.0	35.1	33.7	34.4	23.5
474	-	-	45.0	34.8	34.8	34.8	22.5
480	-	-	45.0	35.7	35.1	35.4	21.3
489	41.5	41.3	41.4	33.2	32.8	33.0	20.3
495	-	-	41.4	33.6	33.2	33.4	19.3
501	-	-	41.4	34.4	32.8	33.6	18.8
507	37.5	35.3	36.4	32.8	30.8	31.8	12.6
514	-	-	36.4	33.5	32.5	33.0	9.3

523	41.8	41.6	41.7	35.9	34.3	35.1	15.8
529	-	-	41.7	38.1	36.5	37.3	10.6
538	-	-	41.7	38.0	37.8	37.9	9.1
544	-	-	41.7	37.7	36.5	37.1	11.0
547	45.6	45.6	45.6	35.3	34.7	35.0	23.2
553	-	-	45.6	36.5	35.3	35.9	21.3
559	-	-	45.6	36.1	35.5	35.8	21.5
571	44.5	44.1	44.3	35.0	34.0	34.5	22.1
577	-	-	44.3	35.3	34.3	34.8	21.4
584	46.0	45.6	45.8	36.6	36.0	36.3	20.7
589	-	-	45.8	36.9	36.7	36.8	19.7
592	40.7	38.5	39.6	34.0	32.6	33.3	15.9
598	-	-	39.6	35.0	35.0	35.0	11.6
604	-	-	39.6	36.3	34.3	35.3	10.9
610	42.1	42.1	42.1	34.8	34.0	34.4	18.3
616	-	-	42.1	34.0	33.6	33.8	19.7
622	-	-	42.1	34.9	33.3	34.1	19.0
628	43.9	43.7	43.8	35.8	35.4	35.6	18.7
634	-	-	43.8	36.1	34.1	35.1	19.9
640	-	-	43.8	35.6	35.4	35.5	18.9
646	40.6	39.8	40.2	32.3	31.9	32.1	20.1
652	-	-	40.2	32.9	30.9	31.9	20.6
658	-	-	40.2	33.5	33.5	33.5	16.7
664	42.9	40.9	41.9	34.7	33.5	34.1	18.6
670	-	-	41.9	34.4	33.2	33.8	19.3
676	-	-	41.9	32.6	32.0	32.3	22.9
678	44.7	43.1	43.9	35.4	35.0	35.2	19.8
684	-	-	43.9	34.6	33.6	34.1	22.3
690	-	-	43.9	35.3	34.3	34.8	20.7
696	39.8	37.2	38.5	30.7	29.7	30.2	21.6
702	-	-	38.5	32.0	31.0	31.5	18.2
708	-	-	38.5	31.0	30.6	30.8	20.0
714	42.3	39.5	40.9	32.4	31.2	31.8	22.2
720	-	-	40.9	31.6	31.2	31.4	23.2
726	-	-	40.9	32.5	31.7	32.1	21.5

732	42.7	40.7	41.7	34.0	34.0	34.0	18.5
738	-	-	41.7	35.5	33.5	34.5	17.3
744	-	-	41.7	33.8	33.8	33.8	18.9
750	40.9	38.1	39.5	31.4	31.0	31.2	21.0
756	-	-	39.5	33.3	32.3	32.8	17.0
762	-	-	39.5	32.7	30.9	31.8	19.5
768	40.1	40.1	40.1	33.7	32.7	33.2	17.2
774	-	-	40.1	33.5	31.5	32.5	19.0
780	-	-	40.1	32.2	31.0	31.6	21.2

Table C-7 Data for Figure 4-14 COD performance of MABR during operation at different phases

Time (Day)	Influent COD (mg/L)			Effluent COD (mg/L)			Removal (%)
	Rep 1	Rep 2	Mean	Rep 1	Rep 2	Mean	
0	532	506	519	122	102	112	78
2	534	504	519	87	77	82	84
3	533	505	519	87	67	77	85
4	527	511	519	86	58	72	86
6	529	509	519	96	80	88	83
8	503	481	492	99	79	89	82
10	501	483	492	98	76	87	82
11	507	477	492	74	52	63	87
12	500	484	492	68	38	53	89
14	500	484	492	58	48	53	89
16	501	483	492	64	36	50	90
18	505	479	492	62	42	52	89
19	484	454	469	73	47	60	87
20	482	456	469	53	37	45	90
21	484	454	469	78	68	73	84
23	480	458	469	97	71	84	82
25	480	458	469	91	63	77	84
27	539	515	527	90	74	82	84
29	539	515	527	100	70	85	84
31	541	513	527	101	85	93	82
32	539	515	527	122	102	112	79
34	537	517	527	129	99	114	78

35	540	514	527	120	106	113	79
37	539	515	527	136	112	124	76
39	505	479	492	86	70	78	84
41	506	478	492	91	67	79	84
44	503	481	492	89	69	79	84
46	506	478	492	61	45	53	89
49	501	483	492	62	46	54	89
51	503	481	492	64	44	54	89
53	548	532	540	103	81	92	83
55	555	525	540	71	47	59	89
58	550	530	540	81	59	70	87
61	553	527	540	81	63	72	87
63	553	527	540	84	68	76	86
65	541	513	527	108	92	100	81
70	542	512	527	89	77	83	84
73	539	515	527	97	75	86	84
77	537	517	527	97	83	90	83
80	710	686	698	123	99	111	84
86	711	685	698	47	27	37	95
89	706	690	698	48	28	38	95
92	711	685	698	66	54	60	91
95	712	684	698	81	55	68	90
98	514	486	500	67	55	61	88
101	509	491	500	60	32	46	91
104	508	492	500	47	33	40	92
107	509	491	500	40	30	35	93
110	439	419	429	50	32	41	90
113	444	414	429	42	28	35	92
116	441	417	429	61	31	46	89
119	442	416	429	70	56	63	85
122	442	416	429	78	48	63	85
125	276	260	268	66	56	61	77
128	282	254	268	63	45	54	80
131	277	259	268	91	69	80	70
134	279	257	268	66	54	60	78

137	282	254	268	70	56	63	76
140	203	177	190	69	53	61	68
143	198	182	190	71	41	56	71
146	202	178	190	70	40	55	71
149	203	177	190	73	43	58	69
152	204	176	190	73	63	68	64
155	185	167	176	68	38	53	70
158	191	161	176	70	50	60	66
161	189	163	176	69	57	63	64
164	184	168	176	76	46	61	65
167	188	164	176	67	57	62	65
170	311	287	299	94	72	83	72
173	312	286	299	75	55	65	78
176	310	288	299	83	57	70	77
179	309	289	299	86	68	77	74
182	308	290	299	66	36	51	83
185	225	207	216	54	38	46	79
188	224	208	216	72	50	61	72
191	227	205	216	70	46	58	73
194	225	207	216	66	52	59	73
197	231	201	216	71	51	61	72
200	227	205	216	96	66	81	63
203	329	309	319	90	66	78	76
206	327	311	319	72	46	59	82
209	334	304	319	74	48	61	81
212	333	305	319	75	61	68	79
215	244	218	231	83	59	71	69
218	246	216	231	67	55	61	74
221	244	218	231	103	75	89	61
224	241	221	231	77	65	71	69
227	218	200	209	68	50	59	72
230	217	201	209	65	45	55	74
233	219	199	209	70	52	61	71
236	222	196	209	80	56	68	67
239	224	194	209	87	59	73	65

242	211	185	198	74	52	63	68
245	211	185	198	68	54	61	69
248	208	188	198	70	48	59	70
251	208	188	198	67	39	53	73
254	211	185	198	64	44	54	73
257	230	204	217	68	46	57	74
260	231	203	217	66	36	51	76
263	228	206	217	72	44	58	73
266	231	203	217	61	45	53	76
269	227	207	217	58	42	50	77
272	272	246	259	71	59	65	75
275	270	248	259	76	66	71	73
278	273	245	259	85	59	72	72
281	269	249	259	83	63	73	72
284	270	248	259	83	55	69	73
287	267	251	259	83	59	71	73
290	231	215	223	78	50	64	71
293	232	214	223	76	54	65	71
296	232	214	223	76	60	68	70
299	231	215	223	83	59	71	68
302	238	208	223	70	54	62	72
305	216	198	207	59	49	54	74
308	218	196	207	57	45	51	75
311	221	193	207	68	48	58	72
314	218	196	207	62	38	50	76
317	203	177	190	57	41	49	74
320	200	180	190	57	31	44	77
323	198	182	190	67	51	59	69
326	199	181	190	56	46	51	73
329	200	180	190	62	38	50	74
332	190	162	176	53	33	43	76
335	189	163	176	63	49	56	68
338	184	168	176	62	40	51	71
341	184	168	176	64	36	50	72
344	186	166	176	64	34	49	72

347	190	170	180	58	34	46	74
350	193	167	180	73	49	61	66
353	188	172	180	71	43	57	68
356	192	168	180	63	45	54	70
359	195	165	180	62	40	51	72
362	194	164	179	68	40	54	70
365	191	167	179	69	51	60	66
368	190	168	179	58	48	53	70
371	192	166	179	69	59	64	64
374	194	164	179	62	48	55	69
377	211	191	201	69	51	60	70
380	209	193	201	66	52	59	71
383	210	192	201	76	48	62	69
386	209	193	201	78	50	64	68
389	215	187	201	78	68	73	64
392	200	172	186	76	46	61	67
395	199	173	186	64	48	56	70
398	199	173	186	69	47	58	69
401	194	178	186	58	40	49	74
404	198	174	186	62	32	47	75
407	194	178	186	68	40	54	71
410	205	177	191	76	46	61	68
413	200	182	191	69	57	63	67

Table C-8 Data for Figure 4-15 AEF performance of MABR during operation at different phases

Time (Day)	Influent COD (mg/L)			Effluent COD (mg/L)			Removal (%)
	Rep 1	Rep 2	Mean	Rep 1	Rep 2	Mean	
0	15.3	14.7	15.0	14.4	14.0	14.2	5.1
1	-	-	15.0	14.2	14.2	14.2	5.1
2	-	-	15.0	13.7	13.7	13.7	8.6
3	-	-	15.0	16.0	15.0	15.5	-3.2
5	-	-	15.0	16.0	15.0	15.5	-3.5
7	15.4	14.9	15.2	15.0	14.2	14.6	4.1
9	-	-	15.2	13.8	12.8	13.3	12.5
10	-	-	15.2	13.5	12.5	13.0	14.2

11	-	-	15.2	14.0	13.6	13.8	9.2
13	-	-	15.2	12.3	12.3	12.3	18.8
15	-	-	15.2	12.2	11.6	11.9	22.0
17	-	-	15.2	12.7	12.1	12.4	18.6
19	15.7	13.7	14.7	12.5	11.5	12.0	18.3
20	-	-	14.7	12.0	11.8	11.9	19.3
22	-	-	14.7	13.1	12.5	12.8	13.1
24	-	-	14.7	13.7	12.7	13.2	10.5
25	-	-	14.7	13.9	12.9	13.4	8.9
26	-	-	14.7	13.7	12.7	13.2	10.2
27	13.7	12.1	12.9	10.8	10.0	10.4	19.2
29	-	-	12.9	11.7	10.9	11.3	12.2
30	-	-	12.9	11.1	10.1	10.6	17.5
32	-	-	12.9	11.0	10.4	10.7	16.9
33	-	-	12.9	11.0	10.6	10.8	16.5
35	-	-	12.9	10.5	10.5	10.5	18.7
37	-	-	12.9	12.8	12.6	12.7	1.5
41	15.8	13.8	14.8	14.1	13.9	14.0	5.5
43	-	-	14.8	12.8	12.0	12.4	16.2
46	-	-	14.8	12.7	12.5	12.6	14.7
49	-	-	14.8	13.0	13.0	13.0	11.9
51	-	-	14.8	13.5	13.1	13.3	9.9
53	16.4	15.2	15.8	11.9	11.5	11.7	25.9
55	-	-	15.8	12.6	12.4	12.5	21.0
57	-	-	15.8	13.3	13.1	13.2	16.7
60	-	-	15.8	12.3	12.3	12.3	22.0
63	-	-	15.8	13.3	12.9	13.1	16.8
70	14.4	13.2	13.8	12.5	11.7	12.1	12.5
73	-	-	13.8	11.5	11.5	11.5	16.6
77	-	-	13.8	12.0	11.0	11.5	17.0
80	-	-	13.8	11.1	10.1	10.6	23.0
89	-	-	13.8	9.8	9.6	9.7	29.5
92	-	-	13.8	10.8	9.8	10.3	25.1
95	-	-	13.8	11.7	11.1	11.4	17.8
98	13.4	11.6	12.5	11.1	10.1	10.6	14.8

101	-	-	12.5	10.9	10.1	10.5	15.5
104	-	-	12.5	10.6	9.8	10.2	18.5
107	-	-	12.5	10.2	10.2	10.2	18.2
110	20.9	19.9	20.4	16.6	16.2	16.4	19.3
116	-	-	20.4	16.1	15.9	16.0	21.3
119	-	-	20.4	16.3	15.3	15.8	22.4
122	-	-	20.4	15.4	15.0	15.2	25.3
125	18.1	16.7	17.4	15.6	15.4	15.5	10.7
128	-	-	17.4	15.1	14.9	15.0	13.8
137	-	-	17.4	14.3	14.1	14.2	18.2
140	22.3	20.7	21.5	18.8	18.0	18.4	14.4
143	-	-	21.5	18.5	18.5	18.5	13.9
146	-	-	21.5	18.3	17.7	18.0	16.1
149	-	-	21.5	14.7	13.7	14.2	33.9
152	-	-	21.5	15.0	14.8	14.9	30.7
155	14.6	13.2	13.9	9.5	8.9	9.2	33.8
161	-	-	13.9	10.3	10.3	10.3	25.9
167	13.4	11.4	12.4	10.8	10.0	10.4	16.1
173	-	-	12.4	10.9	10.7	10.8	12.9
179	-	-	12.4	10.2	10.0	10.1	18.5
185	13.5	12.7	13.1	10.7	9.9	10.3	21.4
191	-	-	13.1	10.2	10.2	10.2	22.1
197	-	-	13.1	10.8	10.6	10.7	18.3
203	17.6	17.2	17.4	12.7	12.5	12.6	27.6
209	-	-	17.4	13.7	13.1	13.4	23.0
215	16.4	15.4	15.9	12.3	12.3	12.3	22.6
221	-	-	15.9	12.8	12.2	12.5	21.4
230	16.5	15.1	15.8	13.0	13.0	13.0	17.7
236	-	-	15.8	12.6	12.0	12.3	22.2
239	14.3	12.5	13.4	11.0	10.6	10.8	19.4
243	-	-	13.4	11.1	10.9	11.0	17.9
245	-	-	13.4	11.4	10.4	10.9	18.7
251	15.9	14.1	15.0	11.1	10.9	11.0	26.7
257	-	-	15.0	12.5	11.5	12.0	20.0
263	20.0	18.0	19.0	14.3	13.7	14.0	26.3

270	-	-	19.0	16.5	15.5	16.0	15.8
276	-	-	19.0	13.2	12.8	13.0	31.6
282	17.0	15.0	16.0	11.2	10.8	11.0	31.3
288	-	-	16.0	12.0	12.0	12.0	25.0
294	-	-	16.0	13.5	12.5	13.0	18.8
300	18.9	17.1	18.0	11.0	11.0	11.0	38.9
306	-	-	18.0	12.4	11.6	12.0	33.3
312	-	-	18.0	11.2	10.8	11.0	38.9
318	-	-	18.0	15.0	15.0	15.0	16.7
324	14.2	13.8	14.0	11.0	11.0	11.0	21.4
330	-	-	14.0	10.2	9.8	10.0	28.6
336	-	-	14.0	9.4	8.6	9.0	35.7
342	-	-	14.0	11.4	10.6	11.0	21.4
348	17.6	16.4	17.0	13.5	12.5	13.0	23.5
354	-	-	17.0	14.4	13.6	14.0	17.6
360	-	-	17.0	12.3	11.7	12.0	29.4
366	-	-	17.0	12.3	11.7	12.0	29.4
372	19.3	18.7	19.0	13.5	12.5	13.0	31.6
378	-	-	19.0	14.4	13.6	14.0	26.3
384	-	-	19.0	12.3	11.7	12.0	36.8
390	-	-	19.0	13.0	13.0	13.0	31.6
396	-	-	18.0	13.5	12.5	13.0	27.8
402	-	-	18.0	12.4	11.6	12.0	33.3
408	-	-	18.0	12.4	11.6	12.0	33.3
414	-	-	18.0	11.4	10.6	11.0	38.9

Table C-9 Data for Figure 4-17 Adsorption isotherm of COD in MABR effluent onto GAC at 21°C

C_e (mg/L)	q_e (mg/g)
49.8	808.08
31.5	789.09
29.7	759.79
15.9	777.83
12.9	753.88
6.4	626.23

2.6	422.45

Table C-10 Data for Figure 4-18 Breakthrough curve of the GAC column with 30 min EBCT

Day	Effluent concentration (mg/L)
0	1
7	1
14	1
21	1
28	1
35	1
42	1
49	1
56	1
63	2
70	1
84	1
91	67
98	65
105	67

Table C-11 Data for Figure 4-19 Performance evaluation of each operational component when the process train was at stable state

Sample Name	COD concentration (mg/L)				AEF concentration (mg/L)			
	Rep 1	Rep 2	Mean	Error	Rep 1	Rep 2	Mean	Error
Raw OSPW	238	228	233	5	65.0	55.8	60.4	4.6
MBBR IN	154	132	143	11	47.6	34.6	41.1	6.5
MBBR OUT	117	109	113	4	38.5	32.7	35.6	2.9
COP IN	118	104	111	7	34.7	29.5	32.1	2.6
COP OUT	112	98	105	7	18.4	14.0	16.2	2.2
MABR IN	111	93	102	9	17.4	13.2	15.3	2.1
MABR OUT	69	57	63	6	15.3	8.5	11.9	3.4
AP IN	66	52	59	7	13.5	9.5	11.5	2.0
AP OUT	20	14	17	3	3.8	2.0	2.9	0.9

Table C-12 Data for Figure 4-20 BOD value and BOD/COD ratio of each operational component when the process train was at stable state

Sample name	Rep 1	Rep2	Mean	Error bar	BOD/COD ratio
Raw OSPW	3	2	3	1	0.01
MBBR influent	244	265	255	10	0.48
MBBR effluent	2	4	3	1	0.03
MBBR effluent after ozonation	18	21	19	2	0.17
MABR influent	73	96	85	12	0.40
MABR effluent	4	5	4	1	0.06
Standard solution	198	196	197	1	-

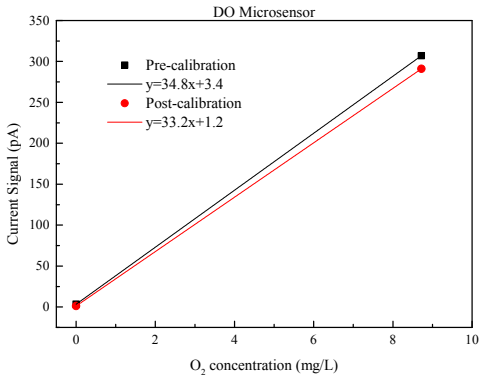

(a)

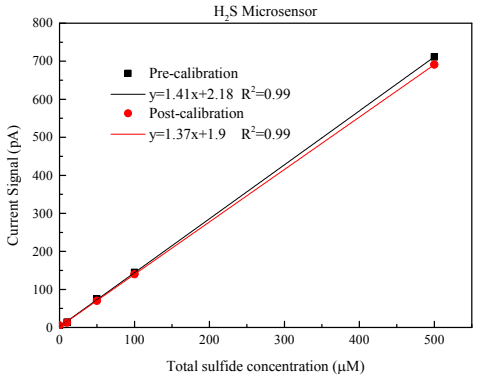

(b)

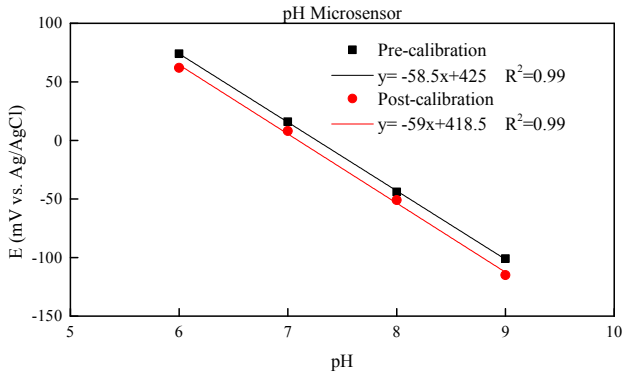

(c)

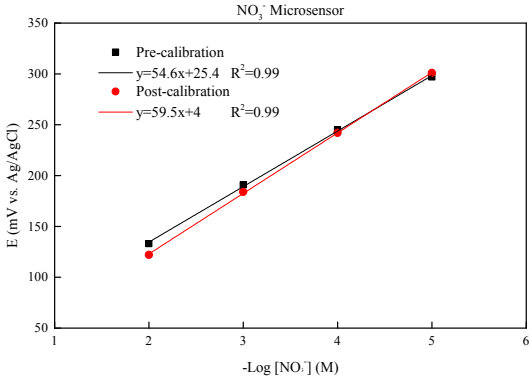

(d)

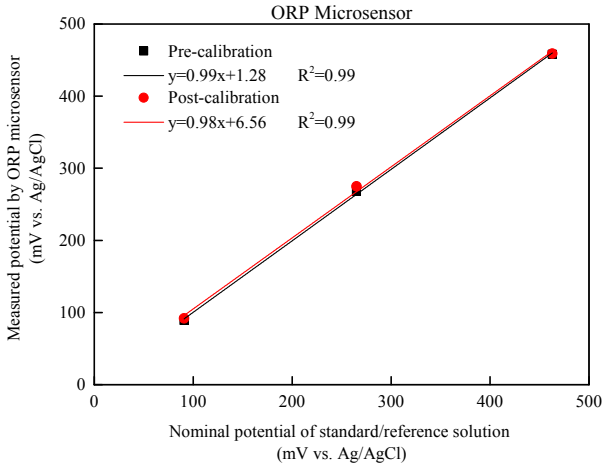

(e)

Figure C-1 Calibration curve for each microsensor

Table C-13 Data for Figure S-3 Calibration curve for each microsensor

DO microsensor

O_2 concentration (mg/L)	Pre-calibration	Post-calibration
	Current signal (pA)	Current signal (pA)
0	3.4	1.2
8.72	307	291

H_2S microsensor

Total sulfide concentration (μM)	Pre-calibration	Post-calibration
	Current signal (pA)	Current signal (pA)
0	2	5
10	14	13
50	75	70
100	145	140
500	711	691

ORP microsensor

Reference solutions	Nominal potential* (mV Vs. Ag/AgCl)	Pre-calibration	Post-calibration
		Measured potential (mV Vs. Ag/AgCl)	Measured potential (mV Vs. Ag/AgCl)

pH 4 Quinhydrone solution	265	268	275
pH 7 Quinhydrone solution	90.8	89	92
Ferrous-Ferric Standard solution	463	458	459

* The values of nominal potentials were for 21°C

NO_3^- microsensor

Molar concentration of NO_3^- (M)	-Log [NO_3^-]	Pre-calibration	Post-calibration
		Potential (mV Vs. Ag/AgCl)	Potential (mV Vs. Ag/AgCl)
10^{-2}	2	133	122
10^{-3}	3	191	184
10^{-4}	4	245	242
10^{-5}	5	297	301

pH microsensor

pH standard solution	Pre-calibration	Post-calibration
	Potential (mV Vs. Ag/AgCl)	Potential (mV Vs. Ag/AgCl)
6	74	62
7	16	8
8	-44	-51
9	-101	-115

Table C-14 Data for Figure 5-3 Chemical profiles inside MBBR biofilm

Distance from biofilm surface (μm)	NO_3^- (mg/L)	DO (mg/L)	pH	H_2S (mg/L)	ORP (mV)
-350	-	3.5	-	0.0	-
-300	15.1	3.1	7.9	0.0	-
-250	14.7	3.6	7.8	0.0	413
-200	13.8	3.1	7.9	0.0	403
-150	13.5	3.7	7.7	0.0	405
-100	12.9	3.4	7.9	0.0	412
-50	12.3	2.8	7.9	0.0	400
0	11.9	3.3	7.9	0.0	398
50	9.4	3.1	7.8	0.0	400
100	8.1	2.5	7.7	0.0	384
150	6.8	1.9	7.7	0.0	375

200	5.2	1.5	7.8	0.0	359
250	3.1	1.6	7.8	0.0	286
300	2.9	1.4	7.7	0.0	233
350	2.3	1.6	7.6	0.0	179
400	2.0	1.1	7.6	0.0	138
450	1.5	0.9	7.6	0.0	94
500	1.4	0.7	7.6	0.0	48
550	0.9	0.1	7.6	0.0	27
600	0.5	0.0	7.6	0.0	-16
650	0.2	0.1	7.6	0.0	-38
700	0.1	0.0	7.7	0.0	-69
750	0.0	0.0	7.7	0.0	-87
800	0.0	0.0	7.6	0.0	-102
850	0.0	0.0	7.7	0.0	-107
900	0.0	0.0	7.6	0.1	-109
950	0.0	0.0	7.7	0.1	-106
1000	0.0	0.0	7.6	0.2	-125
1050	0.0	-	-	-	-117

Table C-15 Data for Figure 5-5 Chemical profiles inside MABR biofilm

Distance from biofilm surface (μm)	NO_3^- (mg/L)	DO (mg/L)	pH	H_2S (mg/L)	ORP (mV)
-400	3.4	0.9	8.1	0.0	139
-300	3.1	1.1	8.0	0.0	107
-250	2.7	0.9	8.3	0.0	73
-200	2.4	1.0	8.1	0.0	81
-150	2.5	0.9	7.9	0.1	67
-100	2.1	0.5	8.1	0.3	23
-50	2.0	0.2	8.1	0.7	-31
0	1.7	0.1	8.0	0.5	-67
50	1.5	0.1	7.9	0.9	-91
100	1.1	0.0	7.8	0.6	-108
150	0.8	0.0	7.8	0.1	-111
200	0.5	0.0	7.8	0.1	-113
250	0.2	0.0	7.8	0.0	-127
300	0.1	0.0	7.7	0.0	-138

350	0.0	0.0	7.7	0.0	-143
400	0.0	0.0	7.7	0.0	-127
450	0.0	0.0	7.7	0.0	-116
500	0.0	0.0	7.6	0.0	-106
550	0.0	0.0	7.7	0.0	-101
600	0.0	0.0	7.8	0.0	-110
650	0.0	0.0	7.8	0.0	-104
700	0.0	0.0	7.8	0.0	-89
750	0.0	0.0	7.8	0.0	-75
800	0.0	0.1	7.8	0.0	-11
850	0.0	0.3	7.8	0.0	43
900	0.0	0.4	7.7	0.0	94
950	0.0	0.6	7.8	0.0	153
1000	0.0	1.1	7.8	0.0	251
1050	0.0	2.3	7.8	0.0	277
1100	0.0	3.1	7.8	0.0	351
1150	0.0	4.5	7.9	0.0	390
1200	0.0	5.7	7.8	0.0	415
1250	0.0	6.9	7.8	0.0	428
1300	0.0	7.4	7.7	0.0	420
1350	0.0	8.3	7.8	0.0	415
1400	0.0	8.7	7.9	-	419
1450	0.0	9.1	7.9	-	424
1500	0.0	-	7.9	-	421

Table C-16 Data for Figure 5-6 The top 10 most relative abundance of the bacteria at the phylum level

Name	Relative abundance (%)					
	S_0	SA_{B1}	SA_{S2}	SA_{B2}	SB_0	SB_{B1}
Acidobacteria	0.5	2.9	2.5	3.3	4.1	6.2
Actinobacteria	1.9	0.3	0.8	1.3	0.7	1.1
Armatimonadetes	0.0	0.5	0.1	0.0	0.2	0.0
Bacteroidetes	10.2	23.2	21.7	7.2	15.1	10.3
Chlamydiae	0.2	0.0	0.1	0.1	0.0	1.0
Chlorobi	0.0	0.1	0.0	0.0	0.0	2.6

Chloroflexi	0.1	2.2	7.4	17.1	1.5	13.9
Cyanobacteria_Chloroplast	0.1	0.0	0.0	0.0	0.0	0.2
Firmicutes	0.0	5.1	26.7	24.3	13.4	1.7
Gemmatimonadetes	0.0	1.8	0.3	0.4	3.4	0.3
Minor Phyla	0.0	0.1	0.1	0.0	0.1	0.0
Nitrospirae	0.0	3.3	1.7	2.9	0.1	4.8
OD1	0.1	0.0	0.1	0.0	0.2	0.0
Planctomycetes	1.3	1.0	2.3	3.2	2.2	9.8
Proteobacteria	78.1	41.7	25.8	24.2	45.9	21.6
Spirochaetes	0.0	0.0	0.0	0.0	0.1	0.0
TM7	0.2	0.1	0.0	0.0	0.3	0.0
unclassified	3.7	11.6	8.0	13.5	8.1	22.4
Verrucomicrobia	3.4	5.9	2.4	2.2	3.5	4.1
WS3	0.0	0.1	0.0	0.0	1.1	0.0

Table C-17 Data for Figure 5-7 The top 10 most relative abundance of the bacteria at the class level

Name	Relative abundance (%)					
	S_0	SA_{B1}	SA_{S2}	SA_{B2}	SB_0	SB_{B1}
Acidobacteria_Gp4	0.0	0.0	1.8	0.0	3.7	4.8
Actinobacteria	1.9	0.0	0.0	0.0	0.0	0.0
Alphaproteobacteria	14.1	7.0	5.3	7.1	9.3	10.2
Anaerolineae	0.0	0.0	0.0	3.2	0.0	0.0
Bacilli	0.0	5.0	25.2	23.9	13.0	0.0
Betaproteobacteria	29.9	26.0	13.7	12.7	21.7	6.1
Caldilineae	0.0	0.0	5.8	12.2	0.0	11.9
Flavobacteria	5.1	0.0	2.7	0.0	0.0	0.0
Gammaproteobacteria	31.9	8.1	5.2	3.4	13.4	3.6
Gemmatimonadetes	0.0	1.8	0.0	0.0	3.4	0.0
Ignavibacteria	0.0	0.0	0.0	0.0	0.0	2.6
Nitrospira	0.0	3.3	0.0	2.9	0.0	4.8
Opitutae	1.4	0.0	0.0	0.0	0.0	0.0
Planctomycetacia	1.2	0.0	2.3	3.2	2.1	9.7
Sphingobacteria	2.4	20.0	12.0	4.5	10.2	7.0
Subdivision3	1.8	2.8	0.0	0.0	0.0	0.0

unclassified	6.3	14.5	15.1	16.3	12.3	25.5
Verrucomicrobiae	0.0	2.1	0.0	0.0	1.5	0.0
Others	3.9	9.5	11.0	10.6	9.4	13.8

Table C-18 Data for Figure 5-8 Heat map for top 50 most abundant bacteria at genus level

Name	Relative abundance (%)					
	S_0	SA_{B1}	SA_{S2}	SA_{B2}	SB_0	SB_{B1}
3_genus_incertae_sedis	1.81	2.82	0.67	0.81	0.64	2.15
Acetoanaerobium	0.00	0.00	0.56	0.00	0.00	0.00
Aeromonas	0.00	1.76	0.22	0.04	0.00	0.00
Armatimonadetes_gp5	0.00	0.53	0.00	0.04	0.20	0.00
Azoarcus	0.00	0.11	0.72	0.47	0.00	0.00
Caldilinea	0.09	0.98	5.80	12.21	1.13	11.87
Carnobacterium	0.00	0.00	2.29	1.58	0.00	0.06
Desulfobacterium	0.00	0.00	0.00	0.00	0.09	0.00
Desulfobulbus	0.00	0.00	0.17	0.00	0.08	0.00
Desulfomicrobium	0.00	0.00	0.36	0.00	0.00	0.00
Desulfosporosinus	0.00	0.00	0.00	0.00	0.06	0.00
Exiguobacterium	0.00	3.98	0.00	0.00	12.83	0.00
Ferruginibacter	0.89	1.13	0.00	0.00	0.00	0.00
Flavobacterium	0.82	0.56	2.17	0.53	0.14	0.30
Gemmatimonas	0.00	1.78	0.26	0.38	3.41	0.32
Gp3	0.00	1.45	0.10	0.25	0.14	0.63
Gp4	0.32	0.97	1.85	2.52	3.75	4.81
Hydrogenophaga	1.40	1.68	2.45	1.07	0.11	0.12
Ignavibacterium	0.00	0.11	0.00	0.00	0.00	2.58
Janthinobacterium	0.00	0.59	0.14	0.00	0.00	0.07
Leadbetterella	0.00	2.28	0.13	0.00	0.00	0.00
Longilinea	0.00	0.00	0.70	1.21	0.00	0.08
Luteimonas	0.00	0.93	0.00	0.00	9.87	0.00
Lutibacter	3.03	0.00	0.00	0.00	0.00	0.00
Lysobacter	0.00	0.00	0.00	0.00	0.71	0.00
Methylobacter	0.15	0.00	0.00	0.00	0.00	0.00
Methyloversatilis	0.60	0.12	0.00	0.11	0.00	0.67
Nitrospira	0.00	3.32	1.66	2.93	0.06	4.81

Novosphingobium	0.99	0.35	0.00	0.06	0.73	0.00
Ohtaekwangia	1.17	0.20	0.47	0.55	0.00	1.85
Opitutus	1.31	0.95	0.13	0.18	0.18	0.66
Paracoccus	0.00	0.00	0.30	0.75	0.00	0.10
Parvibaculum	2.05	0.00	0.00	0.00	0.00	0.19
Pasteuria	0.00	0.00	0.15	0.48	0.12	0.50
Phenylobacterium	0.18	0.00	0.52	0.00	0.00	0.17
Planctomyces	0.96	0.33	0.00	0.58	1.59	2.99
Porphyrobacter	0.46	0.00	0.00	0.00	0.55	0.00
Prosthecobacter	0.21	2.05	0.75	0.40	0.05	0.80
Pseudomonas	0.55	2.25	1.30	1.04	0.27	0.87
Rheinheimera	0.00	0.62	0.00	0.00	0.00	0.00
Rhodobacter	0.36	1.68	0.51	0.72	1.26	0.60
Shewanella	0.00	0.47	1.63	0.00	0.00	0.00
Singularimonas	1.45	0.00	0.00	0.00	0.00	0.00
Spartobacteria_genera_incertae_sedis	0.00	0.00	0.00	0.00	1.03	0.00
Sphaerobacter	0.00	0.00	0.28	0.64	0.00	0.49
Steroidobacter	0.51	0.00	0.00	0.07	0.00	0.40
Sulfuritalea	0.17	0.00	0.00	0.00	0.00	0.00
Thauera	0.12	4.64	0.00	0.12	11.33	0.00
Trichococcus	0.00	0.95	22.69	21.80	0.00	0.99
Unclassified	74.71	55.27	44.24	43.96	43.64	55.39
WS3_genus_incertae_sedis	0.00	0.07	0.00	0.00	1.08	0.00

Table C-19 Data for Figure 5-9 PCoA analysis

Sample	PC1 (38.19%)	PC2 (26.39%)
S_0	-0.230	0.640
SA_{B1}	-0.293	-0.250
SA_{S2}	0.489	0.0414
SA_{B2}	0.498	-0.0308
SB_0	-0.404	-0.236
SB_{B1}	-0.060	-0.055